

# Direct And Mediated Anodic Oxidation of Organic Pollutants

Marco Panizza\* and Giacomo Cerisola

Department of Chemical and Process Engineering, University of Genoa, P.le J. F. Kennedy 1, 16129 Genoa, Italy

Received April 2, 2009

## Contents

1. Introduction	6541
2. Figures of Merit	6541
2.1. Current Efficiency	6542
2.2. Space-time Yield	6543
2.3. Specific Energy Consumption	6543
2.4. Limiting Current Density	6543
3. Direct Electrolysis	6543
4. Oxidation via Intermediates of Oxygen Evolution	6544
4.1. Ruthenium- and Iridium-based Oxides	6545
4.2. Platinum Anode	6546
4.3. Carbon and Graphite	6547
4.4. Tin Dioxide	6547
4.5. Lead Dioxide	6549
4.6. Boron-Doped Diamond (BDD)	6551
5. Indirect Electrolysis	6556
5.1. Metallic Redox Couple	6556
5.2. Oxidizing Chemicals	6559
5.2.1. Active Chlorine	6559
5.2.2. Ozone	6561
5.2.3. Persulfate, Percarbonate, and Perphosphate	6564
6. Concluding Remarks	6565
7. Acknowledgments	6565
8. References	6565

## 1. Introduction

For many years, the introduction of more stringent pollution regulations, coupled with financial and social pressures for sustainable development, has pressed toward “zero-effluent” processes, as well as to researching and developing new or more efficient wastewater treatment technologies. A basic principle in environmental culture is to reduce waste and pollution to “As Low As Reasonably Achievable” (ALARA) levels. To ensure acceptable levels of environmental impact, however, wastewater systems also have to be engineered in accordance with the principle of “Best Available Techniques Not Entailing Excessive Cost” (BATNEEC).

Because of the extremely diverse features of industrial waste that usually contains a mixture of organic and inorganic compounds, no universal strategy of reclamation is feasible. As to the treatment of effluents polluted with organic compounds, biological oxidation is certainly the cheapest process, but the presence of toxic or biorefractory molecules may hinder this approach. For this reason, physical-chemical

methods (filtration, coagulation, adsorption, and flocculation), chemical oxidation (use of chlorine, ozone, hydrogen peroxide, wet air oxidation), and advanced oxidation processes (AOP) (Fenton’s reaction, ozone + UV radiation, photochemistry) are currently used to treat industrial effluents. However, all these methods have some major drawbacks. For example, filtration and adsorption are not always sufficient to achieve the discharge limits;<sup>1</sup> coagulation and flotation generate a large amount of sludge; chemical oxidations have low capacity rates and need transportation and storage of dangerous reactants; and advanced oxidation processes require high investment costs.

In this context, oxidative electrochemical technologies offer an alternative solution to many environmental problems in the process industry, because electrons provide a versatile, efficient, cost-effective, easily automatizable, and clean reagent.<sup>2</sup> For some decades, a large number of companies have been marketing electrochemical devices for metal ion removal and metal recovery, treatment of liquors containing dissolved chromium, flue-gas desulfurization, desalination, and salt splitting.<sup>3–9</sup> However, so far, the role of electrochemical technologies for the treatment of organic pollutants has been “relatively small”. But nowadays, thanks to intensive investigations that have improved the electrocatalytic activity and stability of electrode materials and optimized reactor geometry, electrochemical technologies have reached a promising state of development and can be effectively used for disinfection and purification of wastewater polluted with organic compounds.<sup>10–13</sup>

In electrooxidation, pollutants can be removed by (i) direct electrolysis, where pollutants exchange electrons directly with the anode surface without involvement of other substances, or (ii) indirect electrolysis, where organic pollutants do not exchange electrons directly with the anode surface but rather through the mediation of some electroactive species regenerated there, which act as intermediaries for electrons shuttling between the electrode and the organic compounds. Indirect electrolysis can be a reversible or an irreversible process, and the redox reagent can be electrogenerated by either anodic or cathodic process. Process selection depends on the nature and structure of the electrode material, experimental conditions, and electrolyte composition.

This review focuses on recent progress in and the literature on direct and mediated anodic processes for the oxidation of organic pollutants.

## 2. Figures of Merit

Before describing the results and the mechanisms involved in the electro-oxidation of organic pollutants, it is necessary

\* Corresponding author. Tel.: +39 010 3536032. Fax: +39 010 3536028. E-mail: marco.panizza@unige.it; giacomo.cerisola@unige.it.



Marco Panizza graduated in Chemical Engineering at the University of Genoa (Italy) in 1997 and received his Ph.D. degree in Chemistry for Engineering at the University of Genoa in 2001. In 2000 he was visiting scientist at the Institute of Chemical Engineering, Ecole Federal Polytechnique of Lausanne in the Laboratory of Prof. Cominellis. From 2001 to 2006, he was contract researcher at the Department of Chemical and Process Engineering of the University of Genoa. In 2006 he reached the staff position of researcher at the Faculty of Engineering of the University of Genoa. He has published more than 40 papers in international journals and 2 book chapters. He was awarded the "Oronzio and Niccolò De Nora Foundation Prize" of the Italian Chemical Society and the "Electrochemical Technology and Engineering Prize" of the International Society of Electrochemistry (ISE). His research interests are focused mainly in environmental electrochemistry, specifically in the study of electrode materials and the operating conditions for the oxidation of organic compounds.



Giacomo Cerisola graduated in Chemical Engineering at the University of Genoa (Italy) in 1975. From 1977 to 1988, he worked as Materials Researcher at SULZER AG. in Swiss, at the Institute of Scientific and Technological Research at Trento (Italy), and at the Materials Department of the University of Trento (Italy). In 1988 he was made an associate professor of chemistry at the Engineering Faculty of the University of Genoa, and in 2000 he reached the position of full professor of chemistry, at the Chemical and Process Engineering Department of the University of Genova. He is the responsible for the Laboratory of Electrochemistry, Corrosion and Protection of Metallic Materials of the Department of Chemical and Process Engineering of the University of Genoa. He published in international journals more than 120 papers dealing with electrochemical testing methods for the characterization of polymeric coatings, study of electrode/solution interface, electrode materials for environmental protection technologies, and electrochemical and corrosion characterization of ferrous and nonferrous alloys.

to review some established performance indicators used for progress and efficiency assessment of electrochemical treatments and for comparing reactors with different geometries.

## 2.1. Current Efficiency

Current efficiency ( $\Phi$ ) is generally defined as the ratio of the charge used for the oxidation of each compound to the total charge passed during electrolysis:

$$\Phi = \frac{\text{charge used to oxidize organics}}{\text{total charge}} \cdot 100 \quad (1)$$

In the literature, different expressions of current efficiency have been proposed: instantaneous current efficiency (ICE), electrochemical oxidation index (EOI), general current efficiency (GCE), and mineralization current efficiency (MCE).

Instantaneous current efficiency (ICE) of electro-oxidation can be determined by the oxygen flow rate (OFR) method or chemical oxygen demand (COD) method, using the following relationships:<sup>14</sup>

$$\text{ICE} = \frac{\dot{V}_0 - (\dot{V}_t)_{\text{org}}}{\dot{V}_0} \quad (2)$$

where  $\dot{V}_0$  is the oxygen flow rate measured in the anodic compartment in the absence of organic pollutants (in  $\text{cm}^3 \text{min}^{-1}$ ) and  $\dot{V}_t$  is the oxygen flow rate at a given time  $t$  in the presence of organic pollutants (in  $\text{cm}^3 \text{min}^{-1}$ ); or

$$\text{ICE} = \frac{(\text{COD}_t - \text{COD}_{t+\Delta t})}{8I\Delta t} FV \quad (3)$$

where  $(\text{COD})_t$  and  $(\text{COD})_{t+\Delta t}$  are the chemical oxygen demands at times  $t$  and  $t + \Delta t$  (in  $\text{gO}_2 \text{dm}^{-3}$ ), respectively,  $I$  is the current (A),  $F$  is Faraday's constant ( $96\,485 \text{ C mol}^{-1}$ ),  $V$  is the electrolyte volume ( $\text{dm}^3$ ), and 8 is the oxygen equivalent mass ( $\text{g eq}^{-1}$ ).

Both COD and OFR techniques have their limitations, e.g., COD is not reliable if volatile organic compounds (VOC) or high concentrations of chloride ions are present, or if insoluble organic products are formed during treatment. On the other hand, OFR requires specialized equipment that may not be available to many workers.

The electrochemical oxidation index (EOI), which is the average value of current efficiency during overall oxidation, is determined from ICE using the following relationship:<sup>14</sup>

$$\text{EOI} = \frac{\int \text{ICE} dt}{\tau} \quad (4)$$

where  $\tau$  is the time at which ICE is almost zero.

General current efficiency (GCE) represents an average value of current efficiency, between the initial time  $t = 0$  and  $t$ . It can be determined from COD using the following relationship:<sup>14</sup>

$$\text{GCE} = FV \frac{(\text{COD}_0 - \text{COD}_t)}{8It} \quad (5)$$

where  $\text{COD}_0$  and  $\text{COD}_t$  are chemical oxygen demands ( $\text{g dm}^{-3}$ ) at times  $t = 0$  (initial) and  $t$ , respectively;  $I$  is the current (A),  $F$  is Faraday's constant ( $96\,485 \text{ C mol}^{-1}$ ),  $V$  is the electrolyte volume ( $\text{dm}^3$ ), and 8 is the oxygen equivalent mass ( $\text{g eq}^{-1}$ ).

Mineralization current efficiency (MCE) for treated solutions at a given time can be calculated from total organic carbon (TOC) using the following equation:

$$\text{MCE} = \frac{\Delta(\text{TOC})_{\text{exp}}}{\Delta(\text{TOC})_{\text{theor}}} \cdot 100 \quad (6)$$

where  $\Delta(\text{TOC})_{\text{exp}}$  is experimental TOC removal and  $\Delta(\text{TOC})_{\text{theor}}$  is theoretical TOC abatement, assuming that the applied charge (=current  $\times$  time) is only consumed in the mineralization reaction.

## 2.2. Space-time Yield

Overall electrochemical oxidation capacity is expressed in terms of space-time yield ( $Y_{\text{ST}}$ ) using the following relationship:

$$Y_{\text{ST}} = \frac{a \cdot i \cdot \text{CE} \cdot M}{n \cdot F} \cdot 3600 \quad (7)$$

where  $a$  is the specific electrode area ( $\text{m}^2 \text{m}^{-3}$ ), defined as the ratio of the electrode area to the reactor volume,  $i$  is the current density ( $\text{A m}^{-2}$ ), CE is the average current efficiency,  $n$  is the number of electrons involved in the reaction,  $F$  is Faraday's constant ( $96\,485 \text{ C mol}^{-1}$ ), and  $M$  is the molar mass ( $\text{g mol}^{-1}$ ).

## 2.3. Specific Energy Consumption

The specific energy consumption ( $E_{\text{sp}}$ ), expressed in  $\text{kWh kg}_{\text{COD}}^{-1}$ , is the energy used to remove a unit mass of COD from wastewater and can be calculated using the following relationship:

$$E_{\text{sp}} = \frac{1}{3600} \cdot \frac{F \cdot V_{\text{c}}}{8 \cdot \Phi} \quad (8)$$

where  $F$  is Faraday's constant ( $96\,485 \text{ C mol}^{-1}$ ),  $V_{\text{c}}$  is the cell potential (V),  $\Phi$  is the average current efficiency, and  $8$  is the oxygen equivalent mass ( $\text{g eq}^{-1}$ ).

The cell potential  $V_{\text{c}}$  has several components:

$$V_{\text{c}} = V_{\text{TD}} + \sum |\eta| + \sum R_{\text{c}} I \quad (9)$$

where  $V_{\text{TD}}$  is the equilibrium value of the cell potential,  $\sum \eta$  is the sum of the overpotentials at the electrodes, and  $\sum R_{\text{c}} I$  is the sum of ohmic potential drops in the electrolyte, in the current feeders, and (possibly) in the separator.

## 2.4. Limiting Current Density

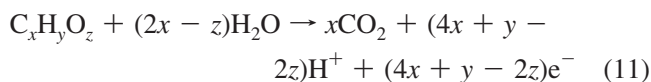
For a process under mass transport control, the maximum production rate (reactor duty) can be expressed via the limiting current density  $i_{\text{lim}}$ :

$$i_{\text{lim}} = n \cdot F \cdot k_{\text{m}} \cdot C_{\text{org}} \quad (10)$$

where  $i_{\text{lim}}$  is the limiting current density for organics oxidation ( $\text{A m}^{-2}$ ),  $n$  is the number of electrons involved in organics mineralization reaction,  $F$  is the Faraday constant ( $96\,485 \text{ C mol}^{-1}$ ),  $k_{\text{m}}$  is the mass transport coefficient ( $\text{m s}^{-1}$ ), and  $C_{\text{org}}$  is the concentration of organics in the solution ( $\text{mol m}^{-3}$ ).

However, in the case of electrooxidation of a mixture of organic compounds or of actual wastewater, it is not easy to

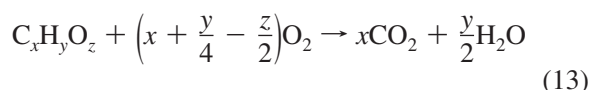
apply this equation and it is preferable to estimate limiting current density from a global parameter, such as COD. The number of exchanged electrons for the mineralization of a generic organic compound can be calculated from the following electrochemical reaction:



Replacing the value of  $n = (4x + y - 2z)$  in eq 10 we obtain:

$$i_{\text{lim}} = (4x + y - 2z) F k_{\text{m}} C_{\text{org}} \quad (12)$$

From the equation of organic compound chemical mineralization (eq 13),



it is possible to obtain the relation between organics concentration ( $C_{\text{org}}$  in  $\text{mol}_{\text{C}_x\text{H}_y\text{O}_z} \text{m}^{-3}$ ) and chemical oxygen demand (COD in  $\text{mol}_{\text{O}_2} \text{m}^{-3}$ ):

$$C_{\text{org}} = \frac{4}{(4x + y - 2z)} \text{COD} \quad (14)$$

From eqs 12 and 14, we can relate the limiting current density of electrochemical organics mineralization with the electrolyte COD (eq 15):<sup>15-17</sup>

$$i_{\text{lim}} = 4 \cdot F \cdot k_{\text{m}} \cdot \text{COD} \quad (15)$$

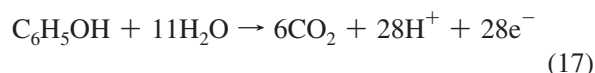
The limiting current density depends only on chemical oxygen demand ( $\text{mol}_{\text{O}_2} \text{m}^{-3}$ ) and hydrodynamic conditions. The hydrodynamic parameters of the electrochemical cell are independent of the chemical nature of the organic compound present in the electrolyte. In order to use eq 15 for a mixture of compounds, the  $k_{\text{m}}$  value of each individual component should be similar.

## 3. Direct Electrolysis

In direct electrolysis, pollutants are oxidized after adsorption on the anode surface, without involvement of any substances other than the electron, which is a "clean reagent":



In electrochemical incineration reactions, oxygen is transferred from water to the organic pollutant using electric energy. This is the so-called electrochemical oxygen transfer reaction (EOTR). A typical example of EOTR is anodic incineration of phenol (eq 17).



In this reaction, water is the source of oxygen atoms for complete phenol oxidation to  $\text{CO}_2$  at the anode of the electrolytic cell. Protons liberated in this reaction are discharged at the cathode to dihydrogen (eq 18).



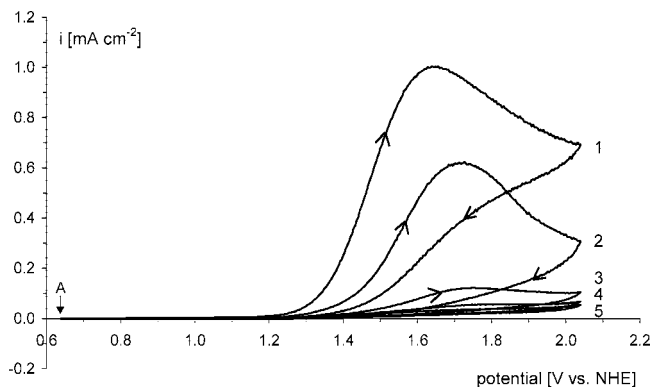


**Figure 1.** Consecutive cyclic voltammograms of 4-chlorophenol 5 mM in 1 M H<sub>2</sub>SO<sub>4</sub>: consecutive cycles 1, 2, 3, 4, and 5. Scan rate 50 mV s<sup>-1</sup>, *T* = 25 °C. (A) Anodic start of the cyclic voltammograms. Reprinted with permission from ref 15. Copyright 2001 The Electrochemical Society.

Direct electro-oxidation is theoretically possible at low potentials, before oxygen evolution, but the reaction rate usually has low kinetics, which depends on anode electrocatalytic activity. High electrochemical rates were observed using noble metals such as Pt and Pd, as well as metal oxide anodes, such as iridium dioxide, ruthenium–titanium dioxide, iridium–titanium dioxide, and lead dioxide.

However, the main problem of electro-oxidation at a fixed anodic potential before oxygen evolution is catalytic activity decrease, commonly called poisoning effect, due to the formation of a polymer layer on the anode surface.

This deactivation depends on (i) adsorption properties of the anode surface and (ii) the concentration and (iii) the nature of organic compounds and their degradation intermediates. In particular, electrocatalytic activity decrease is less pronounced with anodes with weak adsorption properties and inert surface—such as boron-doped diamond<sup>18</sup>—while it is more evident in the presence of high organic concentrations and aromatic substrates, such as phenol,<sup>19–22</sup> chlorophenols,<sup>15,23,24</sup> nitrophenols,<sup>25,26</sup> aniline<sup>27</sup> naphthol,<sup>18</sup> aromatic and aliphatic olefins,<sup>28</sup> herbicides,<sup>29</sup> hydroquinone<sup>30</sup> synthetic dyes,<sup>31–33</sup> pyridine,<sup>34</sup> and industrial wastewater containing aromatic sulfonated acids.<sup>35</sup>

For example, Rodrigo et al.<sup>15</sup> showed that 4-chlorophenol (4-CP) can be directly oxidized at the boron-doped diamond (BDD) anode working in the potential region of water stability. However, direct electron transfer reactions resulted in electrode fouling due to the formation of a polymeric film on its surface. As a matter of fact, during continuous potential cycling in a solution of 4-chlorophenol 5 mM at the BDD electrode, the anodic peak at 1.70 V vs SHE (standard hydrogen electrode) corresponding to the oxidation of 4-chlorophenol decreased with the number of cycles and completely disappeared after about 5 cycles, thus confirming electrode deactivation (Figure 1). The authors postulated that film formation during 4-CP oxidation was a consequence of the coupling of chlorophenoxy cations (or radicals), formed by the initial oxidation step:

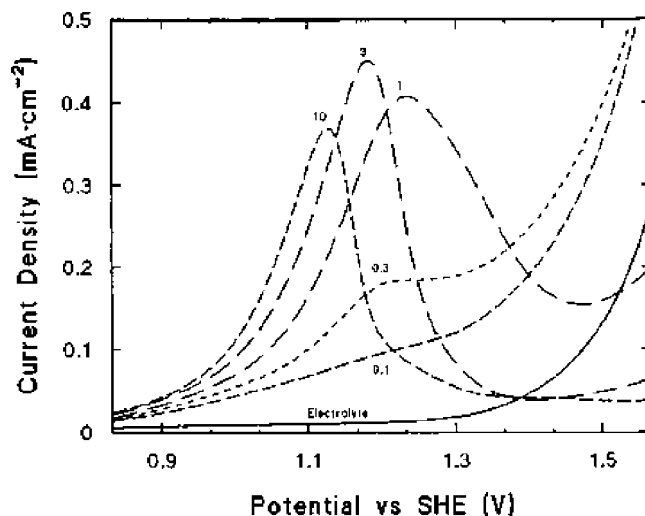
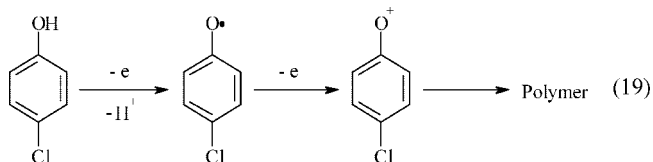


**Figure 2.** Linear sweep voltammograms for the oxidation of different concentrations (0.1–10 mM) of 4-chlorophenol at a Pt anode and pH 6. Reprinted with permission from ref 24. Copyright 1999 American Chemical Society.

This reaction mechanism for polymer formation on BDD is similar to that proposed by Gattrell and Kirk<sup>21</sup> for platinum anode deactivation during phenol oxidation.

Rodgers et al.<sup>24</sup> explored the mechanism of anode fouling by chlorinated phenols and compared structure versus reactivity for phenols differing in the extent of chlorination. At a fixed scan rate of 0.1 V s<sup>-1</sup> (Figure 2), the peak current for 4-chlorophenol was not proportional to concentration above 1 mM, and it shifted to less positive potentials as concentration increased. Simultaneously, the oxidation of water shifted to more positive potentials. This behavior is consistent with previous observations of anode fouling during bulk electrolyses of phenols,<sup>21,36</sup> and in particular, it means that a lower concentration allows more positive potentials to be reached before fouling occurs. Moreover, they observed that, during linear sweep voltammograms of more chlorinated phenols, the anodic current peak shifted to less positive potentials as the number of chlorine atoms increased, unlike what might have been intuitively expected, because highly chlorinated compounds are generally more resistant to oxidation.

The poisoning effect can be avoided by performing oxidation in the potential region of water discharge, with simultaneous oxygen evolution, or by indirect electrolysis, by generating a redox reagent in situ, as a chemical reactant to oxidize the organics.

#### 4. Oxidation via Intermediates of Oxygen Evolution

Electrochemical oxidation of organic compounds in aqueous solution can be obtained without electrode fouling, by performing the electrolysis at high anodic potentials in the region of water discharge due to the participation of intermediates of oxygen evolution. This process does not need to add oxidation catalysts to the solution and does not produce any byproducts. However, current efficiency is diminished by the secondary reaction of oxygen evolution occurring during oxidation. Generally, removal efficiency has been observed to be strictly related to operating conditions and, above all, to selected electrode materials.

Johnson et al.<sup>37–47</sup> speculated that O-transfer reactions at high anodic potential involve the production of adsorbed  $\cdot\text{OH}$

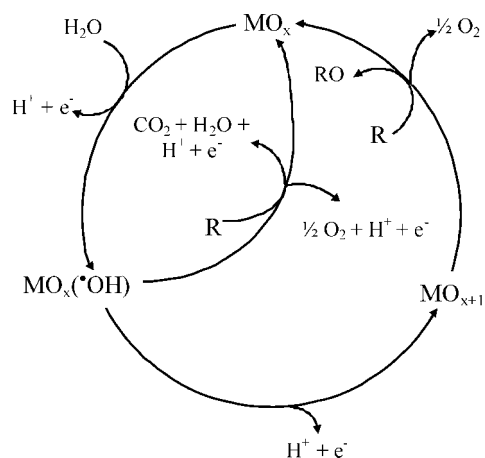
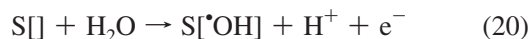


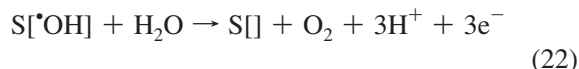
**Figure 3.** Scheme of the electrochemical oxidation of organic compounds on “active” and “nonactive” anodes. Adapted from ref 48.

radicals generated from the discharge of water:



where S represents the surface sites for adsorption of  $*OH$  species.

An inevitable but undesirable concomitant reaction is oxygen evolution through water oxidation:



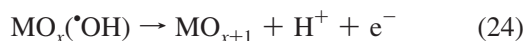
Comninellis et al.<sup>48–51</sup> found that the electrode material nature strongly influences both process selectivity and efficiency; in particular, several anodes favored partial and selective oxidation of pollutants (i.e., conversion), while others favored complete combustion to  $CO_2$ . In order to interpret these observations, they proposed a comprehensive model for oxidation of organics at metal oxide electrodes with simultaneous oxygen evolution (Figure 3).

Similar to the mechanism proposed by Johnson, the first step in oxygen transfer reaction is the discharge of water molecules to form adsorbed hydroxyl radicals:



The following steps depend on the nature of electrode materials and make it possible to distinguish between two limiting classes of electrodes, defined as “active” and “nonactive” anodes:

(a) At “active” electrodes, where higher oxidation states are available on the electrode surface, adsorbed hydroxyl radicals may interact with the anode, forming the so-called higher oxide:



The surface redox couple  $MO_{x+1}/MO_x$ , which is sometimes called chemisorbed “active oxygen”, can act as a mediator in the conversion or selective oxidation of organics on “active” electrodes:

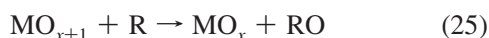
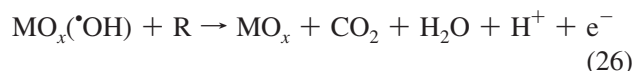


**Table 1.** Potential for Oxygen Evolution Reaction on Different anodes in  $H_2SO_4$ ; Standard Potential for Oxygen Evolution is 1.23 V vs SHE

anode	value vs SHE	conditions
$RuO_2$	1.47	0.5 M $H_2SO_4$
$IrO_2$	1.52	0.5 M $H_2SO_4$
Pt	1.6	0.5 M $H_2SO_4$
oriented pyrolytic graphite	1.7	0.5 M $H_2SO_4$
$SnO_2$	1.9	0.05 M $H_2SO_4$
$PbO_2$	1.9	1 M $H_2SO_4$
BDD	2.3	0.5 M $H_2SO_4$

(b) At “non-active” electrodes, where the formation of a higher oxide is excluded, hydroxyl radicals, called physisorbed “active oxygen”, may assist the nonselective oxidation of organics, which may result in complete combustion to  $CO_2$ :



However, both chemisorbed and the physisorbed “active oxygen” undergo a competitive side reaction, i.e., oxygen evolution, resulting in decreased anodic process efficiency.

According to this mechanism, anodes with low oxygen evolution overpotential (i.e., anodes that are good catalysts for oxygen evolution reaction), such as carbon, graphite,  $IrO_2$ ,  $RuO_2$ , or platinum (Table 1) have an “active” behavior, allowing only partial oxidation of organics, while anodes with high oxygen evolution overpotential (i.e., anodes that are poor catalysts for oxygen evolution reaction), such as antimony-doped tin oxide, lead dioxide, or boron-doped diamond (Table 1), have a “non-active” behavior and favor complete oxidation of the organics to  $CO_2$ . Therefore, they are ideal electrodes for wastewater treatment.

In practice, however, most anodes will exhibit a mixed behavior, since both parallel reaction paths participate in organic oxidation and oxygen evolution reactions.

#### 4.1. Ruthenium- and Iridium-based Oxides

Anodes made of a titanium base metal covered with a thin conducting ruthenium or iridium oxide layer—commonly called dimensionally stable anodes (DSA)—are good catalysts for chlorine and oxygen evolution, respectively. For several decades, they have been commercially used by the chlor-alkali industry and in other electrochemical processes, such as water electrolysis and metal electrowinning. Recently, DSA with a different coating composition have also been studied for applications in the oxidation of organics.<sup>18,28,32,52–58</sup> However, using these anodes, organic oxidation is expected to yield low current efficiency for complete combustion, since they favor the secondary reaction of oxygen evolution.

For example, Feng and Li<sup>52,53</sup> studied phenol oxidation on three  $RuO_2$ -based anodes and compared the results with  $PbO_2$  and Pt electrodes. As shown in Figure 4, phenol degradation performance of the three  $RuO_2$  electrodes follows the order:  $Ti/Sb-Sn-RuO_2-Gd > Ti/Sb-Sn-RuO_2 > Ti/RuO_2$ , but they are less efficient than Pt and  $PbO_2$  electrodes. At all  $RuO_2$  anodes, the aromatic ring opens and phenol is decomposed into aromatic intermediates, such as benzoquinone and hydroquinone, or several carboxylic acids, such as maleic acid, succinic acid, and oxalic acid. No full mineralization to  $CO_2$ , nor complete TOC removal, could be obtained with  $RuO_2$  anodes. This occurred only at the  $PbO_2$  anode.

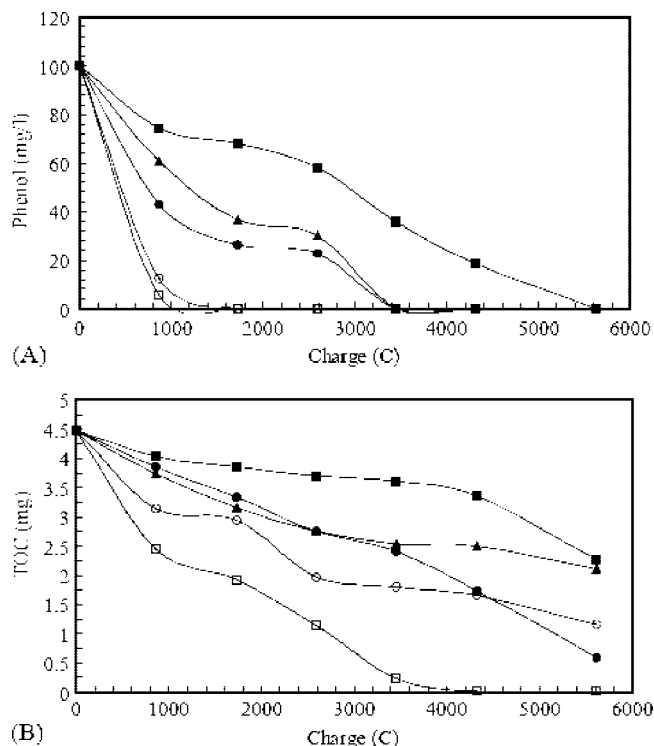


**Figure 4.** Electrochemical degradation of 100 ppm phenol in 60 mL of electrolyte as a function of charge passed for different electrode materials,  $i = 10 \text{ mA cm}^{-2}$ , (A) phenol removal; (B) TOC removal; (—■—) Ti/RuO<sub>2</sub>; (—▲—) Ti/Sb-Sn-RuO<sub>2</sub>; (—●—) Ti/Sb-Sn-RuO<sub>2</sub>-Gd; (—□—) Ti-PbO<sub>2</sub>; and (—○—) Pt. Reprinted with permission from ref 53. Copyright 2003 Elsevier.

Similar results were also obtained by Coteiro and Andrade<sup>59</sup> for 4-chlorophenol oxidation at Ti/Ru<sub>0.3</sub>Ti<sub>0.7</sub>O<sub>2</sub> and Ti/Ru<sub>0.3</sub>Sn<sub>0.7</sub>O<sub>2</sub> prepared by thermal decomposition through two different routes: inorganic precursors dissolved in isopropanol and polymeric precursors. The anodes are very promising for 4-chlorophenol degradation, although—with maximum 52% TOC removal—mineralization of the starting material is not complete. The cleavage of the aromatic ring occurred preferentially in the case of electrodes prepared by decomposition of inorganic precursors, while oxalic acid oxidation was favored on the anode prepared through decomposition of polymeric precursors.

Many studies on organic compounds oxidation with Ti/IrO<sub>2</sub> electrodes have been carried out by Cominellis' group.<sup>20,50,51,60,61</sup> At Ti/IrO<sub>2</sub> anode, detoxification of a 1,4-benzoquinone solution results in the rupture of the aromatic ring to produce aliphatic intermediates. However, these compounds are then poorly degraded<sup>61</sup> (Figure 5). Furthermore, it has been reported that isopropanol is not completely mineralized at IrO<sub>2</sub> anodes, but it is only converted to acetone as a final product with over 90% selectivity and with moderate constantly decreasing current efficiency.<sup>51</sup>

However, several authors have reported that DSA, coated with a RuO<sub>2</sub> or IrO<sub>2</sub> layer and with other oxides—owing to their chlorine evolution activity—can be effectively used for organic disposal by indirect electrolysis, generating in situ active chlorine (see section 5.2.1).

## 4.2. Platinum Anode

Platinum anodes have been used for a long time as electrode materials, because of their good conductivity and chemical stability even at high potentials. They have also

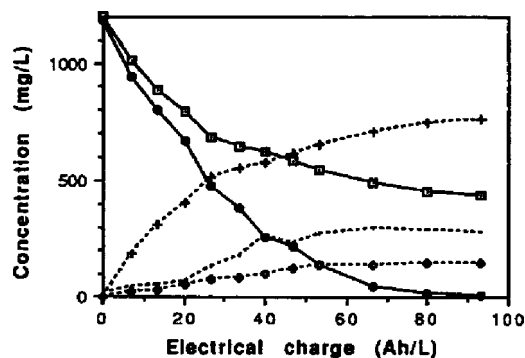


**Figure 5.** Evolution of benzoquinone, intermediates, and COD during the oxidation of benzoquinone at Ti/IrO<sub>2</sub> anodes as a function of charge: □ COD; ● benzoquinone; ◇ aliphatic acids; — others; + CO<sub>2</sub>. Reprinted with permission from ref 61. Copyright 1994 Elsevier.

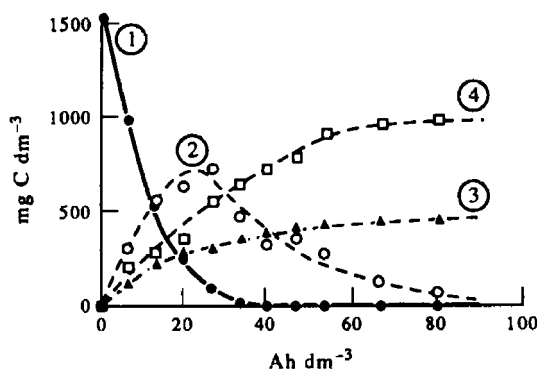


**Figure 6.** Evolution of (1) phenol; (2) aromatic intermediates; (3) aliphatic acids; and (4) CO<sub>2</sub> during oxidation of phenol at Pt anode;  $i = 50 \text{ mA cm}^{-2}$ ,  $T = 70 \text{ }^\circ\text{C}$ . Reprinted with permission from ref 48. Copyright 1994 Elsevier.

been used for oxidation of various organic pollutants, such as phenol,<sup>14,21,48,52,53</sup> chlorophenols,<sup>24,43</sup> glucose,<sup>62</sup> benzene,<sup>63</sup> hydroxybenzoic acid,<sup>64</sup> methanol and formic acid,<sup>65</sup> synthetic dyes,<sup>32</sup> herbicides,<sup>66</sup> and naphthalene-sulfonic acids.<sup>57,67</sup>

The overpotential for oxygen evolution of Pt anodes is not very high (i.e., 1.6 V vs SHE in 0.5 M H<sub>2</sub>SO<sub>4</sub>); therefore, its behavior for organic oxidation is similar to that of ruthenium- or iridium-based anodes. It permits only selective conversion of pollutants with low current efficiency for mineralization.

For example, Cominellis and Pulgarin<sup>14,48</sup> showed that phenol is oxidized at Pt anodes in two steps: at the beginning of electrolysis, aromatic intermediates (hydroquinone, catechol, benzoquinone) are formed, and in the second step the aromatic ring opens, with formation of aliphatic acids (e.g., maleic, fumaric, and oxalic acid) that are stable toward further electro-oxidation (Figure 6). Because of the formation of these intermediates, complete TOC removal cannot be obtained and current efficiency decreased during electrolysis. EOI was slightly influenced by current density and temperature, but it increased with pH and phenol concentration. However, even at pH = 12.5, EOI obtained during oxidation of 0.01 mol dm<sup>-3</sup> of phenol was only 0.143. A similar behavior for phenol oxidation was also obtained by Feng and Li,<sup>52,53</sup> that is, fast phenol concentration decrease down to zero. However, residual TOC suggests that the degradation reaction might slow down significantly for some intermediate products (Figure 4).

Torres et al.<sup>68</sup> reported that also the nature of the substituents affects electrochemical degradation of *p*-substi-

**Table 2. EOI for Several *p*-Substituted Phenols at Ti/Pt Electrodes in Acidic and Basic Media; Adapted from Ref 68**

compound	pH 2	pH 11
<i>p</i> -NO <sub>2</sub>	0.045	0.107
<i>p</i> -COOH	0.049	0.108
phenol	0.056	0.139
<i>p</i> -Cl	0.058	0.155
<i>p</i> -NH <sub>2</sub>	0.077	0.185

tuted phenols. In general, phenols with electron-donor groups (e.g., OH<sup>-</sup> and NH<sub>2</sub><sup>-</sup>) are more easily oxidized than those with electron-withdrawing groups (Table 2). Alkaline pH, high temperature, and low current increased process efficiency, but even under the best conditions and while all parent compounds degraded, no total conversion to CO<sub>2</sub> could be attained.

### 4.3. Carbon and Graphite

Carbon and graphite electrodes have been widely used for organics removal in electrochemical reactors with three-dimensional electrodes (e.g., packed bed, fluidized bed, carbon particles, porous electrode, etc.), because they are very cheap, have a large surface area, and can combine adsorption and electrochemical degradation of pollutants. However, with these materials, electro-oxidation at high potentials is generally accompanied by surface corrosion that reduces their service life.

Many types of carbon-based electrodes can be employed for the treatment of organic compounds, such as carbon felt,<sup>69,70</sup> carbon pellet,<sup>71</sup> carbon black slurry,<sup>72,73</sup> carbon fibers,<sup>74–81</sup> glassy carbon,<sup>82</sup> graphite particles,<sup>83–87</sup> and graphite Rashig rings.<sup>88</sup>

Gattrell and Kirk<sup>82</sup> studied phenol oxidation using reticulated glassy carbon anodes in a flow-by cell, and observed that, at low potential, there was a rapid reaction rate decrease, caused by the electrode surface being clogged with insoluble polymeric products that were slow to oxidize or desorb. Conversely, high temperature and high applied potentials (i.e., greater than 1.9 V vs SCE) resulted in more complete phenol oxidation but also decreased current efficiency and faster electrode corrosion. This corrosion led to loss of material and increased electrode resistance (Figure 7).

The electrochemical removal of 2-chlorophenol and 2,6-dichlorophenol from aqueous solutions using porous carbon felt<sup>70</sup> or a fixed bed of carbon pellets<sup>71</sup> in a flow cell was investigated by Polcaro's group. Both carbon-based anodes

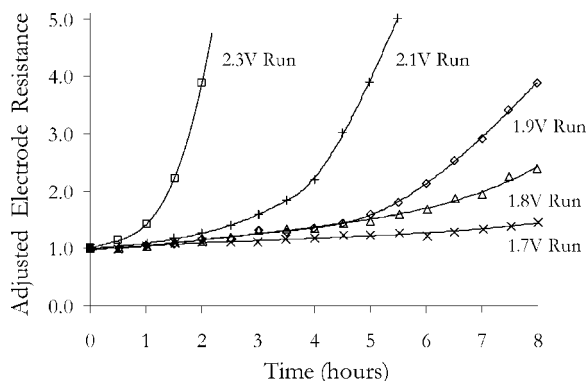


**Figure 7.** Evolution of the electrode resistance (normalized to the initial electrode resistance) as a function of time for runs at various potentials. Reprinted with permission from ref 82. Copyright 1990 John Wiley & Sons, Inc.

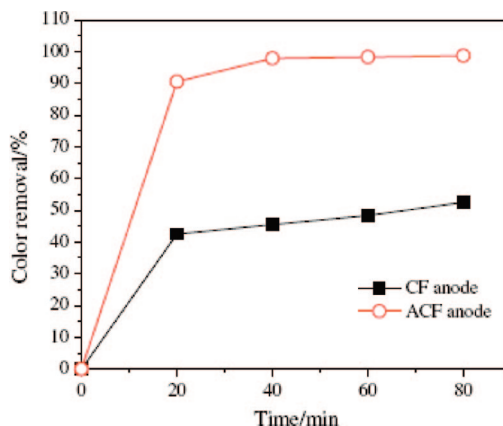


**Figure 8.** Comparison of color removal using ACF and CF anode during the oxidation of Alizarin Red S. Reprinted with permission from ref 80. Copyright 2008 Springer.

effectively removed chlorophenols, as well as their reaction intermediates. Electrolyte velocity through the electrode did not affect the reaction behavior, while the most important parameter was current density per unit electrode volume: using applied current density of 5 mA cm<sup>-2</sup> of electrode, average current efficiency values ranged from 25 to 30%. Moreover, under these conditions, they observed only low corrosion effects on anode surface, even after they had been working for several hours.

Activated carbon fibers (ACF) possess a high specific surface area, good conductivity, and excellent adsorption capability. Therefore, they have recently been used in wastewater treatment as novel three-dimensional electrodes. The potential for oxygen evolution on ACF electrode is 1.7 V, which is approximately equal to that on platinum electrode.<sup>76</sup>

Fan et al.<sup>76</sup> studied Amaranth degradation on ACF electrode under potentiostatic conditions. During the treatment of solutions containing 80 mg dm<sup>-3</sup> of dye, color removal was about 94.5%; however, COD and TOC removal ratios were about 35 and 30%, respectively, indicating that electro-oxidation with ACF can easily destroy the azo bond of the dye molecule, but it cannot completely mineralize all the intermediates.

Yi and Chen<sup>78,80</sup> studied the electrochemical treatment feasibility of Alizarin Red S dye wastewater using ACF as anode material. They observed that ACF anode is more effective for color removal than the carbon fiber anode (Figure 8), and, in particular for ACF anodes, a larger specific surface area and higher mesopore percentage could ensure a more effective electrochemical degradation of the dye. Maximum color and COD removal were about 98% and 76.5%, respectively.

### 4.4. Tin Dioxide

Pure SnO<sub>2</sub> is an n-type semiconductor with a band gap of 3.5 eV and low conductivity at room temperature; hence, it cannot be used as electrode material. However, its conductivity can be improved by doping with Ar, B, Bi, F, Cl, P, and, in particular, Sb, which is commonly used in electrochemical applications.<sup>89–92</sup>

Antimony-doped SnO<sub>2</sub> electrodes have a good conductivity and an overpotential for oxygen evolution of about 1.9 V vs SHE (i.e., 600 mV higher than Pt), which makes it attractive electrode material for anodic oxidation of organics.

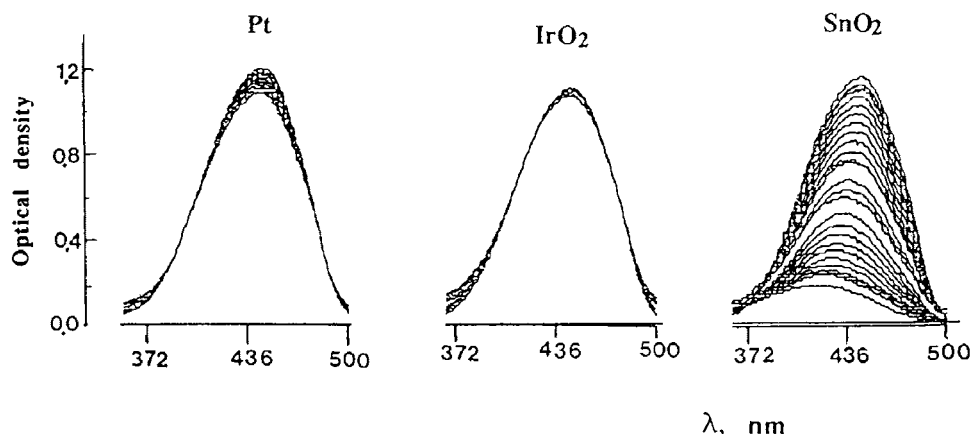


**Figure 9.** Adsorption spectra of aqueous RNO solution obtained at 5 min intervals during 2 h galvanostatic electrolysis with different anode materials:  $i = 20 \text{ mA cm}^{-2}$ ;  $\text{pH} = 7.1$ ;  $T = 25 \text{ }^\circ\text{C}$ . Reprinted with permission from ref 48. Copyright 1994 Elsevier.

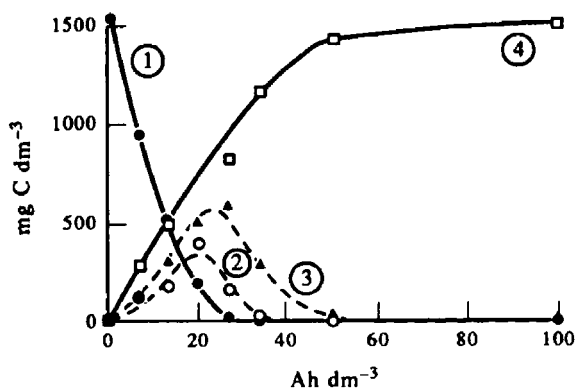


**Figure 10.** Evolution of (1) phenol; (2) aromatic intermediates; (3) aliphatic acids; and (4)  $\text{CO}_2$  during oxidation of phenol at  $\text{SnO}_2$  anode:  $i = 50 \text{ mA cm}^{-2}$ ,  $T = 70 \text{ }^\circ\text{C}$ . Reprinted with permission from ref 48. Copyright 1994 Elsevier.

The use of *N,N*-dimethyl-*p*-nitrosoaniline (RNO) as a spin trap has shown that oxygen evolution at the  $\text{SnO}_2$  electrode involves the production of  $\cdot\text{OH}$  radicals on the electrode surface, differently from  $\text{IrO}_2$  and Pt anodes (Figure 9); thus, the oxidation of organics is unselective and results in complete combustion.<sup>48</sup> In fact, Figure 9 shows that, during electrolysis of  $2 \times 10^{-5} \text{ mol dm}^{-3}$  of RNO solution with Pt and  $\text{IrO}_2$  anodes, there was only a slight decrease in the adsorption spectra at 440 nm. On the contrary, using  $\text{SnO}_2$  anode, there was a rapid decrease of optical density. These results indicated an accumulation of  $\cdot\text{OH}$  at only the  $\text{SnO}_2$  surface.

Kotz et al.<sup>93</sup> first reported the use of antimony-doped tin oxide deposited on a titanium base metal ( $\text{Ti}/\text{SnO}_2\text{-Sb}_2\text{O}_5$ ) for electrochemical wastewater treatment. Complete TOC removal of a wide range of organic compounds was obtained independently of pH, with average efficiency five times higher than with Pt anodes (Table 3).

Similar results were also obtained by Cominellis and Pulgarin<sup>48,94</sup> and by Li et al.<sup>52</sup> for phenol oxidation. EOI achieved with a  $\text{SnO}_2$  anode (EOI = 0.25) was much higher than the value obtained with a Pt anode (EOI = 0.10), because  $\text{SnO}_2$  enabled a rapid removal of phenol oxidation intermediates, mainly aliphatic acids (Figure 10), which, on the contrary, were practically inactive on Pt anodes (Figure 6).

Many other papers demonstrated the great potential of  $\text{SnO}_2$  for wastewater treatment;<sup>61,95–106</sup> however, these electrodes are not currently commercially available, because of

**Table 3. Electrochemical Oxidation Index Obtained for the Oxidation of Various Organic Compounds at Pt and  $\text{SnO}_2$  Anode; Adapted from Ref 93**

organic species	initial electrochemical oxidation index (EOI)	
	platinum anode	$\text{SnO}_2\text{-Sb}_2\text{O}_5$ anode
ethanol	0.02	0.49
acetone	0.02	0.21
acetic acid	0.00	0.09
formic acid	0.01	0.05
oxalic acid	0.01	0.05
malonic acid	0.01	0.21
maleic acid	0.00	0.15
benzoic acid	0.10	0.79
naphthalene-2-sulfonic acid	0.04	0.51
phenol	0.15	0.6
EDTA	0.30	0.30
	Average=0.05	Average=0.34

their short service life—a major drawback.<sup>107,108</sup> Therefore, these anodes are under investigation in many laboratories for further improvement.

The addition of an  $\text{IrO}_2$  interlayer between the Ti substrate and the  $\text{SnO}_2\text{-Sb}_2\text{O}_5$  coating has been demonstrated to strongly increase anode service life (by about 2 orders of magnitude) due to the isomorphous structure of  $\text{IrO}_2$  with  $\text{TiO}_2$  and  $\text{SnO}_2$ .<sup>102,108</sup> However, onset potential for oxygen evolution of  $\text{Ti}/\text{IrO}_2/\text{SnO}_2$  lies between those of  $\text{Ti}/\text{IrO}_2$  and  $\text{Ti}/\text{SnO}_2\text{-Sb}_2\text{O}_5$  and depends on  $\text{IrO}_2$  interlayer thickness: the thicker the layer, the lower is its onset potential.

Zanta et al.<sup>102</sup> reported that, in the case of a high  $\text{SnO}_2\text{-Sb}_2\text{O}_5$  coating relative to the  $\text{IrO}_2$  interlayer loading (i.e., 20–30%), electrode service life can be increased without significantly affecting the electrode ability to carry out *p*-CP oxidation. Anode potential evolution, *p*-CP concentration, and TOC during *p*-CP oxidation are shown in Figure 11 for a  $\text{SnO}_2\text{-Sb}_2\text{O}_5$  with and without  $\text{IrO}_2$  interlayer. The presence of an  $\text{IrO}_2$  interlayer decreases the electrode potential and allows operation at constant potential during almost the entire process, thus indicating a higher stability. Conversely,  $\text{Ti}/\text{SnO}_2\text{-Sb}_2\text{O}_5$  electrode anode potential rapidly increases after  $150 \text{ Ah dm}^{-3}$ , thus indicating electrode deactivation. Furthermore, both electrodes behave similarly toward *p*-CP oxidation and TOC removal, suggesting that organic oxidation at the  $\text{Ti}/\text{IrO}_2/\text{SnO}_2\text{-Sb}_2\text{O}_5$  electrode occurs only through the  $\text{SnO}_2\text{-Sb}_2\text{O}_5$  component without  $\text{IrO}_2$  interlayer interference.

Other authors have also demonstrated that the addition of platinum to  $\text{SnO}_2\text{-Sb}_2\text{O}_5$  electrodes increased their stability,



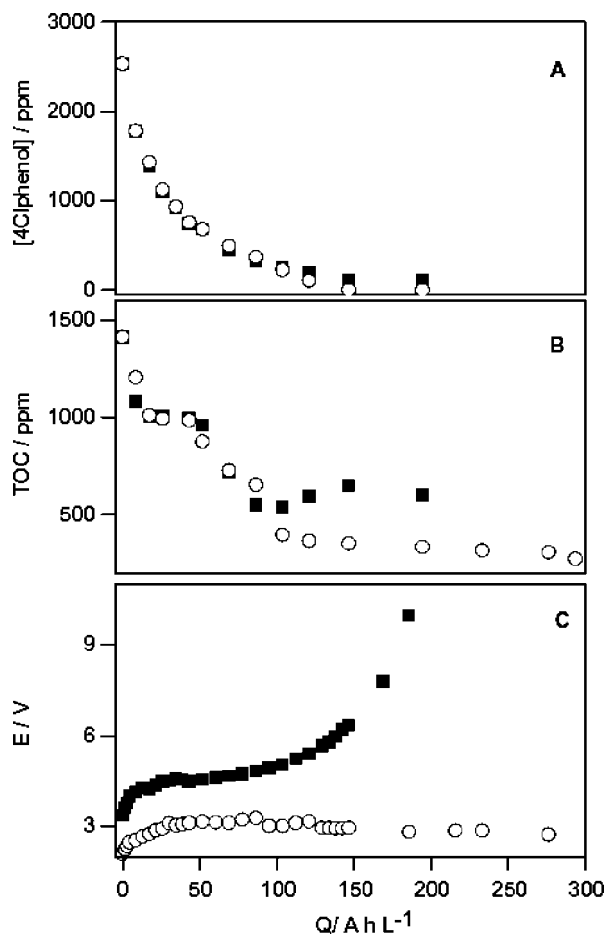


**Figure 11.** (A) *p*-CP concentration, (B) TOC, and (C) anode potential as a function of specific anodic charge (○) Ti/IrO<sub>2</sub>/SnO<sub>2</sub>-Sb<sub>2</sub>O<sub>3</sub> and (■) Ti/SnO<sub>2</sub>-Sb<sub>2</sub>O<sub>3</sub>. Conditions: *i* = 30 mA cm<sup>-2</sup>, *T* = 30 °C. Reprinted with permission from ref 102. Copyright 2003 Springer.

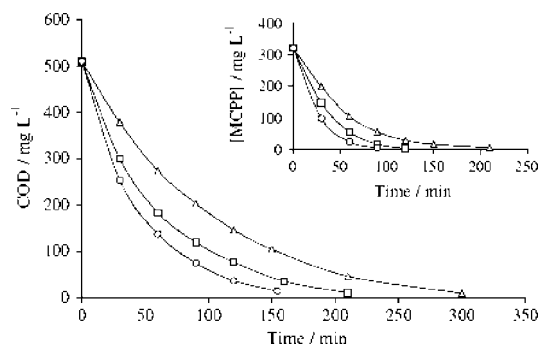


**Figure 12.** Effect of temperature on the evolution of COD and MCPP concentration with time during the electrolyses of 320 mg dm<sup>-3</sup> of MCPP in 0.05 M Na<sub>2</sub>SO<sub>4</sub> using the PbO<sub>2</sub> anode. Flowrate = 300 dm<sup>3</sup> h<sup>-1</sup>; *i* = 40 mA cm<sup>-2</sup>; *T*: (Δ) 25 °C; (□) 40 °C; (○) 50 °C. Reprinted with permission from ref 135. Copyright 2008 Springer.

but oxidation efficiency of the composite Pt-SnO<sub>2</sub> electrodes is even lower than those of pure Pt electrodes.<sup>62</sup>

#### 4.5. Lead Dioxide

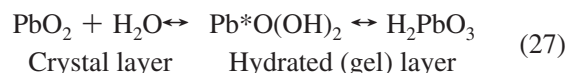
Lead dioxide anodes are inexpensive and easy to prepare, with good conductivity, chemical stability, and a large area. Hence, they have wide industrial applications. Moreover, there is a great interest in the development of PbO<sub>2</sub> anodes for the oxidation of organics, because of their large over-

potential for oxygen evolution in acidic media, which enables the production of hydroxyl radicals during water discharge.

Evidence for active hydroxyl radical generation on the PbO<sub>2</sub> surface has been shown by electron spin resonance spectroscopy (ESR) using 5,5-dimethyl-1-pyrroline-*N*-oxide (DMPO) as spin trapping agent,<sup>109</sup> by high-performance liquid chromatography (HPLC) using salicylic acid as spin trap agent,<sup>110</sup> or by UV absorbance using *N,N*-dimethyl-*p*-nitrosoaniline (RNO) as spin trap agent.<sup>60</sup> The mechanism for hydroxyl radical generation and the electrochemical reactions that occur at the PbO<sub>2</sub> electrode during organic oxidation are still difficult to understand, and no final conclusions have so far been drawn.

As mentioned above (eqs 20–22), Johnson and co-workers<sup>37–47</sup> speculated that the O-transfer step occurs from adsorbed hydroxyl radicals generated by water discharge at PbO<sub>2</sub> sites and adsorbed reactant species.

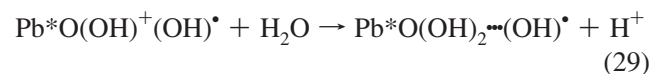
Pavlov et al.<sup>111,112</sup> proposed a more complex mechanism that interpreted the electrochemical processes taking place during oxygen evolution in the light of the gel-crystal structure of the PbO<sub>2</sub> layer. There is an equilibrium between crystal zones, made of PbO<sub>2</sub> exhibiting electron conductivity, and gel zones, composed of hydrated lead dioxide, PbO(OH)<sub>2</sub>, that forms linear polymer chains with electron and proton conductivity:



Pb\*O(OH)<sub>2</sub> is an active center located in the hydrous layer. Upon anodic polarization, an electrochemical reaction is triggered in the active centers:



Electrons move along the polymer chains and reach the crystal zones, as a result of which electric current passes through the electrode. The active centers are charged positively. Their electric charge is neutralized through the following chemical reaction:



where “⋯” is the connection between •OH radical and active center. Therefore, as a result of reaction 29, the active centers contain •OH that could break away from the active centers and react with the contaminants in the solution.

Thanks to the effective production of •OH radicals, PbO<sub>2</sub> is expected to perform quite well for organics mineralization. For this reason, it has been used for the oxidation of several compounds such as phenol,<sup>113–119</sup> chlorophenol,<sup>99,120–122</sup> nitrophenol,<sup>123,124</sup> methoxyphenol,<sup>125</sup> dichloroethane,<sup>126</sup> aniline,<sup>127</sup> naphthol,<sup>56</sup> benzoquinone<sup>41,128</sup> maleic acid,<sup>128</sup> chloroanilic acid,<sup>60</sup> oxalic acid,<sup>129,130</sup> glucose,<sup>62</sup> synthetic dyes,<sup>32,131,132</sup> indoles,<sup>133</sup> 4-chloroguaiacol,<sup>134</sup> herbicides and pesticides,<sup>135,136</sup> landfill leachate,<sup>98</sup> tannery wastewater,<sup>137</sup> and anionic surfactants.<sup>138</sup>

Early papers<sup>113,114</sup> studied phenol oxidation using a packed-bed reactor with PbO<sub>2</sub> pellets. Greater conversion to CO<sub>2</sub> was achieved with high current, temperature, dissolved oxygen, and low phenol concentration.

Phenol electrochemical oxidation was also widely studied by Tahar and Savall<sup>116–118</sup> using Ta/PbO<sub>2</sub> anodes. Phenol and its intermediates (benzoquinone, maleic and fumaric

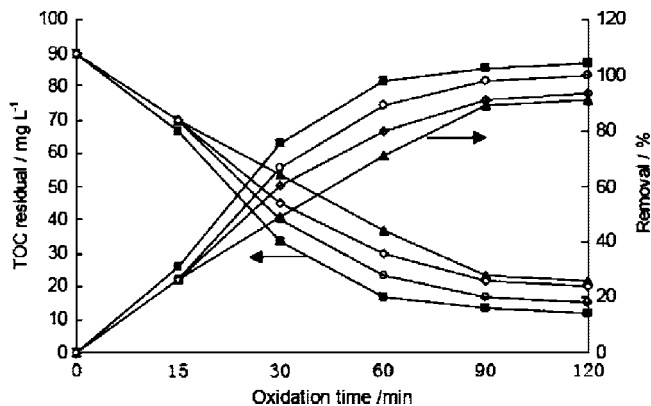


**Figure 13.** Variation of TOC amounts of *o*-nitrophenol (ONP) with time on different PbO<sub>2</sub> electrodes: (—■—) Ti/Bi–PbO<sub>2</sub>; (—▲—) Ti/Co–PbO<sub>2</sub>; (—○—) Ti/Co–Bi–PbO<sub>2</sub>; (—□—) Ti/PbO<sub>2</sub>, [ONP]<sub>0</sub> = 50 mg dm<sup>-3</sup>; *i* = 30 mA cm<sup>-2</sup>. Reprinted with permission from ref 124. Copyright 2008 Springer.

acids) were completely eliminated through the intermediation of hydroxyl radicals adsorbed at the active site of the electrode. An increase in initial phenol concentration and decrease in applied current improves the faradic yield by favoring oxidation reactions of organics at the expense of competitive O<sub>2</sub> evolution. They also observed that a temperature increase from 60 to 90 °C favored phenol oxidation. Looking at activation energy (i.e., 19 kJ mol<sup>-1</sup>), they speculated that probably the limiting step is not thermal but rather of a diffusional nature.

Recently, Panizza et al.<sup>135</sup> studied the influence of the main operating parameters—such as current density, hydrodynamic conditions, pH, and temperature—on Mecoprop herbicide (MCP) oxidation in Na<sub>2</sub>SO<sub>4</sub>. Within the studied range, total mineralization (>97% COD abatement) of MCP was obtained, regardless of operating conditions. In agreement with Tahar and Savall<sup>116–118</sup> and other authors,<sup>42,62,113,114,123</sup> they reported that temperature increase resulted in an increase of COD and MCP removal (Figure 12). However, they explained this behavior in terms of electrogeneration of inorganic oxidizing agents. Actually, it has been demonstrated<sup>139,140</sup> that ozone can be formed during electrolyses with PbO<sub>2</sub> electrodes at high potentials:



These reagents are known to be powerful oxidants that can act as mediators for organics oxidation. The oxidation rate of organic compounds with ozone, hydrogen peroxide, and all oxidants as a whole increases with temperature. They

also reported that Mecoprop decay kinetics follows a pseudo-first-order reaction, and the rate constant increases with current density and recycle flow rate, while it is almost unaffected by solution pH.<sup>135</sup>

The electrochemical properties of electrodeposited PbO<sub>2</sub> as well as its stability are strongly affected by the crystal structure and the incorporation of doping species such as Fe, Co, Bi, F, etc. Abaci et al.<sup>141</sup> observed that highly crystalline β-PbO<sub>2</sub> films had stronger performance on phenol degradation, thanks to a porous structure that provides an enhanced active surface area, increasing the formation of ·OH and favoring the anodic oxidation process.

Johnson's group<sup>37,39</sup> showed that the electrocatalytic properties and fouling resistance of PbO<sub>2</sub> film electrodes were enhanced by the incorporation in the films of metallic species, such as Fe, Bi, or As. For example, current efficiency for electrochemical incineration of 10 mM of benzoquinone at 10 mA cm<sup>-2</sup> increased from 7.4% to 23.5%, when the PbO<sub>2</sub> anode was replaced with a Fe–PbO<sub>2</sub> one.

The electrochemical performance of pure PbO<sub>2</sub> or F-, Fe-, Co-, Fe,F-, and Co,F-doped PbO<sub>2</sub> electrodes in the oxidation of simulated wastewaters containing Blue Reactive 19 dye or phenol using a filter-press reactor was investigated by Andrade et al.<sup>119,131</sup> TOC reduction during Blue Reactive 19 dye oxidation<sup>131</sup> was greater for the PbO<sub>2</sub>–Fe,F electrode obtained from an electrodeposition bath containing 1 mM Fe<sup>3+</sup> and 30 mM F<sup>-</sup>. For phenol oxidation,<sup>119</sup> the best results were attained with PbO<sub>2</sub> electrodes doped with a low-Co content (1 mM Co<sup>2+</sup> in the electrolytic bath) along with F<sup>-</sup>: COD and TOC of simulated wastewaters were removed by about 75% and 50%, respectively (Table 4).

Liu et al.<sup>124</sup> characterized various kinds of PbO<sub>2</sub> electrodes doped with Bi and/or Co oxide in terms of their morphological (SEM) and structural (XRD) features and electrocatalytic activity for *o*-nitrophenol oxidation. The Ti/Bi–PbO<sub>2</sub> electrode has the highest TOC removal of *o*-nitrophenol (87.0%), followed by Ti/Co–Bi–PbO<sub>2</sub>, Ti/β-PbO<sub>2</sub>, and Ti/Co–PbO<sub>2</sub>, whose TOC removal rates are 83.3%, 77.8%, and 75.9%, respectively (Figure 13). They associated the good electrocatalytic activity of the Ti/Bi–PbO<sub>2</sub> electrode with the doping manner of Bi atoms in PbO<sub>2</sub>. Bi doping diminished the size of the crystal particles, thus increasing the specific surface area and resulting in crystal cell expansion and structure defects. These two factors increased the active sites on the surface of the PbO<sub>2</sub> electrode, making it more conducive to the generation of hydroxyl radicals, so as to enhance the electrocatalytic activity of this electrode.

Conversely, other authors<sup>117</sup> reported that a pure PbO<sub>2</sub> anode is more efficient than perchlorate- or bismuth-doped lead dioxide for complete phenol combustion. Although phenol is oxidized at the same rate on the three deposits,

**Table 4.** Reaction Apparent Rate Constant (*k*<sub>ap</sub>), Apparent Mass Transport Coefficient (*k*<sub>m</sub>), Compounds' Concentrations, COD and TOC Removals, Average Current Efficiencies (ACE), and Energy Consumptions (EC) in the Electrolysis (100 mA cm<sup>-2</sup>) of a Simulated Phenol Wastewater (1000 mg dm<sup>-3</sup> Phenol) Using Pure and Co,F-doped PbO<sub>2</sub> Electrodes (Adapted from Ref 119. Copyright 2008 Elsevier.)

	pure PbO <sub>2</sub>	1 mM Co,F-doped PbO <sub>2</sub>	5 mM Co,F-doped PbO <sub>2</sub>
<i>k</i> <sub>ap</sub> (h <sup>-1</sup> )	3.32	1.98	3.21
[benzoquinone] (mg dm <sup>-3</sup> )	43.1	82.2	182.0
[hydroquinone] (mg dm <sup>-3</sup> )	2.2	3.9	19.0
[fumaric acid] (mg dm <sup>-3</sup> )	8.65	2.86	26.8
COD removal (%)	63.4	75.4	48.8
TOC removal (%)	43.4	50.7	36.6
ACE (%)	14.6	18.2	11.6
EC (kWh kg <sub>COD</sub> <sup>-1</sup> )	132	105	165

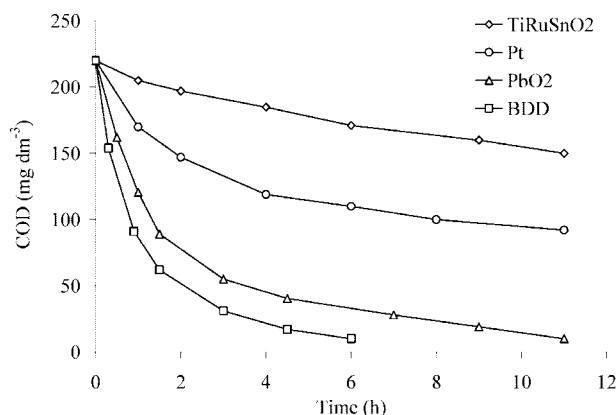


**Figure 14.** Comparison of the trend of COD during the oxidation of 200 mg dm<sup>-3</sup> of Methyl Red in 0.5 M Na<sub>2</sub>SO<sub>4</sub> at different anodes. Conditions:  $I = 500$  mA; flow rate = 180 dm<sup>3</sup> h<sup>-1</sup>. Reprinted with permission from ref 32. Copyright 2007 Elsevier.

perchlorate-doped PbO<sub>2</sub> and Bi<sub>2</sub>O<sub>5</sub>-PbO<sub>2</sub> required more charge for intermediates mineralization to CO<sub>2</sub>. In particular, the higher the degree of doping, the more difficult it is to completely remove TOC from the solution.

Many papers compared the performance of PbO<sub>2</sub> anodes with other electrode materials for the oxidation of several organic compounds.<sup>18,56,60,62,98,99,117,120,126,129,130,132,136,138</sup> For almost all pollutants, PbO<sub>2</sub> permits faster mineralization than Pt, iridium oxide, ruthenium oxide, and doped-SnO<sub>2</sub>, but it is less efficient than BDD anodes under the same operating conditions. To explain this behavior, Gherardini et al.<sup>120</sup> speculated that on PbO<sub>2</sub>, which has a hydrated surface, hydroxyl radicals are more strongly adsorbed and, consequently, less reactive than on BDD, which has an inert surface with weak adsorption properties.

For example, Bonfatti et al.<sup>62</sup> studied the electrochemical incineration of glucose and its metabolites (gluconic and glucaric acid) at Pt, SnO<sub>2</sub>, and PbO<sub>2</sub> electrodes, at different current densities and temperature values. Larger EOI values were found at PbO<sub>2</sub> electrodes under all conditions of current density and temperature.

Panizza and Cerisola<sup>32</sup> studied the influence of electrode materials (i.e., platinum, boron-doped diamond, lead dioxide, and Ti-Ru-Sn ternary oxide) for Methylene Red electrochemical oxidation and reported that Pt and TiRuSnO<sub>2</sub> electrodes permit only partial dye oxidation, but no complete mineralization, while complete COD and color removal is achieved using lead dioxide and BDD. In particular, a faster oxidation rate is achieved using BDD (Figure 14).

Similar results were also obtained by Huitle et al.<sup>136</sup> during the oxidation of methamidophos (MMD), a highly toxic pesticide, on Pb/PbO<sub>2</sub>, Ti/SnO<sub>2</sub>, and Si/BDD. Under galvanostatic conditions, electrode material performance is influenced by pH and current density, but under all conditions, the current efficiency for MMD removal follows the sequence BDD > PbO<sub>2</sub> > SnO<sub>2</sub>.

It is reported that PbO<sub>2</sub> has the same performance as BDD only during oxalic acid incineration, because this compound has a strong interaction with Pb(IV) sites that promote anodic oxidation.<sup>129,130</sup> However, despite their high removal ability of organic pollutants and low price, the major drawback of PbO<sub>2</sub> anodes is the likely release of toxic ions, especially in basic solutions. In fact, lead ions can damage nervous connections and cause blood and brain disorders. These effects limit the practical application of PbO<sub>2</sub> anodes in wastewater treatment. Other materials, which are nontoxic

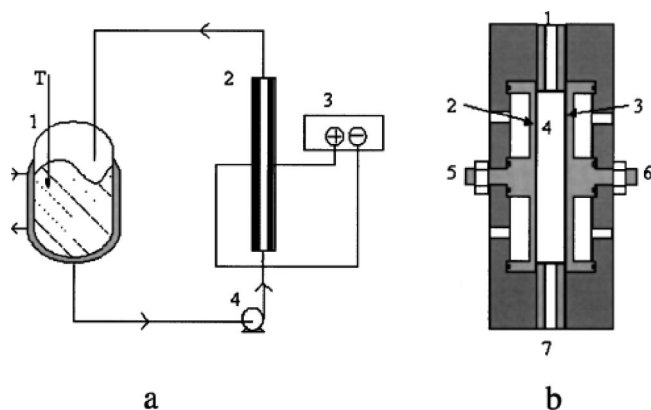


**Figure 15.** Electrochemical cell for bulk oxidation of organics on diamond electrode. (a) Setup used: 1, thermoregulated reservoir; 2, electrochemical cell; 3, power supply; 4, pump. (b) Electrochemical cell: 1, outlet; 2, anode; 3, cathode; 4, electrolysis compartment; 5 and 6, electrical contacts; 7, inlet.

or do not dissolve, may be much more preferable to such inexpensive electrodes which are, however, quite toxic themselves.<sup>128</sup>

#### 4.6. Boron-Doped Diamond (BDD)

Synthetic boron-doped diamond (BDD) thin film is a new electrode material that has recently received great attention, thanks to the development of technologies for synthesizing high-quality conducting diamond films at a commercially feasible deposition rate.<sup>142-147</sup> Diamond films are grown on nondiamond materials, usually silicon, tungsten, molybdenum, titanium, niobium, tantalum, or glassy carbon, by energy-assisted (plasma or hot-filament) chemical vapor deposition. In order to make diamond films conducting, they are doped with different concentrations of boron atoms. The doping level of boron in the diamond layer expressed as B/C ratio is about 1 000–10 000 ppm. High-quality BDD electrodes possess several technologically important properties that distinguish them from conventional electrodes, such as

- An extremely wide potential window in aqueous and nonaqueous electrolytes: in the case of high-quality diamond, hydrogen evolution commences at about  $-1.25$  V vs SHE and oxygen evolution commences at  $+2.3$  V vs SHE; therefore, the potential window may exceed 3 V.<sup>148</sup>
- Corrosion stability in very aggressive media: diamond electrode morphology is stable during long-term cycling from hydrogen to oxygen evolution, even in acidic fluoride media.<sup>149</sup>
- Inert surface with low adsorption properties and strong tendency to resist deactivation: the voltammetric response toward ferri/ferrocyanide is remarkably stable for up to two weeks of continuous potential cycling.<sup>150</sup>
- Very low double-layer capacitance and background current: the diamond–electrolyte interface is ideally polarizable and the current between  $-1000$  and  $+1000$  mV vs SCE is  $<50$   $\mu\text{A cm}^{-2}$ . Double-layer capacitance is by 1 order of magnitude lower than that of glassy carbon.<sup>151</sup>

Thanks to these properties, during electrolysis in the region of water discharge, BDD anodes promote the production of weakly adsorbed hydroxyl radicals, which unselectively and completely mineralize organic pollutants with a high current efficiency:





Experiments conducted to confirm this mechanism, using 5,5-dimethyl-1-pyrroline-*N*-oxide (DMPO) and salicylic acid as spin trapping, demonstrated that the oxidation process on BDD electrodes involves hydroxyl radicals as electrogenerated intermediates.<sup>152</sup>

So far, the number of laboratories investigating this material for wastewater treatment and the number of related publications have rapidly increased during the last two decades.<sup>12,153,154</sup> Many papers have demonstrated that BDD anodes allow complete mineralization—up to near 100% current efficiency—of a large number of organic pollutants, such as carboxylic acids,<sup>155–160</sup> benzoic acid,<sup>161,162</sup> cyanides,<sup>163,164</sup> cresols,<sup>165</sup> herbicides,<sup>29,66,166–169</sup> drugs,<sup>170</sup> naphthol,<sup>16,56</sup> phenolic compounds,<sup>19,26,171–187</sup> polyhydroxybenzenes,<sup>188</sup> polyacrylates,<sup>189</sup> surfactants,<sup>138,190–192</sup> and real wastewaters.<sup>35,193–198</sup> The experimental conditions and some results of the most relevant research on this electrode material are summarized in Table 5.

Comninellis and co-workers<sup>15,16,22,34,120,155,161,163,189</sup> investigated the behavior of Si/BDD anodes for the oxidation of a wide range of pollutants using an undivided electrolytic flow cell illustrated in Figure 15. They observed that, independently of organic pollutant nature, current efficiency and the amount of intermediates were affected by local concentration of  $\cdot\text{OH}$  relative to organics concentration on the anode surface. In particular, for high organic concentrations or low current densities, COD decreased linearly, forming a large amount of intermediates, while ICE remained

about 100%, indicating a kinetically controlled process. Conversely, for low organic concentrations or high current densities, pollutants were directly mineralized to  $\text{CO}_2$  but ICE was below 100%, due to mass transport limitation and side reactions of oxygen evolution. For example, Figure 16 shows COD and ICE trends during electrochemical oxidation of different concentrations of naphthol. In order to describe these results, the authors developed a comprehensive kinetic model to predict COD trends and current efficiency for the electrochemical combustion of the organic with BDD electrodes, as well as to estimate energy consumption during the process.<sup>16,17,120,199</sup> The model, developed for an electrochemical reactor operating in a batch recirculation mode under galvanostatic conditions, was formulated on limiting current density estimates from COD value using eq 15.

Depending on applied current density ( $i_{\text{appl}}$ ) with respect to limiting current density ( $i_{\text{lim}}$ ), which decreased during treatment, two different operating regimes were identified:

- $i_{\text{appl}} < i_{\text{lim}}$ : When the applied current was low or the concentration of the organics was sufficiently high, electrolysis was under current limited control, current efficiency was 100% and COD decreased linearly over time.
- $i_{\text{appl}} > i_{\text{lim}}$ : When the applied current was high or the concentration of the organics was low, electrolysis was under mass-transport control and secondary reactions (such as oxygen evolution) commenced, resulting in current efficiency decrease. In this regime, COD removal, due to mass-transport limitation, followed an exponential trend.

A graphical representation of the proposed kinetic model and the equations that describe the trends over time of COD

**Table 5. Some Examples of Organic Compounds Oxidized on Diamond Electrodes**

pollutant	experimental conditions	remarks	ref
carboxylic acids	$i = 30 \text{ mA cm}^{-2}$ ; $T = 30 \text{ }^\circ\text{C}$ ; 1 M $\text{H}_2\text{SO}_4$	average current efficiency: 70–90%	155–158
benzoic acid	$i = 7\text{--}36 \text{ mA cm}^{-2}$ ; 0.5 M $\text{HClO}_4$	oxidation intermediates: salicylic acid, hydroquinone, hydroxybenzoic acid	161, 162
cyanides	$i = 36 \text{ mA cm}^{-2}$ ; 1 M KCN + 1 M KOH	95% of $\text{CN}^-$ elimination after passage of 220 Ah/l	163, 164
<i>o</i> - and <i>p</i> -cresol	$27\,129 \leq Re \leq 42\,631$ , $i = 15\text{--}60 \text{ mA cm}^{-2}$	<i>o</i> -cresol is more recalcitrant than <i>p</i> -cresol	165
herbicides	$i = 30\text{--}150 \text{ mA cm}^{-2}$ ; pH = 2–12, $T = 15\text{--}60 \text{ }^\circ\text{C}$	herbicides decay follows a pseudo-first-order kinetics	29, 66, 166–170
naphthol	$i = 15\text{--}75 \text{ mA cm}^{-2}$ ; $T = 30\text{--}60 \text{ }^\circ\text{C}$ , 1 M $\text{H}_2\text{SO}_4$	efficiency increases with naphthol concentration	16, 56
phenol	flow-cell, batch one compartment cell, bipolar trickle tower reactor	microwave and ultrasound enhanced phenol oxidation	171–175
phenols, chlorophenols, and nitrophenols	$i = 15\text{--}60 \text{ mA cm}^{-2}$ ; 5000 mg/L $\text{Na}_2\text{SO}_4$ or 1 M $\text{H}_2\text{SO}_4$	without diffusion limitation the current efficiency is 100%	19, 25, 26, 176–182
phenolic compounds and Triazines	$i = 50 \text{ mA cm}^{-2}$ ; impinging cell	efficiency of 100% up to the near-complete mineralization	183–185
mixture of phenols	$i = 30 \text{ mA cm}^{-2}$ ; 0.1 M $\text{Na}_2\text{CO}_3$	model proposed for the degradation of mixture of organics	186, 187
polyhydroxybenzenes	$i = 15\text{--}60 \text{ mA cm}^{-2}$	influence of temperature, pH and, supporting media was studied	188
polyacrylates	$i = 1\text{--}30 \text{ mA cm}^{-2}$ ; 1 M $\text{HClO}_4$	initial current efficiency 100%	189
surfactants	$i = 4\text{--}30 \text{ mA cm}^{-2}$ ; SDBS = 25–300 mg $\text{dm}^{-3}$	complete removal of COD and TOC	138, 190–192
tridecane dicarboxylic acid wastewater	$E = 1.6\text{--}5 \text{ V}$ , pH = 3.4–8.26, COD about 10 000 mg $\text{dm}^{-3}$	COD removal rate 99%, specific energy consumption 6.4 kWh $\text{kg}_{\text{COD}}^{-1}$ .	159
malic acid, EDTA, and triethanolamine	$i = 7\text{--}36 \text{ mA cm}^{-2}$ ; initial COD 1500–8000 mg $\text{dm}^{-3}$	current efficiency of 85–100%	160
olive mill wastewater	$T = 25 \text{ }^\circ\text{C}$ ; $i = 30 \text{ mA cm}^{-2}$	complete mineralization with high efficiency	193–195
effluent of a fine chemical plant	$i = 150\text{--}600 \text{ A m}^{-2}$ ; pH = 2–12; $T = 25\text{--}60 \text{ }^\circ\text{C}$	efficiencies of the process depend on the pH and the temperature	196
Ink-manufacturing process wastewater	$i = 15\text{--}60 \text{ mA cm}^{-2}$ ; $T = 25\text{--}60 \text{ }^\circ\text{C}$	Oxidation favored by the formation of electrogenerated oxidants.	197
wastewater from the automotive industry	initial COD > 2500 mg $\text{dm}^{-3}$	current efficiency > 90% for COD values higher 500 mg $\text{dm}^{-3}$ .	198
industrial effluent	$i = 20\text{--}60 \text{ mA cm}^{-2}$ ; $Q = 60\text{--}180 \text{ dm}^3 \text{ h}^{-1}$ .	total mineralization of the aromatic sulphonated acids	35

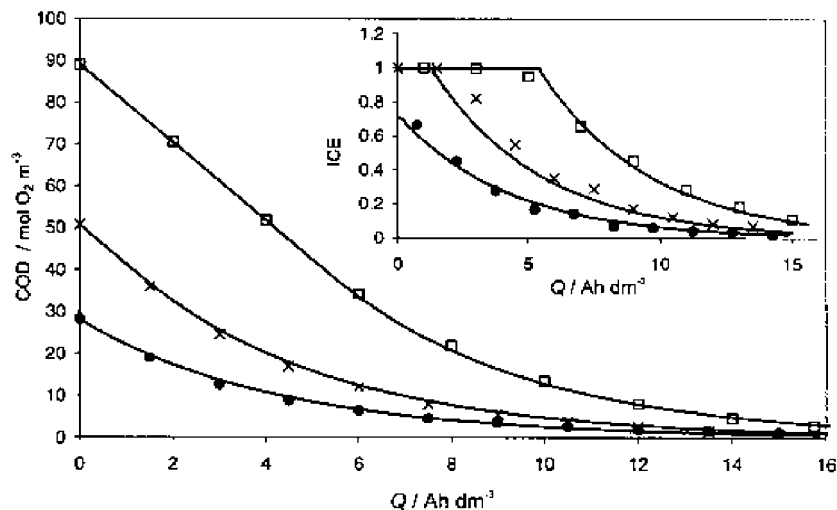


**Figure 16.** Influence of 2-naphthol concentration on the evolution of COD and ICE (inset) with the specific electrical charge passed during the electrolyses on boron-doped diamond anode. Conditions:  $T = 30\text{ }^{\circ}\text{C}$ ; applied current density  $i = 30\text{ mA cm}^{-2}$ ; initial 2-naphthol concentration: ( $\square$ ) 9 mM; ( $\times$ ) 5 mM; ( $\bullet$ ) 2 mM. The solid lines represent model prediction. Reprinted with permission from ref 16. Copyright 2001 Elsevier.

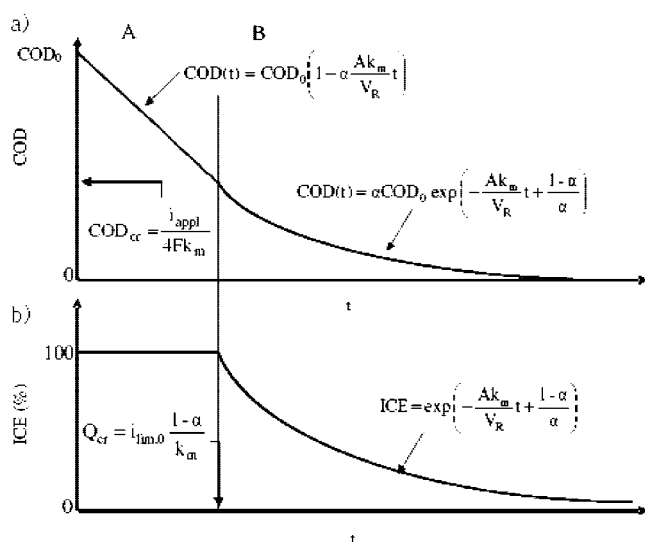


**Figure 17.** Evolution of (a) COD and (b) ICE as a function of time (or specific charge); (A) represents the charge transport control; (B) represents the mass transport control.

and ICE in both regimes are given in Figure 17. The main advantage of this model is that it does not include any adjustable parameters. Hence, the system behavior can be predicted if the experimental conditions (applied current intensity, organic concentration, and mass-transfer coefficient) are known. The model was applied to the electrochemical treatment of solutions containing acetic acid,<sup>199</sup> isopropanol,<sup>199</sup> naphthol,<sup>16</sup> phenol,<sup>22</sup> chlorophenols,<sup>120</sup> polyacrylates,<sup>189</sup> benzoic acid,<sup>161</sup> and chloromethylphenoxy herbicides.<sup>29</sup> A good agreement between the experimental and modeling results obtained in all cases validated the assumptions on which the model is based. Figure 16 shows, for example, the excellent concordance between experimental and theoretical evolution of COD and ICE, observed during naphthol oxidation under different experimental conditions.

Recently Panizza et al.,<sup>200</sup> studying 3,4,5-trihydroxybenzoic acid oxidation, observed that, while with low current density a high current efficiency and a low energy consumption can be obtained, organic mineralization required a long electrolysis time, because some of the reactor capacity is underused. Conversely, when operating current exceeds the

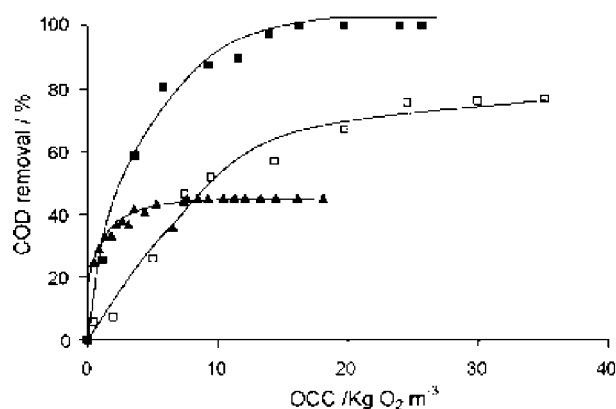


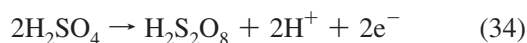
**Figure 18.** Changes in the removal percentage of COD as a function of the OCC during CDEO ( $\blacksquare$ ), ozonation ( $\square$ ), and Fenton oxidation ( $\blacktriangle$ ) of a fine chemical industry wastewater. Experimental conditions of BDD electrolysis:  $i = 300\text{ A m}^{-2}$ . Experimental conditions of ozonation: pH 12; ozone production  $0.99\text{ g h}^{-1}$ . Experimental conditions of Fenton oxidation: pH 3;  $\text{Fe}^{2+}$   $850\text{ mg dm}^{-3}$ . Reprinted with permission from ref 196. Copyright 2006 Elsevier.

limiting one, electrolysis is fast, but current efficiency decreases; hence, energy consumption increases, because a portion of the current is wasted on the secondary oxygen evolution reaction (Table 6). They proposed that a simple way to minimize secondary reactions and maximize reactor performance could be to operate with multiple current steps electrolysis, in which the applied current is adjusted during electrolysis not to exceed the instantaneous limiting current. Therefore, they adapted the equations of the previous model<sup>16,17,120,199</sup> to calculate the time for each step, so that it would remain below the instantaneous limiting current. By comparing the results obtained with the current steps electrolysis and those at constant currents, the former was found to permit a fast oxidation rate, comparable with high current density electrolysis, but with nearly 100% current efficiency and low energy consumption, as in low current density electrolysis (Table 6). Furthermore, if the number of current steps is sufficiently high, i.e., working in a semicontinuous control mode, the reactor performance is comparable with the one achievable in an ideal diffusion-controlled process, with 100% efficiency.

**Table 6. Comparison of the Results Obtained during Constant Currents Electrolysis and Current Steps Electrolysis for the Oxidation of 3,4,5-Trihydroxybenzoic Acid at BDD Anode (Reprinted with Permission from Ref 200. Copyright 2008 Elsevier.)**

applied current density	average current efficiency $\eta$ (-)	electrolysis time $\tau$ (min)	specific energy consumption $E_{sp}$ (kWh kgCOD <sup>-1</sup> )
10 mA cm <sup>-2</sup>	0.96	200	13
60 mA cm <sup>-2</sup>	0.28	108	68
four current step	0.94	126	14.5
semicontinuous control electrolysis	0.97	115	14.0

BDD application for wastewater treatment has also been widely studied by the group of Canizares,<sup>19,25,26,30,156,164,176,177,179,180,182,188,197,201</sup> using an experimental setup similar to that illustrated in Figure 15. They obtained complete mineralization of organic wastes, independently of their characteristics (initial concentration, pH, and supporting media) and operating conditions (temperature and current density). They also found that, depending on electrolyte composition, the organics were oxidized on the electrode surface—by reaction with hydroxyl radicals—as well as in the bulk of the solution by inorganic oxidants electrogenerated on BDD anodes, such as peroxodisulfuric acid from sulfuric acid oxidation:



This group has recently compared conductive-diamond electrochemical oxidation (CDEO) with two other advanced oxidation processes, Fenton oxidation and ozonation, for the treatment of synthetic and real wastewaters.<sup>157,194,196</sup> To compare the performance of different AOP, they introduced a new parameter, namely, oxygen-equivalent chemical oxidation capacity (OCC), which quantifies, in arbitrary units, the oxidants added to the waste and is defined as the kg of O<sub>2</sub>, which is equivalent to the quantity of oxidant reagents used in each process to treat 1 m<sup>3</sup> of wastewater. This parameter is related to the various oxidants used in the three advanced oxidation processes and can be calculated according to the following equations:

$$\text{OCC (kg}_{\text{O}_2}\text{ m}^{-3}) = 0.298Q \text{ (kAhm}^{-3}) \quad (35)$$

$$\text{OCC (kg}_{\text{O}_2}\text{ m}^{-3}) = 1.000[\text{O}_3] \text{ (kg}_{\text{O}_3}\text{ m}^{-3}) \quad (36)$$

$$\text{OCC (kg}_{\text{O}_2}\text{ m}^{-3}) = 0.471[\text{H}_2\text{O}_2] \text{ (kg}_{\text{H}_2\text{O}_2}\text{ m}^{-3}) \quad (37)$$

For both synthetic and real wastewaters, CDEO was the only technology capable of completely reducing COD and TOC content. Conversely, ozonation and mainly the Fenton process led to the buildup of significant concentrations of oxidation-refractory organic compounds. The percentages of refractory compounds increase significantly depending on initial waste concentration. For example, Figure 18 shows the evolution of COD removal obtained during the treatment of fine chemical industry wastewater using BDD anode, Fenton oxidation, and ozonation. They also observed that energy requirements are significantly lower for electrochemical oxidation than for ozonation. This indicates that electrochemical technology could successfully compete with other commonly used AOP (like ozonation).

Panizza et al.<sup>202</sup> studied the use of electrochemical oxidation as a refining technology to guarantee the quality of a real effluent containing high concentrations of naphthalene sulfonates and other recalcitrant organic compounds. They

coupled a biofilm airlift suspension (BAS) reactor with an electrochemical cell equipped with a BDD anode. The degradation yield evolution during the combined biological–electrochemical process showed that overall degradation efficiency of BAS did not exceed 70% owing to the recalcitrant nature of some aromatic sulfonates in the effluent. However, these compounds were completely mineralized by electrochemical oxidation (Figure 19). The results suggested that the combined process allowed for the minimization of aeration volumes required for biological oxidation, as well as the energy required for electrochemical oxidation. Similar results were also obtained by Canizares et al.<sup>201</sup> for waste treatment from a door-manufacturing process.

The group of Brillas<sup>29,166,167,170</sup> demonstrated that anodic oxidation with BDD is very effective for complete mineralization of herbicides and pharmaceutical drugs. Experiments carried out in batch under steady conditions using a flow reactor reveal that the removal of pollutants is practically pH-independent, but it gets faster with increasing herbicide concentration, current density, temperature, and liquid flow rate (Figure 20). They reported that herbicide decay follows a pseudo-first-order kinetics, and that these persistent organic compounds are mainly destroyed by reaction with <sup>•</sup>OH produced at BDD surface, while generated weak oxidants, such as H<sub>2</sub>O<sub>2</sub> and peroxodisulfate ions, have little influence on TOC decay.

Polcaro et al.<sup>169,183,184</sup> showed that the crucial point to obtain high faradic yields during pollutants oxidation on BDD anodes is the rate of mass transfer of the reactant toward the electrode surface. Thus, they used an impinging cell that enabled the obtaining of a high mass transfer coefficient ( $\sim 10^{-4}$  m s<sup>-1</sup>) for degradation of phenolic compounds, diuron, and 3,4-dichloroaniline. The results indicated that, if a minimum value of current density is imposed, suitable initial conditions can be set at which the process is carried out at a faradic yield close to 1, up to near-complete disappearance of total organic load.<sup>184</sup>

The use of BDD anodes was also widely investigated for the removal of synthetic dyes from wastewaters.<sup>31–33,132,203–218</sup>

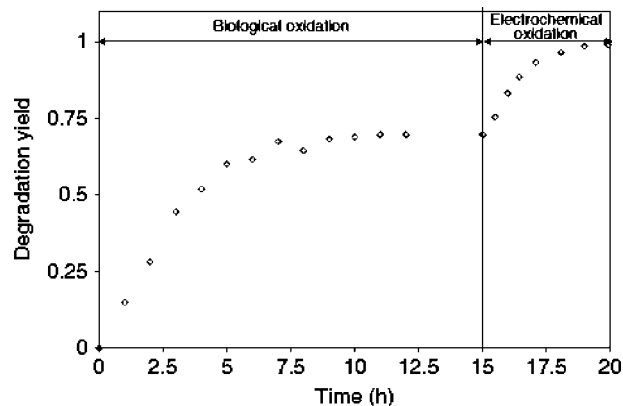


**Figure 19.** Degradation yields for biological and electrochemical oxidation of organic molecules. Reprinted with permission from ref 202. Copyright 2006 John Wiley & Sons, Inc.

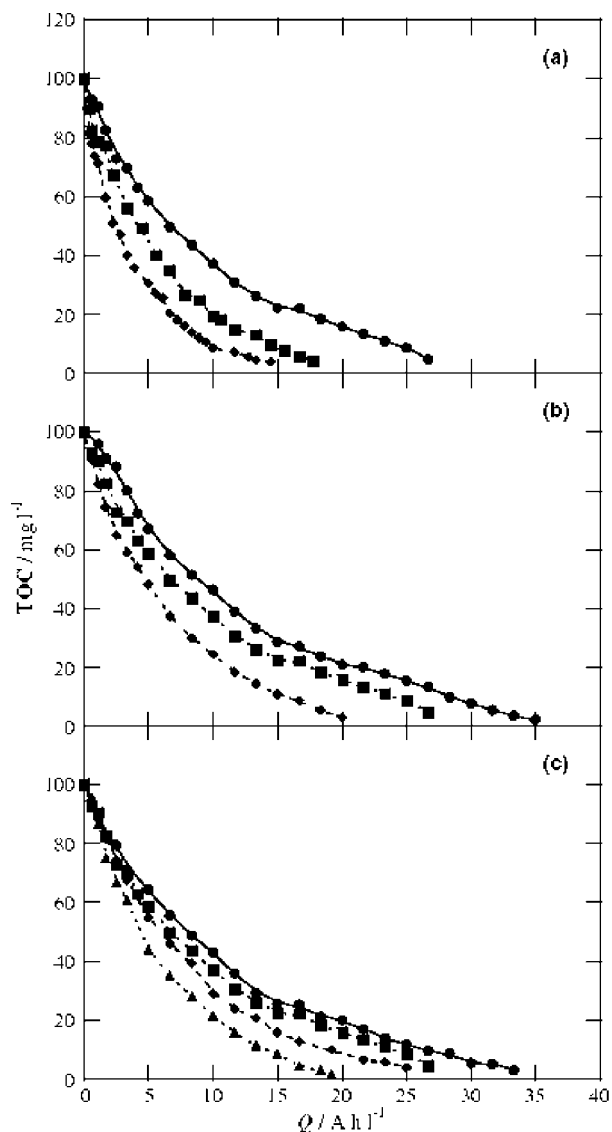


**Figure 20.** Effect of experimental parameters on TOC decay for the degradation of 1.8 L of  $178 \text{ mg dm}^{-3}$  of Mecoprop herbicide using a BDD anode. (a) Current density = (●) 150, (■) 100, and (◆)  $50 \text{ mA cm}^{-2}$ ,  $T = 40 \text{ °C}$ , liquid flow rate =  $130 \text{ dm}^3 \text{ h}^{-1}$ . (b) Current density =  $150 \text{ mA cm}^{-2}$ ,  $T =$  (●) 15, (■) 40, and (◆)  $60 \text{ °C}$ , liquid flow rate =  $130 \text{ dm}^3 \text{ h}^{-1}$ . (c) Current density =  $150 \text{ mA cm}^{-2}$ ,  $T = 40 \text{ °C}$ , liquid flow rate = (●) 230, (■) 170, (◆) 130, and (▲)  $75 \text{ dm}^3 \text{ h}^{-1}$ . Reprinted with permission from ref 166. Copyright 2006 Elsevier.

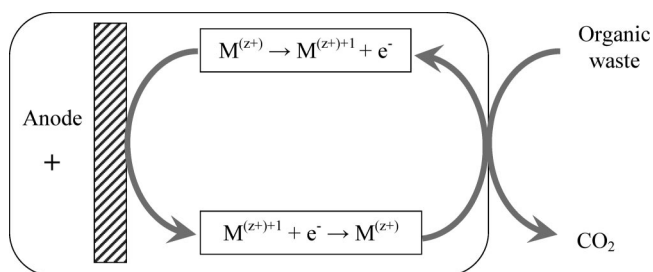


**Figure 21.** Principle of the MEO process.

The efficacy of these electrodes was pointed out in the removal of color as well as mineralization of these pollutants. For example, the effects of operational variables on Orange II oxidation at a boron-doped diamond electrode using Ti as a substrate (Ti/BDD) were systematically examined by Chen et al.<sup>204</sup> They reported that high temperature and low

current density were beneficial for Orange II oxidation. Nevertheless, the effect of pH and electrolyte concentration was not significant. At high COD values, nearly 100% current efficiency was obtained.

Canizares et al.<sup>31</sup> studied the oxidation of synthetic waste polluted with three azoic dyes (Eriochrome Black T, Methyl Orange, and Congo Red) using a Si/BDD anode. Results showed that complete COD and color removal was obtained for all solutions. Current efficiency did not seem to depend on the molecule of oxidized azoic dyes but only on its concentration range.

Conversely, other authors<sup>33</sup> compared Alizarin Red (an anthraquinone dye) and Eriochrome Black T (an azoic compound) oxidation and demonstrated that pollutant nature and especially the presence of functional groups (such as the azoic group) seem to strongly affect the oxidation mechanism and efficiency of the electrochemical process. Alizarin Red electrochemical oxidation led to an almost direct generation of carbon dioxide, without any build-up of large amounts of intermediates in the system, while Eriochrome Black T oxidation process started with the breakage of the azoic group and formation of a great amount of intermediates. It then continued with the mineralization of all generated intermediates.

Many researchers compared BDD degradation ability with traditional electrodes, such as  $\text{SnO}_2$ ,  $\text{PbO}_2$ ,  $\text{RuO}_2$ , and  $\text{IrO}_2$ , and they demonstrated that, under all experimental conditions, BDD enables the highest oxidation rate and current efficiency.<sup>51,56,60,120,129,130,136,138,168,174,205</sup> To explain its best performance, Cominellis and co-workers<sup>120</sup> speculated that on BDD—which has an inert surface with weak adsorption properties—electrogenerated hydroxyl radicals are weakly adsorbed and consequently more reactive toward organic oxidation. Furthermore, they assumed that  $\cdot\text{OH}$  action is extended to a “reaction cage” in the vicinity of the electrode surface, rather than limited to the surface itself.

For example, Panizza and Cerisola<sup>32</sup> compared electrocatalytic properties of BDD, Ti–Ru–Sn ternary oxide, platinum, and lead dioxide anodes for Methyl Red oxidation by potentiodynamic measurements and bulk electrolysis. They verified that faster mineralization and higher current efficiency were obtained at BDD (Figure 14). Similarly, Chen et al.<sup>205</sup> reported that the current efficiency obtained with Ti/BDD in oxidizing acetic acid, maleic acid, phenol, and dyes was 1.6-, 4.3-fold higher than that obtained with the Ti/Sb<sub>2</sub>O<sub>5</sub>–SnO<sub>2</sub> electrode.

Weiss et al.<sup>174</sup> have recently studied phenol oxidation in a one-compartment flow cell with BDD or PbO<sub>2</sub> anodes and demonstrated that phenol, TOC, and COD removals were achieved more quickly with BDD than with PbO<sub>2</sub>. In particular, the energy required for 99% removal of aromatic compounds was 80 and 330 kWh m<sup>-3</sup> for BDD and PbO<sub>2</sub> anodes, respectively.

Other papers have demonstrated that Si/BDD electrodes are able to achieve faster oxidation and better incineration efficiency than Ti/PbO<sub>2</sub> in the treatment of naphthol,<sup>56</sup> 4-chlorophenol,<sup>120</sup> chloranilic acid<sup>60</sup> surfactants,<sup>138</sup> and herbicides.<sup>136,168</sup>

Despite the numerous advantages of diamond electrodes, their high cost and especially the difficulties in finding an appropriate substrate for thin diamond layer deposition are their major drawbacks. Indeed, really stable diamond films are mainly deposited on silicon, tantalum, niobium, and tungsten, but these materials are not suitable for large-scale

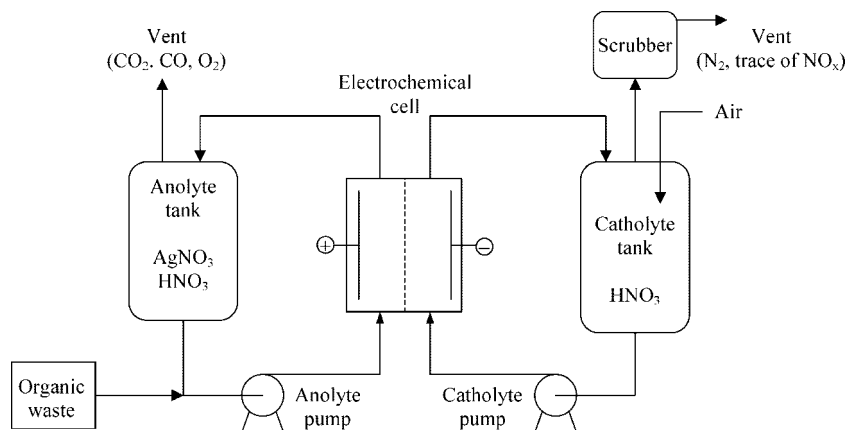


**Figure 22.** Scheme of a silver-mediated electrochemical oxidation process.

use. As a matter of fact, a silicon substrate is very brittle and its conductivity is poor, while tantalum, niobium and tungsten are too expensive.

Titanium is a preferable choice as a substrate, due to its good conductivity, high strength, low price, high anticorrosion, and quick repassivation behavior. However, service life of a Ti/BDD electrode is relatively short, because of large thermal residual stress due to substrate cooling from about 850 °C to ambient temperature, as well as due to the formation of a TiC interlayer reducing diamond film adhesion to the substrate.<sup>219</sup>

Service life improvement of Ti/BDD anodes is now under investigation in many laboratories. Chen and co-workers found that, by applying a silicon interlayer between Ti and diamond, accelerated lifetime tests of the Ti/Si/BDD was extended from 264 to 320 h for Ti/BDD.<sup>220</sup> They also reported that the use of two-temperature-stage hot filament chemical vapor deposition permits the manipulation of TiC interlayer properties, thus significantly increasing accelerated lifetime tests to 804 h.<sup>221</sup> A further improvement in Ti/BDD stability will open the door to potential industrial applications of such electrode material.

## 5. Indirect Electrolysis

The idea of indirect electrolysis is to prevent electrode fouling, avoiding direct electrons exchange between organics and anode surface. Therefore, in indirect electrolysis, pollutants are oxidized through the mediation of some electrochemically generated redox reagents, which act as an intermediary for electrons shuttling between the electrode and the organics.

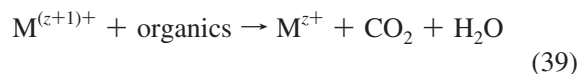
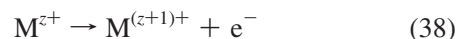
The main requirements for obtaining high efficiencies in indirect electrolytic processes are the following:<sup>2</sup>

- The potential at which the intermediate species is produced must not be near oxygen evolution potential.
- The intermediate generation rate must be high.
- The reaction rate of the intermediate species and the pollutant must be higher than the rate of any competing reactions.
- Pollutant adsorption must be minimized.

Oxidation mediators can be metallic redox couples, such as Ag(II), Ce(IV), Co(III), Fe(III), and Mn(III), or strong oxidizing chemicals, such as active chlorine, ozone, hydrogen peroxide, persulfate, percarbonate, and perphosphate.

### 5.1. Metallic Redox Couple

Indirect electrolysis using metallic couples as redox reagent is called mediated electrochemical oxidation (MEO). The principles of this process are shown in Figure 21. Metal ions in acidic solutions are anodically oxidized from their stable oxidation state ( $M^{z+}$ ) to the higher reactive oxidation state ( $M^{(z+1)+}$ ) in which they attack the other organic feed, breaking it down into carbon dioxide, insoluble inorganic salts, and water:



This reaction brings the couple back to a stable state ( $M^{z+}$ ), and it is then recycled through the cell to continuously regenerate further reactions. MEO has the advantage of operating at low temperature values (up to 90 °C) and at near-atmospheric pressure; it is easily controllable by switching off power supply to the electrochemical cell; and it does not produce toxins. This process is preferably used to treat solid waste or concentrated solutions, with an organic content higher than 20%, in order to avoid or limit the separation of the metallic redox couples from the solution. For total organics oxidation, a redox pair with a high oxidation potential, such as Ag(I/II) ( $E^\circ = 1.98$  V), Co(II/III) ( $E^\circ = 1.82$  V), or Ce(III/IV) ( $E^\circ = 1.44$  V), must be chosen.

A MEO diagram throughout the oxidizing species Ag(II) regeneration process is presented in Figure 22. The core of the plant is the divided electrochemical cell, where Ag(II) ions are generated by anodic oxidation of Ag(I) ions in concentrated nitric acid, forming a dark brown complex with nitrate ions, which slows down silver(II) reduction by water:



The corresponding cathodic reaction is the reduction of nitric acid to nitrous acid or NO, which can be further oxidized to nitric acid by bubbling oxygen through it or by oxidative absorption in columns.<sup>6</sup>

Cells, divided by a porous separator or an ion-exchange membrane, have to be used to prevent Ag(II) reduction at the cathode and the mixing of anolyte and catholyte streams; otherwise, Ag(II) produced at the anode will react with  $\text{HNO}_2$  produced at the cathode, to reform  $\text{AgNO}_3$  again, instead of mineralizing the pollutants, hence reducing process efficiency.



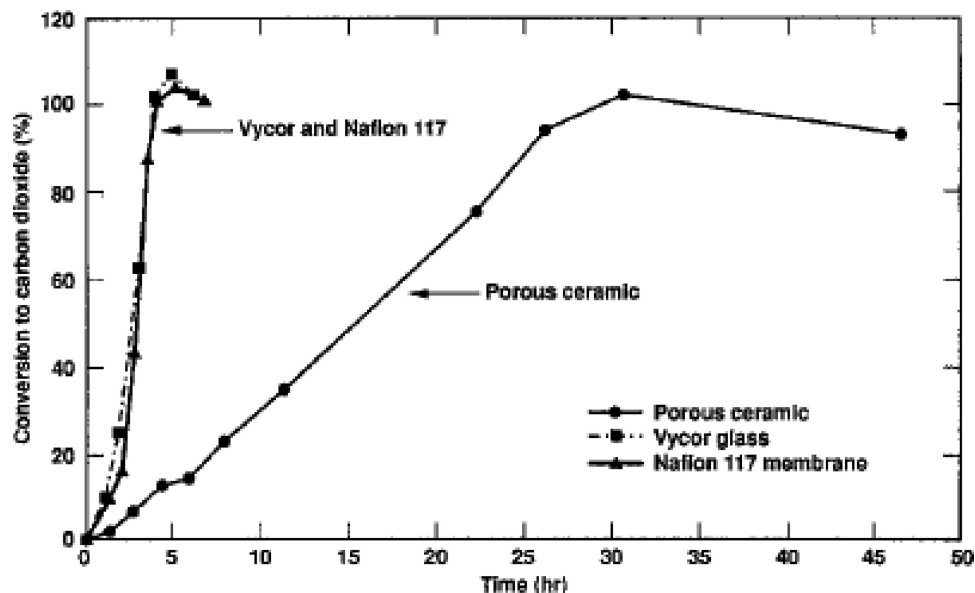
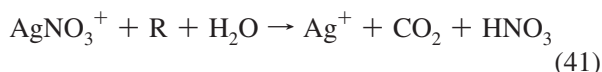


**Figure 23.** Comparison of rates of EG conversion to CO<sub>2</sub> in reactors with porous ceramic, Vycor microporous glass, and Nafion 117 cation-exchange membrane separators. Reprinted with permission from ref 225. Copyright 1992 The Electrochemical Society.

**Table 7. Materials Treated by the Silver II Process; Adapted from Ref 234**

industry	pollutants	plant scale	destruction efficiency	current efficiency
nuclear materials	TBP/OK, IX resin, cellulose, oil	laboratory—12 kW	complete	70–95%
chemical warfare	VX, HT, GB, HD, HT, DMMP, TBP/OK	0.15–12 kW	99.9999–99.99999%	50–90%,
energetic compounds	RDX, TNT, triple base, TETRIL, nitroglycerine, DEMEX, OTTO fuel, M28, DNT, TETRYTOL	laboratory—12 kW	99.999%	80–100%.

Organic waste is fed to the anolyte, with an appropriate mixer to ensure its dispersal, and then mineralized by Ag(II) ions to carbon dioxide, insoluble inorganic salts, and water:



During oxidation, the anolyte remains clear because the bulk AgNO<sub>3</sub><sup>+</sup> concentration was essentially zero. Then, when the solution turns dark brown, it is evidence of AgNO<sub>3</sub><sup>+</sup> in the anolyte and of organics destruction.

Platinum is the anode material generally used for silver couple regeneration,<sup>222–224</sup> because of its good corrosion resistance in nitric acid. However, other electrodes can be used, such as gold,<sup>225</sup> antimony-doped tin dioxide,<sup>226</sup> and boron-doped diamond electrodes.<sup>227</sup>

Silver-mediated electrolysis was developed in the 1980s for refractory plutonium oxide dissolution in nuclear waste processing units.<sup>223,224,228,229</sup> Later, it was also applied to the treatment of various organic pollutants and waste streams including persistent organic pollutants (POPs),<sup>230</sup> kerosene,<sup>231</sup> urea<sup>232</sup> and organic acids.<sup>233</sup>

Accentus Plc<sup>234</sup> developed and applied a silver MEO (Silver II Process) for the mineralization of a wide range of organic substrates, as summarized in Table 7. Nuclear materials were completely mineralized with current efficiencies in the range of 70–95%, working from laboratory scale to 12 kW plant. Warfare chemical agents were removed with 99.9999–99.99999% destruction efficiency and 50–90% current efficiencies, while the range of energetic compounds were also successfully treated with 80–100% current efficiency.<sup>234</sup>

Steele<sup>223</sup> used a cell with a platinum anode and a platinum cathode, AgNO<sub>3</sub> (1M) in HNO<sub>3</sub> (6M) as anolyte, HNO<sub>3</sub> (12

M) as catholyte for the treatment of rubber gloves, anionic and cationic exchange resins, and hydraulic oil, obtaining complete destruction of all the compounds.

Farmer et al.<sup>225</sup> investigated silver MEO of ethylene glycol (EG) and benzene (BZ). EG, BZ, and their intermediates were completely converted to CO<sub>2</sub> (100% conversion efficiency) with 83–88% Coulombic efficiencies, by applying a current of about 24–40% the limiting current for mediator generation. They also investigated three separator materials to prevent anolyte and catholyte mixing: a porous ceramic, Vycor microporous glass, and a Nafion 117 cation-exchange membrane. Porous ceramic frits allowed HNO<sub>2</sub> to migrate from catholyte to anolyte, thereby reducing process efficiency. Conversely, Vycor microporous glass and Nafion 117 were effective barriers to HNO<sub>2</sub> migration; therefore, they allowed faster conversion (Figure 23).

The main drawbacks of this process are the loss of silver by AgCl precipitation during the oxidation of chlorinated compounds, the relatively high cost of silver, HNO<sub>2</sub> and NO<sub>x</sub> generation at the cathode, corrosion problems, high quantities of Ag leakage through the separator, and the need to completely regenerate the silver ions, because they are considered a hazardous waste by themselves.

Co(III) is another powerful oxidant similar to silver(II), but with some advantages over the latter, including the fact that cobalt chloride is soluble and, hence, does not precipitate. Cobalt is cheaper than silver, and, under appropriate conditions, it can operate in a divided or undivided cell. Working in the divided cell with HNO<sub>3</sub> as electrolyte, Co(III)-mediated electrochemical oxidation was employed for the destruction of aniline<sup>235</sup> and many chlorinated hydrocarbons<sup>222,236</sup> with over 90% current efficiency.

In order to eliminate the problems related to the separator, oxidation can be performed in an undivided cell in sulfuric

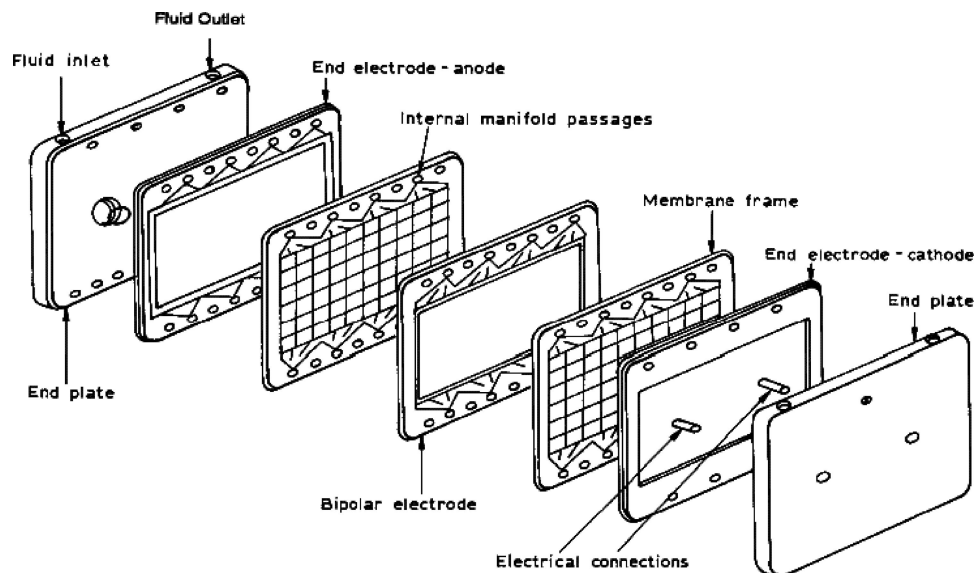


**Figure 24.** Construction details of the  $\text{CeO}_x$  electrochemical cell for wastewater treatment. Reproduced by permission of Platinum Metals Review. Reprinted with permission from ref 243. Copyright 2002 Johnson Matthey PLC.

media. Electrogenerated  $\text{Co(III)}$  immediately reacts with the organics near the anode surface, and the cathodic reduction of  $\text{Co(III)}$  is suppressed by the irreversible character of this redox couple.

The destruction of halogenated organic waste by reaction with  $\text{Co(III)}$  in a cell with no electrode separator has been demonstrated by Farmer et al.<sup>237</sup> Dissolved ethylene glycol (EG), 1,3-dichloro-2-propanol (DCP), 3-monochloro-1-propanol (MCP), and isopropanol (IPA) were completely converted to  $\text{CO}_2$  by reaction with  $\text{Co(III)}$ . They also found a correlation between the total number of  $\text{Co(III)}$  ions required for complete oxidation of a compound and its corresponding Coulombic efficiency. Indeed, about 74% EG oxidation efficiency was obtained, which dropped drastically to 10% for MCP of IPA.

Leffrang et al.<sup>238</sup> used an undivided cell with a concentric cylindrical anode and a cathode made of platinum for the oxidation of various chlorophenols. All substances were totally destroyed with at least 98% conversion rate and 75% current efficiency.

Sanroman et al.<sup>239</sup> demonstrated that the electrochemical process with  $\text{Co(III)}$  redox mediator can efficiently electrocatalyze the oxidation of different mixtures of dyes (Bromophenol Blue, Indigo, Poly R-478, Phenol Red, Methyl Orange, Fuchsine, Methyl Green, and Crystal Violet), thus significantly shortening treatment time versus electrolysis without cobalt ions.

Many papers have demonstrated that the use of cerium as an electrocatalyst has some advantages over silver and cobalt. Actually, (i) It does not form any precipitate with chloro-organic compounds. (ii) The rate of water oxidation by  $\text{Ce(IV)}$  is minimal compared to silver(II) and cobalt(III) ions. (iii) It is not a listed or hazardous compound. (iv) It can be recovered and recycled without much loss.

Chung et al.<sup>235</sup> compared the results of  $\text{Ce(IV)}$ - and  $\text{Co(III)}$ -mediated electrochemical destruction of aniline, showing that  $\text{Ce(IV)}$  was better than  $\text{Co(III)}$  in terms of cost per given amount of aniline treated. Other papers demonstrated that Trimsol cutting oil, Otto Fuel II, and Sarin ( $\text{C}_4\text{H}_{10}\text{FO}_2\text{P}$ ) can be removed with over 99% destruction efficiency using  $\text{Ce(IV)}$ , by operating at a temperature range of 40–100 °C.<sup>240,241</sup>

Nelson et al.<sup>242,243</sup> developed a commercial-scale plant with 80 kW nominal capacity for the destruction of chlorinated pesticides and herbicides using a cerium-catalyzed electrochemical process (CerOx). Oxidation is performed in a series of “tank systems” of plate and frame cells in poly(vinylidene fluoride) (PVDF), with platinum bipolar electrodes separated by a Nafion membrane (Figure 24). Electrolyte concentrations are 1.0 M cerium in 3.5 M nitric acid for the anolyte and 4 M nitric acid for the catholyte. Experiments were carried out at a temperature between 90–95 °C and at atmospheric pressure. This system allowed the complete destruction (>99.995%) of chlorinated organics such as Chlordane, Ambush, Keldane, or 2,4-D with about 88% current efficiency.

More recently, Moon’s group successfully tested a cerium-MEO in batch and continuous mode for the mineralization of various model compounds (e.g., ethylenediaminetetraacetic acid (EDTA), phenol, benzoquinone, hydroquinone, catechol, maleic acid, and oxalic acid).<sup>244–251</sup> They used 1 M cerium nitrate and 3 M nitric acid as anolyte and 4 M nitric acid as catholyte. The electrochemical cell was equipped with a mesh-type  $\text{Ti/IrO}_2$  anode and a Ti cathode separated by a Nafion 324 membrane. Destruction efficiency (D.E.), evaluated measuring the evolved  $\text{CO}_2$  or solution TOC, was higher than 95% for all the organics studied, with 88–92% Coulombic efficiency (Table 8).

They also studied the effect of various parameters for EDTA destruction, such as EDTA concentration, temperature, cerium and nitric acid concentrations, and organic feeding time. An excellent destruction efficiency was achieved for the following conditions: EDTA concentration = 67 mM; temperature = 95 °C; cerium concentration = 0.95 M; and nitric acid concentration = 3 M.

$\text{Fe(II)/Fe(III)}$  or  $\text{Mn(II)/Mn(III)}$  are not suited for total oxidation of organics, because of their low oxidation potential, but they can be used for selective partial oxidation of organic substances.<sup>252–254</sup>

Mediated electrochemical oxidation has been applied also for off-gas purification. In this process, the chemical reaction between gas pollutant and redox mediator can be achieved either in the electrochemical cell—where the mediators are

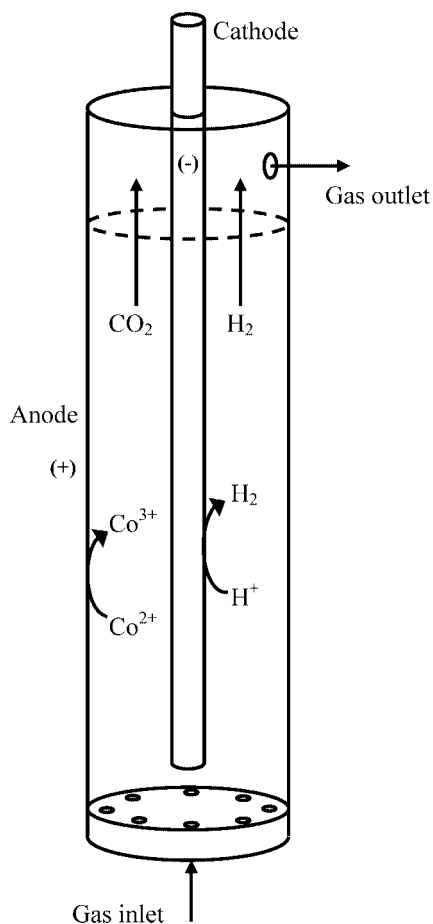


**Figure 25.** Scheme of inner-cell processes for gas purification by cobalt-mediated electrochemical oxidation.

regenerated (inner-cell process)—or in adsorption towers/scrubbing devices (outer-cell process).

Farmer et al.<sup>255</sup> patented an inner-cell assembly for the treatment of air contaminated with halide-containing organics, by Co(III)-mediated electrochemical oxidation. The cell is cylindrical and undivided, with a cylindrically shaped cathode disposed along the center of the cylindrical anode, both made of platinum. Air containing organic waste is fed from the bottom through a distributor. As bubbles progress through the  $\text{CoSO}_4/\text{H}_2\text{SO}_4$  electrolyte within the cell, organics are dissolved and react with electrogenerated Co(III) to form  $\text{CO}_2$ . Hydrogen, which has evolved at the cathode, and  $\text{CO}_2$  exit from the top of the cell. A diagram of this cell is reported in Figure 25.

## 5.2. Oxidizing Chemicals

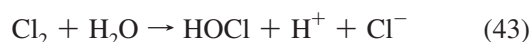
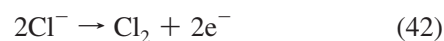
For the disposal of wastewaters containing low concentrations of organic pollutants (i.e., organic content lower than 20%), MEO is not recommended, since metallic redox couples may require a solution–solution separation step, which may not be desirable. These effluents can be treated by indirect electrolysis generating in situ chemical reactants and converting them into less harmful products.

The oxidizing chemicals can be electrogenerated either by anodic oxidation (such as active chlorine, ozone, or persulfates) or by cathodic reduction (hydrogen peroxide). Although indirect  $\text{H}_2\text{O}_2$ -mediated electrolysis is an effective and promising process, it is not discussed here because it is a cathodic process. Also, it is the subject of another review.<sup>256</sup>

### 5.2.1. Active Chlorine

Among anodically generated oxidizing chemicals, active chlorine is the most traditional one and the most widely employed for wastewater treatment. Chlorine-mediated electrolysis has been reported in the oxidation of a wide range of model pollutants,<sup>191,257–280</sup> but it is particularly suitable for the treatment of real wastewaters with high sodium chloride concentrations (even more than  $5 \text{ g dm}^{-3}$ ), such as olive oil wastewater, textile, and tannery effluents.<sup>67,103,137,281–313</sup> Some examples are summarized in Table 9.

Despite the wide use of chlorinated inorganic species as redox mediator, the electrochemical and chemical reactions that take place during electro-oxidation of organic pollutants in chloride-containing solutions are complex and not entirely known. Indeed, oxygen transfer to organic molecules can be attained both on the electrode surface through adsorbed oxychloro species (such as chloro and oxychloro radicals) or in the bulk of the solution, through long-lifetime oxidants (such as chlorine, hypochlorous acid, or hypochlorite) anodically produced by the oxidation of chloride ions, according to the following reactions:



An explanation of the mediating role of chloride ions and a reaction mechanism have been proposed by De Battisti's group<sup>62,260,261</sup> (Figure 26). They extended the diagram for electrochemical oxygen transfer reactions proposed by Comninellis<sup>48</sup> to the cases where oxygen transfer is carried out by adsorbed oxychloro species—which are intermediates in chlorine evolution reaction—instead of by hydroxyl radicals. The presence of chloride ions seems to inhibit oxygen-evolution reaction, causing an increase in anode potential and, therefore, a higher reactivity of adsorbed chloride–oxychloro radicals. They also observed that the oxidation of organics in the presence of chloride ions mainly depends on chloride concentration, solution temperature, and pH, and that it is substantially insensitive to electrode surface nature.

In the literature, the most used electrode materials for in situ generation of active chlorine are based on platinum or on a mixture of metal oxides (e.g.,  $\text{RuO}_2$ ,  $\text{TiO}_2$ ,  $\text{IrO}_2$ ) that have good electrocatalytic properties for chlorine evolution, as well as long-term mechanical and chemical stability. However, other electrodes can also be used, such as  $\text{PbO}_2$ <sup>137,260,261,272,273</sup> and graphite.<sup>262,274–277,281</sup>

One of the early papers reporting on the catalytic effect of chloride ions in organic pollutants oxidation was published by Comninellis and Nerini.<sup>278</sup> They showed that the addition of 85 mM NaCl to the solution catalyzed phenol oxidation at Ti/IrO<sub>2</sub> anodes, due to the participation of electrogenerated  $\text{ClO}^-$ , by increasing EOI from about 0.06 to 0.56.

More recently, Panizza et al.<sup>56,314</sup> deeply investigated the influence of operating conditions on the oxidation of 2-naphthol with in situ electrogenerated active chlorine on a Ti–Ru–Sn ternary oxide. Degradation rate increased with NaCl concentration and pH, reaching maximum efficiency (EOI = 0.302) with  $7.5 \text{ g dm}^{-3}$  of NaCl and pH 12 (Figure 27). COD removal rate increased linearly with current, but

**Table 8. Mineralization of Various Organics by Cerium(IV) Mediated Oxidation Process at 80°C, [Ce(IV)] = 0.95 M, [HNO<sub>3</sub>] = 3 M, and Feed Rate = 3 cm<sup>3</sup> min<sup>-1</sup>; Adapted from Ref 246**

organic compound	feed concentration (ppm)	D.E. based on CO <sub>2</sub> (%)	D.E. based on TOC (%)
phenol	10	89.9	99.2
benzoquinone	2,5	90.6	95.0
hydroquinone	10	93.3	99.0
catechol	10	91.4	99.4
maleic acid	10	99.2	99.0
oxalic acid	10	88.5	99.5
EDTA	25	89.8	98.8

there were no significant differences in the amount of electric charge consumed at different current density values (Figure 28). This implies that the faradic yield of the mineralization process does not depend on current density. Similar results were also obtained by De Battisti and co-workers<sup>261</sup> during glucose oxidation with Ti/Pt anode, as well as by Iniesta et al.<sup>273</sup> during phenol oxidation using PbO<sub>2</sub> anodes.

The main drawback of this indirect oxidation is the likely formation of chlorinated organic compounds during electrolysis, resulting in increased wastewater toxicity. Indeed, Panizza et al.<sup>314</sup> detected a small amount of organochlorinated compounds during 2-naphthol electrolysis, reaching a maximum at about 9 Ah dm<sup>-3</sup>, which disappeared during electrolysis.

Conversely, De Battisti et al.<sup>260,261</sup> demonstrated that, by selecting appropriate experimental conditions, glucose can

be incinerated by chlorine-mediated electrolysis without formation of chlorinated organics.

Vlyssides et al.<sup>265</sup> studied the efficiency of chlorine-mediated electrolysis for the treatment of obsolete organophosphoric pesticides (Demeton-S-methyl, Metamidophos, Fenthion, and Diazinon). They used an experimental plant (Figure 29) with a cylindrical electrolytic cell containing 6 dm<sup>3</sup> of brine solution (NaCl 4% w/v) equipped with a Ti/Pt cylindrical anode located inside a perforated 304 stainless steel cylinder, which served as cathode. This construction ensured homogeneous dynamic lines between anode and cathode and provided good waste contact with the electrode. The pesticide solution was added in the electrolytic cell with a centrifugal 3 mL min<sup>-1</sup> flow rate pump. They observed a high reduction of COD and BOD<sub>5</sub> of oxidized pesticides and, in particular, improved biodegradability index (COD/BOD<sub>5</sub> ratio) of investigated pesticides. This is evidence that the initial toxic pesticides solution was highly detoxified, and that electrochemical oxidation could be used as a pretreatment method for pesticide detoxification, followed by biological oxidation. Actually, it is acceptable that a waste with a COD/BOD ratio < 2 can be treated by a biological system, while a COD/BOD ratio > 5 indicates toxic waste.<sup>50</sup>

In order to evaluate process integration feasibility and set some criteria for optimization (i.e., how to maximize degradation efficiency with minimum energy consumption and sludge) in combined biological and electrochemical oxidation of tannery wastewater, Szyrkowicz et al.<sup>296</sup> compared four different combinations of electrochemical and biological processes. Figure 30 gives the main characteristics of the options considered, and computation results are shown in Table 10. They observed that, if cheap energy is available, electro-oxidation can be proposed as a unique treatment process, reducing plant size by about 95%. Placing the

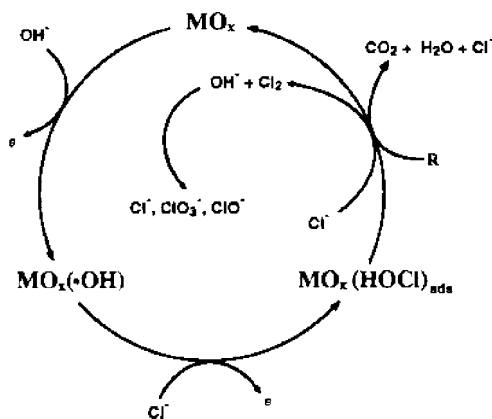


**Figure 26.** Scheme of chlorine-mediated electrolysis proposed by Bonfatti et al. Reprinted with permission from ref 261. Copyright 2000 The Electrochemical Society.

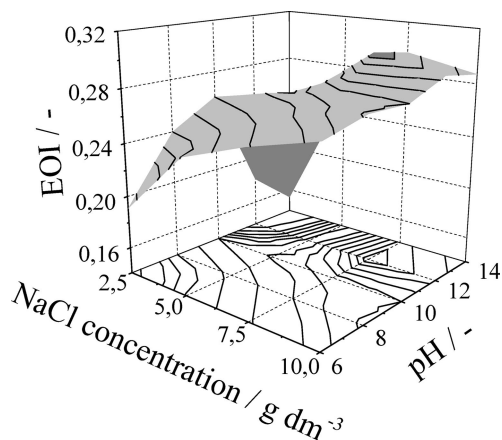


**Figure 27.** 3D representation of the combined effect of NaCl concentration and pH on the values of the EOI during the electrolyses of 2-naphthol on a Ti-Ru-Sn ternary oxide anode. Initial 2-naphthol concentration = 5 mM; applied current density = 75 mA cm<sup>-2</sup>; flowrate = 180 dm<sup>3</sup> h<sup>-1</sup>; and T = 25 °C. Reprinted with permission from ref 56. Copyright 2004 Elsevier.

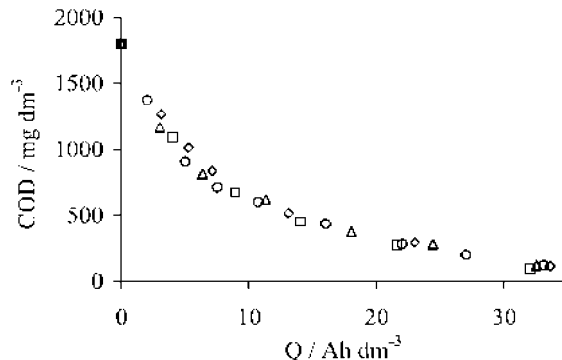


**Figure 28.** Influence of applied current density on the evolution of COD with the specific electrical charge passed during the electrolyses of 2-naphthol on a Ti-Ru-Sn ternary oxide anode. Initial 2-naphthol concentration = 5 mM; T = 25 °C; pH = 10; NaCl concentration = 5 g dm<sup>-3</sup>; applied current density: (◇) *i* = 25 mA cm<sup>-2</sup>, (○) *i* = 50 mA cm<sup>-2</sup>, (△) *i* = 75 mA cm<sup>-2</sup>, (□) *i* = 100 mA cm<sup>-2</sup>. Reprinted with permission from ref 314. Copyright 2003, Elsevier.

**Table 9. Examples of the Indirect Electrochemical Oxidation Electrogenenerating in situ Active Chlorine**

pollutant	anode	comments	ref
anionic surfactants	Ti–Ru–SnO <sub>2</sub>	optimal NaCl concentration: 2.5 g dm <sup>-3</sup>	191
atrazine	Ti/Ru <sub>0.3</sub> Ti <sub>0.7</sub> O <sub>2</sub>	TOC removal dependent on the quantity of NaCl in solution	257
chlorophenol	Ti/TiO <sub>2</sub> RuO <sub>2</sub>	CE 89% at pH 12.6 and current density of 11.39 mA cm <sup>-2</sup>	258
cresol	Ti/TiO <sub>2</sub> –RuO <sub>2</sub> –IrO <sub>2</sub>	optimum conditions were 2.5 g dm <sup>-3</sup> of chlorides and <i>i</i> = 5.4 A dm <sup>-2</sup>	259
glucose	Ti/PbO <sub>2</sub> , Ti/SnO <sub>2</sub> , Ti/Pt	oxidation rate was independent of the electrode but increase with <i>i</i> , pH, and <i>T</i>	260, 261
indigo dyes	graphite	90% of indigo degraded in 120 min with a power consumption of 1.84 kWh m <sup>-3</sup>	262
methylene blue	Ti/RuO <sub>2</sub>	optimal chloride concentration 1.2 g dm <sup>-3</sup>	263
oxalic acid	Ti/Pt	oxidation rate depends on the halides, following the order F <sup>-</sup> > Br <sup>-</sup> > Cl <sup>-</sup>	264
pesticides	Ti/Pt	COD/BOD <sub>5</sub> ratio was improved considerably after electrolysis	265–271
phenol	PbO <sub>2</sub>	complete phenol degradation	272
phenol	PbO <sub>2</sub>	formation of chloroform	273
phenolic compounds	carbon	batch or tubular reactor	274–277
phenol	Ti/IrO <sub>2</sub> , Ti/SnO <sub>2</sub>	EOI = 0.56 independent of the applied current and NaCl concentration	278
phenol	Ti/TiO <sub>2</sub> –RuO <sub>2</sub> –IrO <sub>2</sub>	formation of AOX at the beginning of electrolysis	279
Reactive Orange 4	Ti/PtO <sub>x</sub>	TOC removal of 81% with 20 g dm <sup>-3</sup> of NaCl	280
distillery effluent	graphite	reductions of BOD, COD, and absorbance were 93.5%, 85.2%, and 98.0%	281
paper mill wastewater	Ti/Co/SnO <sub>2</sub> –Sb <sub>2</sub> O <sub>5</sub>	COD removal 86%, color removal 75% at pH 11 and 15 g dm <sup>-3</sup> of NaCl	103
landfill leachate	TiO <sub>2</sub> RuO <sub>2</sub>	reductions of COD, TOC, and color were 73%, 57%, and 86%	282
landfill leachate	graphite, Ti/PbO <sub>2</sub> , Ti/ Sn–Pd–RuO <sub>2</sub>	best treatment with ternary Sn–Pd–Ru oxide	283
landfill leachate	Ti/Pt	COD reduction 84%, complete removal of VSS, N-NH <sub>4</sub> , and total phosphorus	284, 285
industrial paint wastewater	carbon	51.8% of COD removal and complete color and turbidity removals	286
industry wastewater	Ti/TiO <sub>2</sub> –RuO <sub>2</sub> –IrO <sub>2</sub>	organic halogens (AOX) were detected at high concentrations	287
industrial wastewater	Ti/Pt, Ti/RuSnO <sub>2</sub> , carbon	better COD removal with Ti/Pt anode	67
olive mill wastewater	Ti/RuO <sub>2</sub>	energy consumption for COD removal was 0.8 kWh dm <sup>-3</sup> .	288
olive mill wastewater	Ti/Pt	energy consumption = 123 kWh kg <sub>COD</sub> <sup>-1</sup>	289
olive mill wastewater	Ti/Pt	90% decolorization and 85% removal of phenols	290
olive mill wastewater	Ti/Ta–Pt–Ir	removal efficiency of COD reached 85.5%	291
tannery wastewater	Ti/RuO <sub>2</sub> , Ti/PbO <sub>2</sub>	best conditions at <i>i</i> = 600 A m <sup>-2</sup> , pH 10, <i>T</i> = 40 °C	137
tannery wastewater	Ti/Pt, Ti/Pt–Ir, Ti/PbO <sub>2</sub> , Ti/PdCo	complete removal of COD, tannins, ammonium, and sulfide	292–297
tannery wastewater	different DSA	decrease of total phenolic compounds, absorbance, and toxicity	298
reactive dyes	TiO <sub>2</sub> –RuO <sub>2</sub> –IrO <sub>2</sub>	COD and TOC removals were from 39.5 to 82.8% and from 11.3 to 44.7%	299, 300
textile wastewater	Ti/RuTiO <sub>2</sub> ; Ti/IrTiO <sub>2</sub> ; Ti/RuSnO <sub>2</sub>	lower energy consumption using Ti/Ru <sub>0.3</sub> Ti <sub>0.7</sub> O <sub>2</sub> electrode	301
textile dye wastewater	Ti/Pt	COD, BOD, color, and TKN removals were 86%, 71%, 100%, and 35%	302–304
textile wastewater	different DSA	Ti/Pt–Ir anode showed the best performance	305–310
textile dyes	Ti/Ta–Pt–Ir	formation of organochlorinated compounds	311
textile wastewater	oxide-coated titanium	Ti/RuO <sub>2</sub> gives better oxidation than Ti/SnO <sub>2</sub> and Ti/PbO <sub>2</sub>	312, 313

electrochemical reactor as a final polishing stage, after the conventional biological aerobic sludge process, allows an 80% reduction in total plant volume. This solution can be considered competitive, offering high reliability and low plant volume, even if the energy requirement is much higher than that theoretically needed in a single-sludge biological plant.

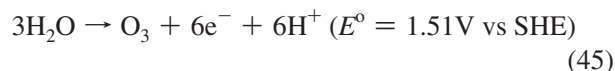
The same authors also investigated the influence of anode materials based on noble metals and metal oxides (Ti/Pt–Ir, Ti/PbO<sub>2</sub>, Ti/PdO–Co<sub>3</sub>O<sub>4</sub>, and Ti/RhO<sub>x</sub>–TiO<sub>2</sub>) on the treatment of tannery wastewater by indirect electrolysis.<sup>297</sup> They observed that only Ti/Pt–Ir and Ti/PdO–Co<sub>3</sub>O<sub>4</sub> gave satisfactory results and that, with these anodes, ammonia, COD, and sulfide removal was well-described by pseudo-first-order kinetics. Conversely, Ti/RhO<sub>x</sub>–TiO<sub>2</sub> was less effective, as it promoted direct discharge of proteins, leading to its partial passivation, while Ti/PbO<sub>2</sub> was subjected to fouling.

### 5.2.2. Ozone

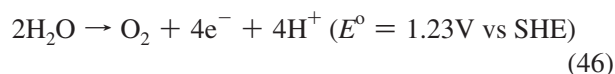
Ozone is another chemical oxidizing agent that can be produced by anodic process and employed for water disinfection and treatment. There is an increasing use of ozone

in wastewater treatment, because it has a high oxidation standard potential ( $E^\circ = 2.1$  V) and it does not produce secondary pollution, since it decomposes into oxygen. Ozone is commonly generated in air by corona discharge at very high voltage. This method, however, also produces a small amount of undesirable products, such as nitrogen oxide. Electrochemical ozone production (EOP) is an attractive alternative, because it requires low voltage and produces ozone in high concentrations directly in water, thus eliminating or minimizing problems of dissolving ozone in water.

The electrochemical ozone generation reaction at the anode can be expressed as



Ozone production efficiency is limited by oxygen evolution occurring at lower potential and it is, therefore, thermodynamically favored:



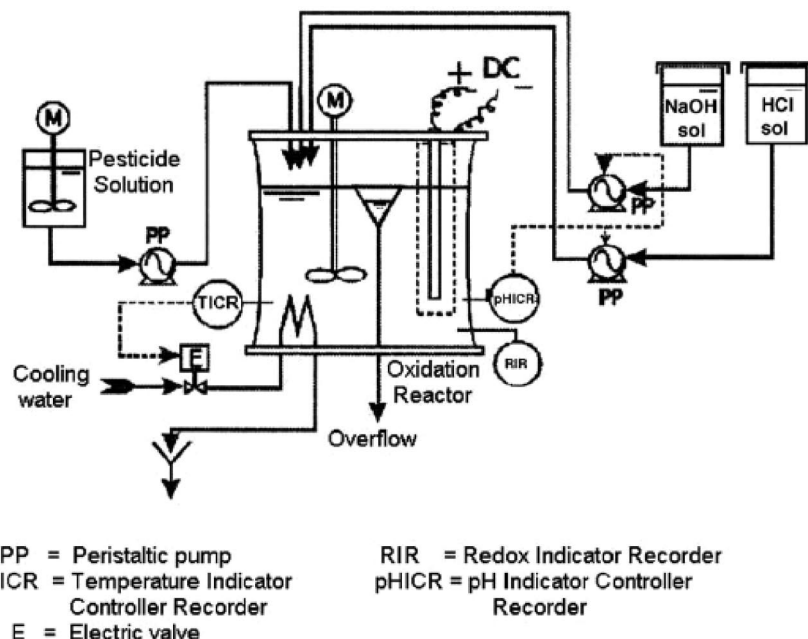


**Figure 29.** Scheme of the laboratory-scale pilot plant used for the destruction of obsolete pesticides stock. Reprinted with permission from ref 265. Copyright 2005 Elsevier.

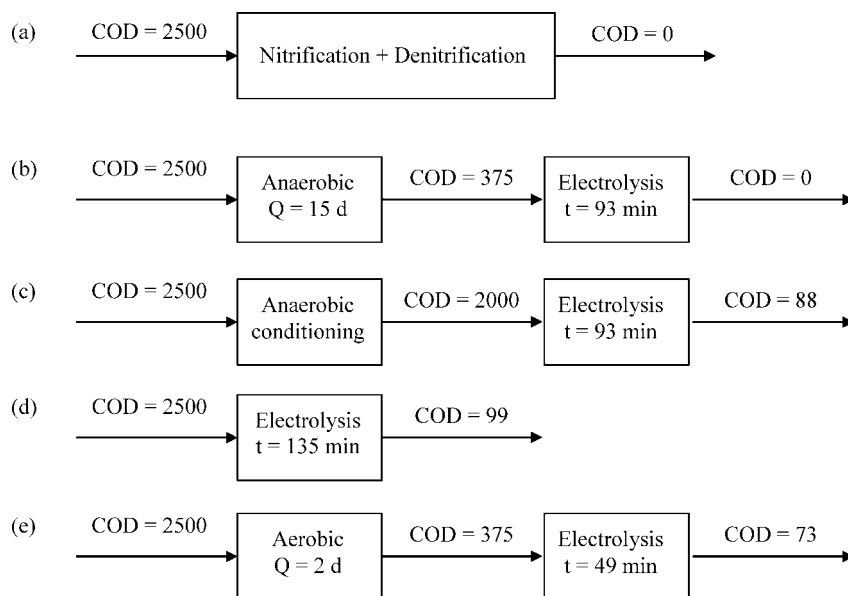


**Figure 30.** Schemes of possible combinations of electrochemical and biological processes. Adapted from ref 296.

In order to obtain the best EOP efficiency, literature reports suggest using electrode materials having high oxygen overpotential and performing electrolysis at low temperature, very low interfacial pH, and high anodic current. As a result, most of the investigations have focused on the use of lead dioxide,<sup>47,140,315–326</sup> however, tin dioxide,<sup>327,328</sup> Ti/IrO<sub>2</sub>–Nb<sub>2</sub>O<sub>5</sub>,<sup>329</sup> Ti/IrO<sub>2</sub>–Ta<sub>2</sub>O<sub>5</sub>,<sup>330</sup> platinum,<sup>331,332</sup> glassy carbon,<sup>333</sup> and diamond<sup>334–336</sup> were also studied.

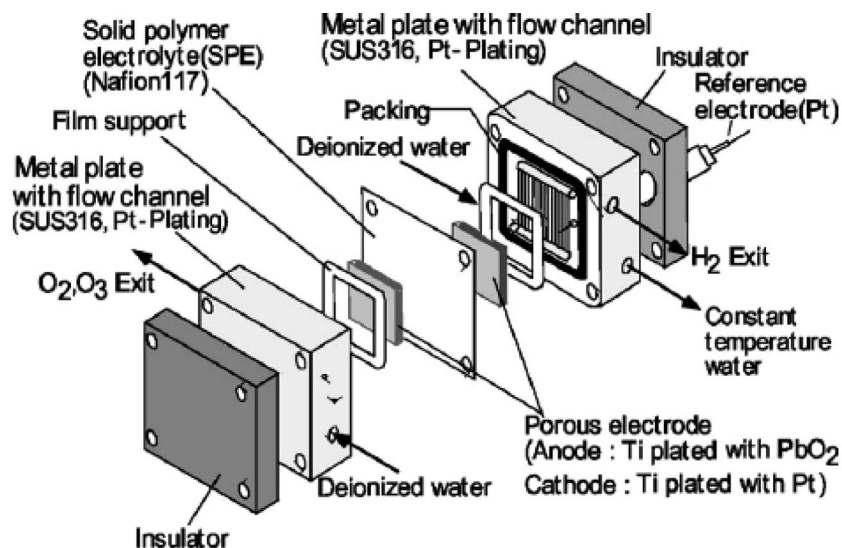
For example, Foller et al.<sup>319</sup> reported that current efficiency of ozone generation was more than 50% at a current density of 0.75 A cm<sup>-2</sup> and  $T = 0$  °C, when lead dioxide and 7.3 M hexafluorophosphoric acid were used as anode and electrolyte solution, respectively.

Using a boron-doped diamond in 10% H<sub>2</sub>SO<sub>4</sub>, Katsuki et al.<sup>334</sup> obtained an ozone concentration from 3 000 to 10 000 ppm, but with low percentage current efficiency, depending on temperature and current density.

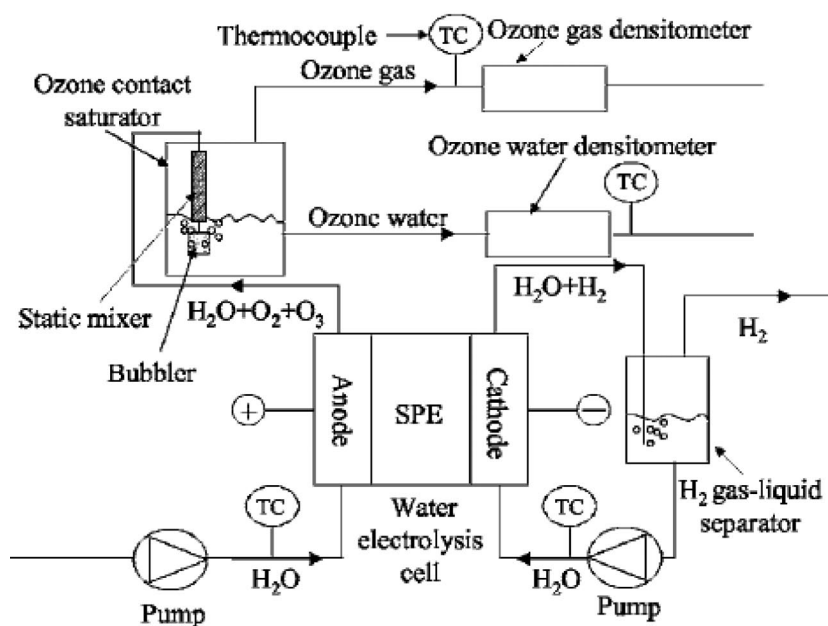
Wang et al.<sup>327</sup> showed that nickel- and antimony-doped tin dioxide electrode is a very efficient anode for ozone production. At room temperature in 0.1 M H<sub>2</sub>SO<sub>4</sub>, ozone concentration reached 34 mg dm<sup>-3</sup> with 36.3% current efficiency.

Together with the nature of electrode material, ozone electrochemical generation performance strongly depends on the composition of the supporting electrolyte.

Da Silva et al.,<sup>317</sup> in agreement with the results of Foller,<sup>319</sup> reported that the introduction of fluoro-compounds in the supporting electrolyte (3.5 M H<sub>2</sub>SO<sub>4</sub>) resulted in oxygen evolution reaction inhibition at high current densities, improving ozone generation efficiency. In particular, current efficiency data as a function of electrolyte composition show improved electrode performance following the following sequence: 3.5 M H<sub>2</sub>SO<sub>4</sub> < (3.5 M H<sub>2</sub>SO<sub>4</sub> + NaF) < (3.5 M H<sub>2</sub>SO<sub>4</sub> + HBF<sub>4</sub>) < (3.5 M H<sub>2</sub>SO<sub>4</sub> + KPF<sub>6</sub>).



(A)



(B)

**Figure 31.** Schematic diagram of (A) the solid polymer electrolyte cell and (B) the experimental apparatus used for electrochemical ozone production. Reprinted with permission from ref 339. Copyright 2005 The Electrochemical Society.

**Table 10. Volumes, Energy Requirements, and Sludge Production for Different Combinations of Electrochemical and Biological Processes (Concentrations in  $\text{mg dm}^{-3}$ ) (Reprinted with Permission from Ref 296. Copyright 2005 Springer.)**

		energy consumption ( $\text{kWh m}^{-3}$ )		required volume ( $\text{m}^3$ )		sludge produced ( $\text{kg day}^{-1}$ )
		for each unit	totally for the option	for each unit	totally for the option	
(a) single sludge	nitrification	3.02	8.47	1153	1925	431
	denitrification	0.55		772		
	pumping	4.90				
(b) anaerobic electrolysis		0.0472	53.31	1736	1800.5	72
		53.30		64.5		
(c) anaerobic conditioning electrolysis		0.0052	53.31	174	238.5	17
		53.30		64.5		
(d) aerobic electrolysis		74.70	74.70	93.75	93.75	0
(e) aerobic electrolysis		1.10	29.00	364	398	546
		27.90		34		

Despite the advantage of high current efficiency, this process has the disadvantage that these electrolytes are highly

corrosive for the cell materials, and ozone gas should be abstracted from electrolyzed water. Therefore, to improve

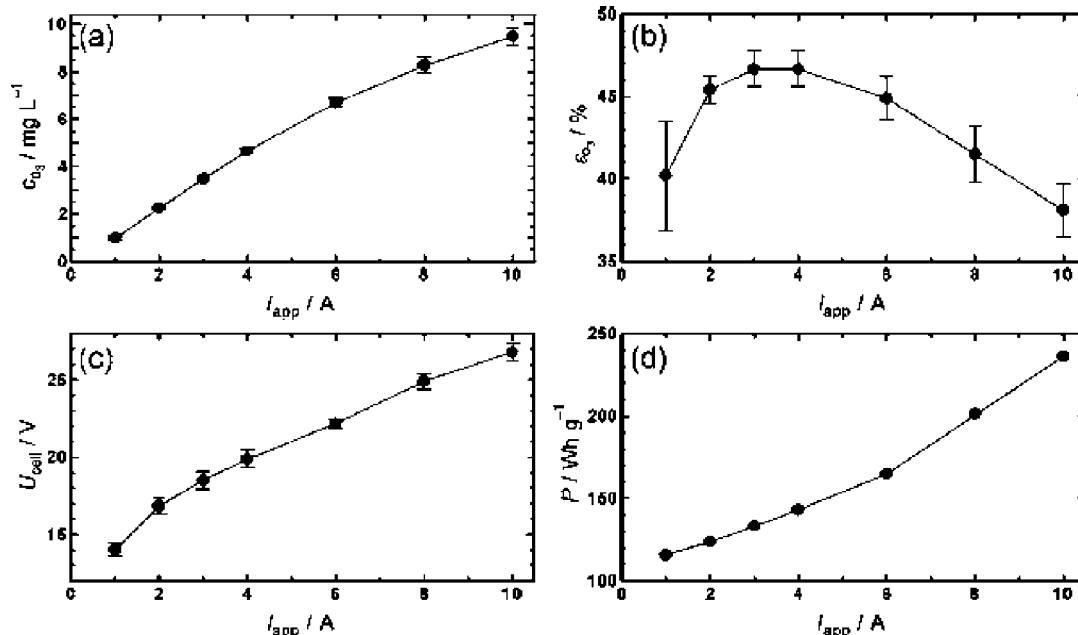


**Figure 32.** Plots of (a) ozone concentration, (b) current efficiency, (c) cell voltage, and (d) specific power consumption with respect to applied current. Ozone water was produced by electrolysis of pure water with freestanding perforated BDD electrodes. Reprinted with permission from ref 335. Copyright 2007 The Electrochemical Society.

the performance and stability of electrochemical ozone production, solid polymer electrolytes (SPEs) can be used.<sup>335,337–339</sup>

In this process, the three-dimensional porous anode and cathode are pressed on a proton-exchange membrane, which acts as electrolyte, forming a sandwich. Ozone is produced in water from the back of the anode at room temperature, while hydrogen evolves from the back of the cathode. Figure 31 shows a schematic diagram of the solid polymer electrolyte cell and the experimental apparatus used by Onda et al.<sup>339</sup> for ozone generation on  $\text{PbO}_2$  anode. With this configuration and under optimal conditions (i.e., temperature = 25–30 °C, water flow rate = 33  $\text{dm}^3 \text{h}^{-1}$ , and current density = 1.0  $\text{A cm}^{-2}$ ), current efficiency for ozone water production is about 8%.

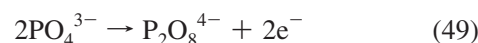
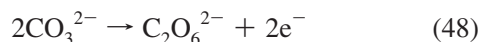
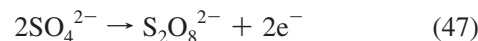
High-concentration ozone-water was obtained by Arihara et al.<sup>335</sup> with a zero-gap electrolytic cell containing a freestanding perforated boron-doped diamond anode. Performance of the freestanding perforated BDD electrodes was proven to be dependent on the number of holes, hole diameter, and electrode thickness. In particular, increasing the number of holes per unit area is the most effective way to improve current efficiency. In the optimal electrode configuration (i.e., 0.54 mm thickness, 1.0 mm hole diameter), maximum current efficiency was improved up to about 47% (Figure 32).

Degradation of reactive dyes used in the textile industry (Reactive Yellow 143 and Reactive Blue 264) with electrochemically generated ozone was investigated in alkaline medium by Da Silva et al.<sup>338</sup> Electrochemical ozonation shows a very good efficiency for both solution decoloration and TOC removal.

### 5.2.3. Persulfate, Percarbonate, and Perphosphate

Other strong oxidants, such as persulfate ( $\text{S}_2\text{O}_8^{2-}$ ), percarbonate ( $\text{C}_2\text{O}_6^{2-}$ ), or perphosphate ( $\text{P}_2\text{O}_8^{4-}$ ), can be used as mediators in indirect electrochemical oxidation of organics. These compounds are produced by anodic oxidation of

sulfate, carbonate, or phosphate ions present in the solution according to the following equations:



Experimental tests have shown that these oxidants are efficiently generated only using anodes with high oxygen evolution overpotential, such as boron-doped diamond or lead dioxide.<sup>16,31,33,135,176,188,193,203,340–342</sup> As reported above, when BDD or  $\text{PbO}_2$  anodes are used, organic pollutants can be efficiently removed by hydroxyl radicals electrogenerated by water discharge. However, a positive contribution of these chemicals is also foreseen during the final treatment step, when oxygen is produced as secondary reaction. The presence of these strong oxidants in wastewater bulk avoids mass-transfer limitation and increases process efficiency.

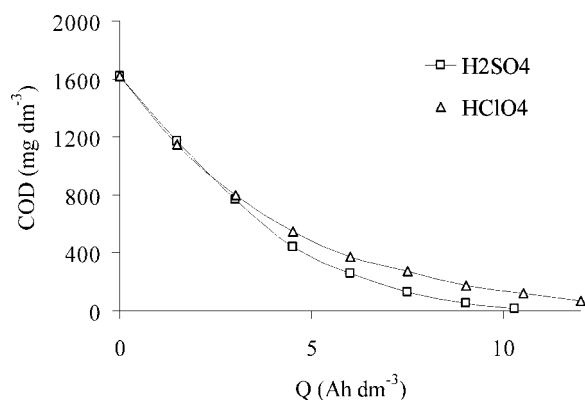


**Figure 33.** Evolution of COD during the electrolysis of 5 mM 2-naphthol at BDD anode. Applied current  $I = 1.5 \text{ A}$ ,  $T = 60 \text{ }^\circ\text{C}$ , electrolyte: ( $\square$ )  $\text{H}_2\text{SO}_4$  1 M, ( $\triangle$ )  $\text{HClO}_4$  1 M.



For example, data collected at our laboratory, based on the comparison in COD evolution during electrolysis of 2-naphthol on BDD anode in perchloric and sulfuric media, point out that persulfate-mediated oxidation promotes removal of organic pollutants (Figure 33). At the beginning of electrolysis, when organics concentration is still high and the process is under charge transfer control, no significant differences are found between the electrolytes. Conversely, when the concentration of organics decreases and the process is under mass-transfer limitation, COD removal is faster in sulfuric media due to persulfates mediation. Similar results were also found by other authors for the removal of triazines,<sup>183</sup> polyhydroxybenzenes,<sup>188</sup> and carboxylic acids.<sup>156</sup>

Canizares et al.<sup>343</sup> also proposed a theoretical model that considers both kinetic and mass-transfer processes and includes the contribution of electrogenerated oxidants (persulfates, perphosphates). According to this model, an electrochemical reactor can be represented as three interconnected stirred-tank reactors, which correspond to the two zones close to the electrodes (i.e., electrochemical reaction zones, where direct oxidation or reduction occur) and to the bulk zone (i.e., chemical reaction zone, where pollutants are oxidized by electrogenerated chemicals). The model was applied to electrochemical treatment using BDD anodes of aqueous wastes containing carboxylic acids (formic, oxalic, and maleic) or phenol. It provided good agreement between the experimental and modeling results.

## 6. Concluding Remarks

Literature results summarized in this review show that there are two main strategies for anodic oxidation of organic compounds. The first is to perform electrolysis at a high anodic potential in the region of water discharge, with the participation of intermediates of electrogenerated hydroxyl radicals. The nature of electrode material strongly affects both process selectivity and efficiency. In particular, anodes with low oxygen evolution overpotential, such as graphite, IrO<sub>2</sub>, RuO<sub>2</sub>, and Pt permit only partial oxidation of organics, while anodes with high oxygen evolution overpotential, such as SnO<sub>2</sub>, PbO<sub>2</sub>, and BDD, favor complete oxidation of organics to CO<sub>2</sub>; therefore, they are ideal electrodes for wastewater treatment. Among them, BDD anodes show the highest removal rate and stability and are, thus, promising anodes for industrial-scale wastewater treatment.

The second strategy is to oxidize pollutants by indirect electrolysis, generating a redox reagent in situ as a chemical reactant. The inorganic mediator can be a metallic redox couple, used for waste material disposal with over 15–20% organic content, or a chemical reagent (e.g., chlorine, ozone, peroxides). With indirect electrolysis, the mass-transfer limitation problems are minimal, but it either requires separation of metallic redox couples or produces secondary pollution.

Although laboratory and pilot tests have been successful, industrial applications of these methods are still limited, due to relatively high energy consumption of the electrochemical methods. However, thanks to the development of new electrode materials, electrochemical oxidation could be increasingly applied in the future, due to specific advantages for certain applications over other technologies. Moreover, energy consumption could be reduced using so-called “advanced electrochemical oxidation processes”, based on the combination of anodic and cathodic electrogeneration of highly oxidizing hydroxyl radicals.

## 7. Acknowledgments

The authors thank American Chemical Society, Electrochemical Society Inc., Elsevier, John Wiley & Sons, Platinum Metals Review, Springer, and all the authors who gave permission for the reproduction of figures and tables.

## 8. References

- (1) Bousher, A.; Shen, X.; Edyvean, R. *Water Res.* **1997**, *31*, 2084–2092.
- (2) Rajeshwar, K.; Ibanez, J. G.; Swain, G. M. *J. Appl. Electrochem.* **1994**, *24*, 1077.
- (3) Pletcher, D.; Walsh, F. C. *Industrial electrochemistry*; Chapman and Hall: London, 1982.
- (4) Grimm, J.; Bessarabov, D.; Sanderson, R. *Desalination* **1998**, *115*, 285.
- (5) Janssen, L. J. J.; Koene, L. *Chem. Eng. J.* **2002**, *85*, 137.
- (6) Juettner, K.; Galla, U.; Schmieder, H. *Electrochim. Acta* **2000**, *45*, 2575.
- (7) Simonsson, D. *Chem. Soc. Rev.* **1997**, *26*, 181.
- (8) Walsh, F.; Mills, G. *Chem. Ind.-London* **1993**, 576.
- (9) Rajeshwar, K.; Ibanez, J. G. *Environmental Electrochemistry. Fundamentals and applications in pollution abatement*; Academic Press, Inc.: London, 1997.
- (10) Martínez-Huitle, C. A.; Ferro, S. *Chem. Soc. Rev.* **2006**, *12*, 1324.
- (11) Chen, G. *Sep. Purif. Technol.* **2004**, *38*, 11.
- (12) Comninellis, C. C.; Guohua, Eds. *Electrochemistry for the Environment*; Springer: Berlin, 2009.
- (13) Panizza, M.; Cerisola, G. In *Advances in Chemistry Research*, Volume 2; Zinger, D. V., Ed.; Nova Science Publishers, Inc.: New York, 2006.
- (14) Comninellis, C.; Pulgarin, C. *J. Appl. Electrochem.* **1991**, *21*, 703.
- (15) Rodrigo, M. A.; Michaud, P. A.; Duo, I.; Panizza, M.; Cerisola, G.; Comninellis, C. *J. Electrochem. Soc.* **2001**, *148*, D60.
- (16) Panizza, M.; Michaud, P. A.; Cerisola, G.; Comninellis, C. *J. Electroanal. Chem.* **2001**, *507*, 206.
- (17) Panizza, M.; Michaud, P. A.; Cerisola, G.; Comninellis, C. *Electrochem. Commun.* **2001**, *3*, 336.
- (18) Panizza, M.; Cerisola, G. *Electrochim. Acta* **2003**, *48*, 3491.
- (19) Canizares, P.; Martínez, F.; Diaz, M.; Garcia-Gomez, J.; Rodrigo, M. A. *J. Electrochem. Soc.* **2002**, *149*, 118.
- (20) Foti, G.; Gandini, D.; Comninellis, C. *Curr. Top. Electrochem.* **1997**, *5*, 71.
- (21) Gattrell, M.; Kirk, D. *J. Electrochem. Soc.* **1993**, *140*, 1534.
- (22) Iniesta, J.; Michaud, P. A.; Panizza, M.; Cerisola, G.; Aldaz, A.; Comninellis, C. *Electrochim. Acta* **2001**, *46*, 3573.
- (23) Rao, T. N.; Terashima, C.; Sarada, B. V.; Tryk, D. A.; Fujishima, A. *Anal. Chem.* **2002**, *74*, 895.
- (24) Rodgers, J. D.; Jedral, W.; Bunce, N. *J. Environ. Sci. Technol.* **1999**, *33*, 1453.
- (25) Canizares, P.; Saez, C.; Lobato, J.; Rodrigo, M. A. *Ind. Eng. Chem. Res.* **2004**, *43*, 1944.
- (26) Canizares, P.; Saez, C.; Lobato, J.; Rodrigo, M. A. *Electrochim. Acta* **2004**, *49*, 4641.
- (27) Mitadera, M.; Spataru, N.; Fujishima, A. *J. Appl. Electrochem.* **2004**, *34*, 249.
- (28) Zanta, C. L. P. S.; De Andrade, A. R.; Boodts, J. F. C. *J. Appl. Electrochem.* **2000**, 467.
- (29) Boye, B.; Brillas, E.; Marselli, B.; Michaud, P.-A.; Comninellis, C.; Farnia, G.; Sandona, G. *Electrochim. Acta* **2006**, *51*, 2872.
- (30) Nasr, B.; Abdellatif, G.; Canizares, P.; Saez, C.; Lobato, J.; Rodrigo, M. A. *Environ. Sci. Technol.* **2005**, *39*, 7234.
- (31) Canizares, P.; Gadri, A.; Lobato, J.; Nasr, B.; Paz, R.; Rodrigo, M. A.; Saez, C. *Ind. Eng. Chem. Res.* **2006**, *45*, 3468.
- (32) Panizza, M.; Cerisola, G. *Appl. Catal., B* **2007**, *75*, 95.
- (33) Saez, C.; Panizza, M.; Rodrigo, M. A.; Cerisola, G. *J. Chem. Technol. Biotechnol.* **2007**, *82*, 575.
- (34) Iniesta, J.; Michaud, P. A.; Panizza, M.; Comninellis, C. *Electrochem. Commun.* **2001**, *3*, 346.
- (35) Panizza, M.; Cerisola, G. *Int. J. Environ. Pollut.* **2006**, *27*, 64.
- (36) Comninellis, C.; Vercesi, G. P. *J. Appl. Electrochem.* **1991**, *21*, 335.
- (37) Chang, H.; Johnson, D. C. *J. Electrochem. Soc.* **1990**, *137*, 2452.
- (38) Chang, H.; Johnson, D. C. *J. Electrochem. Soc.* **1990**, *137*, 3108.
- (39) Feng, J.; Johnson, D. C. *J. Electrochem. Soc.* **1990**, *137*, 507.
- (40) Feng, J.; Johnson, D. C. *J. Electrochem. Soc.* **1991**, *138*, 3328.
- (41) Feng, J.; Houk, L. L.; Johnson, D. C.; Lowery, S. N.; Carey, J. J. *J. Electrochem. Soc.* **1995**, *142*, 3626.
- (42) Houk, L. L.; Johnson, S. K.; Feng, J.; Houk, R. S.; Johnson, D. C. *J. Appl. Electrochem.* **1998**, *28*, 1167.
- (43) Johnson, S. K.; Houk, L. L.; Feng, J.; Houk, R. S.; Johnson, D. C. *Environ. Sci. Technol.* **1999**, *33*, 2638.

- (44) Kawagoe, K. T.; Johnson, D. C. *J. Electrochem. Soc.* **1994**, *141*, 3404.
- (45) Treimer, S. E.; Feng, J.; Scholten, M. C.; Johnson, D. C.; Davenport, A. J. *J. Electrochem. Soc.* **2001**, *148*, E459.
- (46) Vitt, J. E.; Johnson, D. C. *J. Electrochem. Soc.* **1992**, *139*, 774.
- (47) Feng, J.; Johnson, D. C.; Lowery, S. N.; Carey, J. J. *J. Electrochem. Soc.* **1994**, *141*, 2708.
- (48) Comninellis, C. *Electrochim. Acta* **1994**, *39*, 1857.
- (49) Comninellis, C.; De Battisti, A. *J. Chim. Phys.* **1996**, *93*, 673.
- (50) Simond, O.; Schaller, V.; Comninellis, C. *Electrochim. Acta* **1997**, *42*, 2009.
- (51) Foti, G.; Gandini, D.; Comninellis, C.; Perret, A.; Haenni, W. *Electrochim. Solid State* **1999**, *2*, 228.
- (52) Li, X.-Y.; Cui, Y.-H.; Feng, Y.-J.; Xie, Z.-M.; Gu, J.-D. *Water Res.* **2005**, *39*, 1972.
- (53) Feng, Y. J.; Li, X. Y. *Water Res.* **2003**, *37*, 2399.
- (54) Malpass, G. R. P.; Miwa, D. W.; Mortari, D. A.; Machado, S. A. S.; Motheo, A. J. *Water Res.* **2007**, *41*, 2969.
- (55) Miwa, D. W.; Malpass, G. R. P.; Machado, S. A. S.; Motheo, A. J. *Water Res.* **2006**, *40*, 3281.
- (56) Panizza, M.; Cerisola, G. *Electrochim. Acta* **2004**, *49*, 3221.
- (57) Socha, A.; Chrzescijanska, E.; Kusmierek, E. *Dyes Pigm.* **2005**, *67*, 71.
- (58) Gonçalves, M.; Joyce, A.; Alves, M.; Correia, J. P.; Marques, I. P. *Desalination* **2005**, *185*, 351.
- (59) Coteiro, R. D.; De Andrade, A. R. *J. Appl. Electrochem.* **2007**, *37*, 691.
- (60) Martinez-Huitle, C. A.; Quiroz, M. A.; Comninellis, C.; Ferro, S.; De Battisti, A. *Electrochim. Acta* **2004**, *50*, 949.
- (61) Pulgarin, C.; Adler, N.; Peringer, P.; Comninellis, C. *Water Res.* **1994**, *28*, 887.
- (62) Bonfatti, F.; Ferro, S.; Lavezzo, F.; Malacarne, M.; Lodi, G.; De Battisti, A. *J. Electrochem. Soc.* **1999**, *146*, 2175.
- (63) Kim, K.-W.; Kuppaswamy, M.; Savinell, R. F. *J. Appl. Electrochem.* **2000**, *30*, 543.
- (64) De Lima Leite, R. H.; Cognet, P.; Wilhelm, A.-M.; Delmas, H. *J. Appl. Electrochem.* **2003**, *33*, 693.
- (65) Lamy, C.; Leger, J. M.; Clavilier, J.; Parsons, R. *J. Electroanal. Chem.* **1983**, *150*, 71.
- (66) Brillas, E.; Banos, M. A.; Garrido, J. A. *Electrochim. Acta* **2003**, *48*, 1697.
- (67) Panizza, M.; Bocca, C.; Cerisola, G. *Water Res.* **2000**, *34*, 2601.
- (68) Torres, R. A.; Torres, W.; Peringer, P.; Pulgarin, C. *Chemosphere* **2003**, *50*, 97.
- (69) Canizares, P.; Dominguez, J. A.; Rodrigo, M. A.; Villasenor, J.; Rodriguez, J. *Ind. Eng. Chem. Res.* **1999**, *38*, 3779.
- (70) Polcaro, A. M.; Palmas, S. *Ind. Eng. Chem. Res.* **1997**, *36*, 1791.
- (71) Polcaro, A. M.; Palmas, S.; Renoldi, F.; Mascia, M. *Electrochim. Acta* **2000**, *46*, 389.
- (72) Boudenne, J. L.; Cerclier, O.; Galea, J.; Van Der Vlist, E. *Appl. Catal., A* **1996**, *143*, 185.
- (73) Boudenne, J.-L.; Cerclier, O. *Water Res.* **1999**, *33*, 494.
- (74) Han, Y.; Quan, X.; Ruan, X.; Zhang, W. *Sep. Purif. Technol.* **2008**, *59*, 43.
- (75) Jia, J.; Yang, J.; Liao, J.; Wang, W.; Wang, Z. *Water Res.* **1999**, *33*, 881.
- (76) Fan, L.; Zhou, Y.; Yang, W.; Chen, G.; Yang, F. *Dyes Pigm.* **2008**, *76*, 440.
- (77) Fan, L.; Zhou, Y.; Yang, W.; Chen, G.; Yang, F. *J. Hazard. Mater.* **2006**, *137*, 1182.
- (78) Yi, F.; Chen, S.; Yuan, C. *J. Hazard. Mater.* **2008**, *157*, 79.
- (79) Yang, J.; Jia, J.; Liao, J.; Wang, Y. *Water Res.* **2004**, *38*, 4353.
- (80) Yi, F.; Chen, S. *J. Porous Mater.* **2008**, *15*, 565.
- (81) Shen, Z.; Wang, W.; Jia, J.; Ye, J.; Feng, X.; Peng, A. *J. Hazard. Mater.* **2001**, *84*, 107.
- (82) Gattrell, M.; Kirk, D. *Can. J. Chem. Eng.* **1990**, *68*, 997.
- (83) Awad, Y. M.; Abuzaid, N. S. *J. Environ. Sci. Health, Part A* **1997**, *32*, 1393.
- (84) Awad, Y. M.; Abuzaid, N. S. *Sep. Sci. Technol.* **1999**, *34*, 699.
- (85) Awad, Y. M.; Abuzaid, N. S. *Sep. Purif. Technol.* **2000**, *18*, 227.
- (86) Piya-aretham, P.; Shenchunthichai, K.; Hunsom, M. *Water Res.* **2006**, *40*, 2857.
- (87) Fan, L.; Yang, F.; Yang, W. *Sep. Purif. Technol.* **2004**, *34*, 89.
- (88) Ogutveren, U. B.; Toru, E.; Koparal, S. *Water Res.* **1999**, *33*, 1851.
- (89) Hsu, Y.-S.; Ghandhi, S. K. *J. Electrochem. Soc.* **1980**, *127*, 1592.
- (90) Hsu, Y.-S.; Ghandhi, S. K. *J. Electrochem. Soc.* **1980**, *127*, 1595.
- (91) Jarzelski, Z. M.; Marton, J. P. *J. Electrochem. Soc.* **1976**, *123*, 199C.
- (92) Kotz, R.; Stucki, S.; Carcer, B. *J. Appl. Electrochem.* **1991**, *21*, 14.
- (93) Stucki, S.; Kotz, R.; Carcer, B.; Suter, W. *J. Appl. Electrochem.* **1991**, *21*, 99.
- (94) Comninellis, C.; Pulgarin, C. *J. Appl. Electrochem.* **1993**, *23*, 108.
- (95) Borrás, C.; Berzoy, C.; Mostany, J.; Scharifker, B. R. *J. Appl. Electrochem.* **2006**, *36*, 433.
- (96) Borrás, C.; Berzoy, C.; Mostany, J.; Herrera, J. C.; Scharifker, B. R. *Appl. Catal., B* **2007**, *72*, 98.
- (97) Chen, X.; Gao, F.; Chen, G. *J. Appl. Electrochem.* **2005**, *35*, 185.
- (98) Cossu, R.; Polcaro, A. M.; Lavagnolo, M. C.; Mascia, M.; Palmas, S.; Renoldi, F. *Environ. Sci. Technol.* **1998**, *32*, 3570.
- (99) Polcaro, A. M.; Palmas, S.; Renoldi, F.; Mascia, M. *J. Appl. Electrochem.* **1999**, *29*, 147.
- (100) Quiroz, M. A.; Reyna, S.; Sánchez, J. L. S. *J. Solid State Electrochem.* **2003**, *7*, 277.
- (101) Tanaka, S.; Nakata, Y.; Kimura, T.; Yustiawati; Kawasaki, M.; Kuramitz, H. *J. Appl. Electrochem.* **2002**, *32*, 197.
- (102) Zanta, C. L. P. S.; Michaud, P. A.; Comninellis, C.; De Andrade, A. R.; Boодts, J. F. C. *J. Appl. Electrochem.* **2003**, *33*, 1211.
- (103) Wang, B.; Kong, W.; Ma, H. *J. Hazard. Mater.* **2007**, *146*, 295.
- (104) Wang, Y. H.; Chan, K. Y.; Li, X. Y.; So, S. K. *Chemosphere* **2006**, *65*, 1087.
- (105) Grimm, J. H.; Bessarabov, D. G.; Simon, U.; Sanderson, R. D. *J. Appl. Electrochem.* **2000**, *30*, 293.
- (106) Zhu, K.; Zhang, W.; Wang, H.; Xiao, Z. *Clean* **2008**, *36*, 97.
- (107) Lipp, L.; Pletcher, D. *Electrochim. Acta* **1997**, *42*, 1091.
- (108) Correa-Lozano, B.; Comninellis, C.; De Battisti, A. *J. Appl. Electrochem.* **1997**, *27*, 970.
- (109) Cong, Y.; Wu, Z. *J. Phys. Chem. C* **2007**, *111*, 3442.
- (110) Wu, D.; Liu, M.; Dong, D.; Zhou, X. *Microchem. J.* **2007**, *85*, 250.
- (111) Pavlov, D.; Monahov, B. *J. Electrochem. Soc.* **1996**, *143*, 3616.
- (112) Pavlov, D. *J. Electrochem. Soc.* **1992**, *139*, 3075.
- (113) Sharifian, H.; Kirk, D. *J. Electrochem. Soc.* **1986**, *113*, 921.
- (114) Smith-de-Sucre, V.; Watkinson, A. P. *Can. J. Chem. Eng.* **1981**, *59*, 52.
- (115) Iniesta, J.; Exposito, E.; Gonzalez-Garcia, J.; Montiel, V.; Aldaz, A. *J. Electrochem. Soc.* **2002**, *149*, D57.
- (116) Tahar, N. B.; Savall, A. *J. Electrochem. Soc.* **1998**, *145*, 3427.
- (117) Tahar, N. B.; Savall, A. *J. Appl. Electrochem.* **1999**, *29*, 277.
- (118) Tahar, N. B.; Savall, A. *J. New Mater. Electrochem. Syst.* **1999**, *2*, 19.
- (119) Andrade, L. S.; Rocha-Filho, R. C.; Bocchi, N.; Biaggio, S. R.; Iniesta, J.; Garcia-Garcia, V.; Montiel, V. *J. Hazard. Mater.* **2008**, *153*, 252.
- (120) Gherardini, L.; Michaud, P. A.; Panizza, M.; Comninellis, C.; Vatas, N. *J. Electrochem. Soc.* **2001**, *148*, D78.
- (121) Borrás, C.; Laredo, T.; Mostany, J.; Scharifker, B. R. *Electrochim. Acta* **2004**, *49*, 641.
- (122) Borrás, C.; Laredo, T.; Scharifker, B. R. *Electrochim. Acta* **2003**, *48*, 2775.
- (123) Quiroz, M. A.; Reyna, S.; Martinez-Huitle, C. A.; Ferro, S.; De Battisti, A. *Appl. Catal., B* **2005**, *59*, 259.
- (124) Liu, H.; Liu, Y.; Zhang, C.; Shen, R. *J. Appl. Electrochem.* **2008**, *38*, 101.
- (125) Borrás, C.; Rodriguez, P.; Laredo, T.; Mostany, J.; Scharifker, B. R. *J. Appl. Electrochem.* **2004**, *34*, 583.
- (126) Scialdone, O.; Galia, A.; Filardo, G. *Electrochim. Acta* **2008**, *53*, 7220.
- (127) Kirk, D.; Sharifian, H.; Foulkes, F. R. *J. Appl. Electrochem.* **1985**, *15*, 285.
- (128) Bock, C.; MacDougall, B. *J. Electrochem. Soc.* **1999**, *146*, 2925.
- (129) Martinez-Huitle, C. A.; Ferro, S.; De Battisti, A. *Electrochim. Acta* **2004**, *49*, 4027.
- (130) Martinez-Huitle, C. A.; Ferro, S.; De Battisti, A. *J. Appl. Electrochem.* **2005**, *35*, 1087.
- (131) Andrade, L. S.; Ruotolo, L. A. M.; Rocha-Filho, R. C.; Bocchi, N.; Biaggio, S. R.; Iniesta, J.; Garcia-Garcia, V.; Montiel, V. *Chemosphere* **2007**, *66*, 2035.
- (132) Panizza, M.; Cerisola, G. *Ind. Eng. Chem. Res.* **2008**, *47*, 6816.
- (133) Keech, P. G.; Bunce, N. J. *J. Appl. Electrochem.* **2003**, *33*, 79.
- (134) Samet, Y.; Elaoud, S. C.; Ammar, S.; Abdelhedi, R. *J. Hazard. Mater.* **2006**, *138*, 614.
- (135) Panizza, M.; Sires, I.; Cerisola, G. *J. Appl. Electrochem.* **2008**, *38*, 923.
- (136) Martinez-Huitle, C. A.; De Battisti, A.; Ferro, S.; Reyna, S.; Cerro-Lopez, M.; Quiro, M. A. *Environ. Sci. Technol.* **2008**, *42*, 6929.
- (137) Panizza, M.; Cerisola, G. *Environ. Sci. Technol.* **2004**, *38*, 5470.
- (138) Weiss, E.; Groenen-Serrano, K.; Savall, A. *J. New Mater. Electrochem. Syst.* **2006**, *9*, 249.
- (139) Amadelli, R.; De Battisti, A.; Girenko, D. V.; Kovalyov, S. V.; Velichenko, A. B. *Electrochim. Acta* **2000**, *46*, 341.
- (140) Amadelli, R.; Armelao, L.; Velichenko, A. B.; Nikolenko, N. V.; Girenko, D. V.; Kovalyov, S. V.; Danilov, F. I. *Electrochim. Acta* **1999**, *45*, 713.
- (141) Abaci, S.; Tamer, U.; Pekmez, K.; Yildiz, A. *Appl. Surf. Sci.* **2005**, *240*, 112.
- (142) Fujishima, A.; Einaga, Y.; Rao, T. N.; Tryk, D. A. *Diamond Electrochemistry*; Elsevier: Amsterdam, The Netherlands, 2005.
- (143) Pleskov, Y. V. *Russ. J. Electrochem.* **1999**, *68*, 381.
- (144) Rao, T. N.; Fujishima, A. *Diamond Relat. Mater.* **2000**, *9*, 384.

- (145) Swain, G. M.; Anderson, A. B.; Angus, J. C. *MRS Bull.* **1998**, *23*, 56.
- (146) Fryda, M.; Matth e, T.; Mulcahy, S.; Hampel, A.; Sch fer, L.; Tr ster, I. *Diamond Relat. Mater.* **2003**, *12*, 1950.
- (147) Troster, I.; Schafer, L.; Fryda, M.; Matthee, T. *Water Sci. Technol.* **2004**, *49*, 207.
- (148) Martin, H. B.; Argoitia, A.; Landau, U.; Anderson, A. B.; Angus, J. C. *J. Electrochem. Soc.* **1996**, *143*, L133.
- (149) Ramesham, R.; Rose, M. F. *Diamond Relat. Mater.* **1997**, *6*, 17.
- (150) Swain, G. M. *Adv. Mater.* **1994**, *5*, 388.
- (151) Pleskov, Y. V. *Russ. J. Electrochem.* **2002**, *38*, 1275.
- (152) Marselli, B.; Garcia-Gomez, J.; Michaud, P. A.; Rodrigo, M. A.; Comninellis, C. *J. Electrochem. Soc.* **2003**, *150*, D79.
- (153) Panizza, M.; Brillas, E.; Comninellis, C. *J. Environ. Eng. Manage.* **2008**, *18*, 139.
- (154) Panizza, M.; Cerisola, G. *Electrochim. Acta* **2005**, *51*, 191.
- (155) Gandini, D.; Mahe, E.; Michaud, P. A.; Haenni, W.; Perret, A.; Comninellis, C. *J. Appl. Electrochem.* **2000**, *30*, 1345.
- (156) Canizares, P.; Garcia-Gomez, J.; Lobato, J.; Rodrigo, M. A. *Ind. Eng. Chem. Res.* **2003**, *42*, 956.
- (157) Canizares, P.; Paz, R.; S ez, C.; Rodrigo, M. A. *Electrochim. Acta* **2008**, *53*, 2144.
- (158) Scialdone, O.; Galia, A.; Guarisco, C.; Randazzo, S.; Filardo, G. *Electrochim. Acta* **2008**, *53*, 2095.
- (159) Xu, L.; Wang, W.; Wang, M.; Cai, Y. *Desalination* **2008**, *222*, 388.
- (160) Kraft, A.; Stadelmann, M.; Blaschke, M. *J. Hazard. Mater.* **2003**, *103*, 247.
- (161) Montilla, F.; Michaud, P. A.; Morallon, E.; Vazquez, J. L.; Comninellis, C. *Electrochim. Acta* **2002**, *47*, 3509.
- (162) Louhichi, B.; Bensalash, N.; Gadri, A. *Chem. Eng. Technol.* **2006**, *29*, 944.
- (163) Perret, A.; Haenni, W.; Skinner, N.; Tang, X.-M.; Gandini, D.; Comninellis, C.; Correa, B.; Foti, G. *Diamond Relat. Mater.* **1999**, *8*, 820.
- (164) Canizares, P.; Diaz, M.; Dominguez, J. A.; Lobato, J.; Rodrigo, M. A. *J. Chem. Technol. Biotechnol.* **2005**, *80*, 565.
- (165) Nava, J. L.; Nunez, F.; Gonzalez, I. *Electrochim. Acta* **2007**, *52*, 3229.
- (166) Flox, C.; Cabot, P. L.; Centellas, F.; Garrido, J. A.; Rodriguez, R. M.; Arias, C.; Brillas, E. *Chemosphere* **2006**, *64*, 892.
- (167) Sires, I.; Cabot, P. L.; Centellas, F.; Garrido, J. A.; Rodriguez, R. M.; Arias, C.; Brillas, E. *Electrochim. Acta* **2006**, *52*, 75.
- (168) Sires, I.; Brillas, E.; Cerisola, G.; Panizza, M. *J. Electroanal. Chem.* **2008**, *613*, 151.
- (169) Polcaro, A. M.; Mascia, M.; Palmas, S.; Vacca, A. *Electrochim. Acta* **2004**, *49*, 649.
- (170) Brillas, E.; Sires, I.; Arias, C.; Cabot, P. L.; Centellas, F.; Rodriguez, R. M.; Garrido, J. A. *Chemosphere* **2005**, *58*, 399.
- (171) Zhu, X.; Shi, S.; Wei, J.; Lv, F.; Zhao, H.; Kong, J.; He, Q.; Ni, J. *Environ. Sci. Technol.* **2007**, *41*, 6541.
- (172) Yavuz, Y.; Koparal, A. S.; Ogutveren, U. B. *J. Environ. Eng.* **2008**, *134*, 24.
- (173) Zhao, G.; Shen, S.; Li, M.; Wu, M.; Cao, T.; Li, D. *Chemosphere* **2008**, *73*, 1407.
- (174) Weiss, E.; Groenen-Serrano, K.; Savall, A. *J. Appl. Electrochem.* **2008**, *38*, 329.
- (175) Ghanem, M. A.; Compton, R. G.; Coles, B. A.; Psillakis, E.; Kulandainathan, M. A.; Marken, F. *Electrochim. Acta* **2007**, *53*, 1092.
- (176) Canizares, P.; Diaz, M.; Dominguez, J. A.; Garcia-Gomez, J.; Rodrigo, M. A. *Ind. Eng. Chem. Res.* **2002**, *41*, 4187.
- (177) Canizares, P.; Garcia-Gomez, J.; Saez, C.; Rodrigo, M. A. *J. Appl. Electrochem.* **2004**, *34*, 87.
- (178) Canizares, P.; Lobato, J.; Garcia-Gomez, J.; Rodrigo, M. A. *J. Appl. Electrochem.* **2004**, *34*, 111.
- (179) Canizares, P.; Lobato, J.; Paz, R.; Rodrigo, M. A.; Saez, C. *Water Res.* **2005**, *39*, 2687.
- (180) Canizares, P.; Saez, C.; Lobato, J.; Paz, R.; Rodrigo, M. A. *J. Electrochem. Soc.* **2007**, *154*, E37.
- (181) Canzares, P.; Garcia-Gomez, J.; Saez, C.; Rodrigo, M. A. *J. Appl. Electrochem.* **2003**, *33*, 917.
- (182) Canizares, P.; Saez, C.; Lobato, J.; Rodrigo, M. A. *J. Chem. Technol. Biotechnol.* **2006**, *81*, 352.
- (183) Polcaro, A. M.; Vacca, A.; Mascia, M.; Palmas, S. *Electrochim. Acta* **2005**, *50*, 1841.
- (184) Polcaro, A. M.; Vacca, A.; Palmas, S.; Mascia, M. *J. Appl. Electrochem.* **2003**, *33*, 885.
- (185) Mascia, M.; Vacca, A.; Palmas, S.; Polcaro, A. M. *J. Appl. Electrochem.* **2007**, *37*, 71.
- (186) Morao, A.; Lopes, A.; Pessoa de Amorim, M. T.; Goncalves, I. C. *Electrochim. Acta* **2004**, *49*, 1587.
- (187) Pacheco, M. J.; Morao, A.; Lopes, A.; Ciriaco, L.; Goncalves, I. *Electrochim. Acta* **2007**, *53*, 629.
- (188) Canizares, P.; Saez, C.; Lobato, J.; Rodrigo, M. A. *Ind. Eng. Chem. Res.* **2004**, *43*, 6629.
- (189) Bellagamba, R.; Michaud, P. A.; Comninellis, C.; Vatistas, N. *Electrochem. Commun.* **2002**, *4*, 171.
- (190) Louhichi, B.; Ahmadi, M. F.; Bensalah, N.; Gadri, A.; Rodrigo, M. A. *J. Hazard. Mater.* **2008**, *158*, 430.
- (191) Panizza, M.; Delucchi, M.; Cerisola, G. *J. Appl. Electrochem.* **2005**, *35*, 357.
- (192) Weiss, E.; Groenen-Serrano, K.; Savall, A. *J. Appl. Electrochem.* **2007**, *37*, 1337.
- (193) Canizares, P.; Martinez, L.; Paz, R.; Saez, C.; Lobato, J.; Rodrigo, M. A. *J. Chem. Technol. Biotechnol.* **2006**, *81*, 1331.
- (194) Canizares, P.; Lobato, J.; Paz, R.; Rodrigo, M. A.; Saez, C. *Chemosphere* **2007**, *67*, 832.
- (195) Deligiorgis, A.; Xekoukoulotakis, N. P.; Diamadopoulos, E.; Mantzavinos, D. *Water Res.* **2008**, *42*, 1229.
- (196) Canizares, P.; Paz, R.; Lobato, J.; Saez, C.; Rodrigo, M. A. *J. Hazard. Mater.* **2006**, *138*, 173.
- (197) Canizares, P.; Louhichi, B.; Gadri, A.; Nasr, B.; Paz, R.; Rodrigo, M. A.; Saez, C. *J. Hazard. Mater.* **2007**, *146*, 552.
- (198) Troster, I.; Fryda, M.; Herrmann, D.; Schafer, L.; Hanni, W.; Perret, A.; Blaschke, M.; Kraft, A.; Stadelmann, M. *Diamond Relat. Mater.* **2002**, *11*, 640.
- (199) Kapalka, A.; Foti, G.; Comninellis, C. *J. Appl. Electrochem.* **2008**, *38*, 7.
- (200) Panizza, M.; Kapalka, A.; Comninellis, C. *Electrochim. Acta* **2008**, *53*, 2289.
- (201) Canizares, P.; Beteta, A.; Saez, C.; Rodriguez, L.; Rodrigo, M. A. *Chemosphere* **2008**, *72*, 1080.
- (202) Panizza, M.; Zolezzi, M.; Nicolella, C. *J. Chem. Technol. Biotechnol.* **2006**, *81*, 225.
- (203) Panizza, M.; Cerisola, G. *J. Hazard. Mater.* **2008**, *153*, 83.
- (204) Chen, X.; Chen, G. *Sep. Purif. Technol.* **2006**, *48*, 45.
- (205) Chen, X.; Chen, G.; Gao, F.; Yue, P. L. *Environ. Sci. Technol.* **2003**, *37*, 5021.
- (206) Faouzi, A. M.; Nasr, B.; Abdellatif, G. *Dyes Pigm.* **2007**, *73*, 86.
- (207) Hattori, S.; Doi, M.; Takahashi, E.; Kurosu, T.; Nara, M.; Nakamatsu, S.; Nishiki, Y.; Furuta, T.; Iida, M. *J. Appl. Electrochem.* **2003**, *33*, 85.
- (208) Koparal, A. S.; Yavuz, Y.; Gurel, C.; Ogutveren, U. B. *J. Hazard. Mater.* **2007**, *145*, 100.
- (209) Foord, J. S.; Holt, K. B.; Compton, R. G.; Marken, F.; Kim, D.-H. *Diamond Relat. Mater.* **2001**, *10*, 662.
- (210) Faouzi, M.; Canizares, P.; Gadri, A.; Lobato, J.; Nasr, B.; Paz, R.; Rodrigo, M. A.; Saez, C. *Electrochim. Acta* **2006**, *52*, 325.
- (211) Diniz, A. V.; Ferreira, N. G.; Corat, E. J.; Trava-Airoldi, V. J. *Diamond Relat. Mater.* **2003**, *12*, 577.
- (212) Bechtold, T.; Turcanu, A.; Schrott, W. *Diamond Relat. Mater.* **2006**, *15*, 1513.
- (213) Ceron-Rivera, M.; Davila-Jimenez, M. M.; Elizalde-Gonzalez, M. P. *Chemosphere* **2004**, *55*, 1.
- (214) Chen, X.; Chen, G.; Yue, P. L. *Chem. Eng. Sci.* **2003**, *58*, 995.
- (215) Fernandes, A.; Morao, A.; Magrinho, M.; Lopes, A.; Goncalves, I. *Dyes Pigm.* **2004**, *61*, 287.
- (216) Carvalho, C.; Fernandes, A.; Lopes, A.; Pinheiro, H.; Goncalves, I. *Chemosphere* **2007**, *67*, 1316.
- (217) Ammar, S.; Abdelhedi, R.; Flox, C.; Arias, C.; Brillas, E. *Environ. Chem. Lett.* **2006**, *4*, 229.
- (218) Hastie, J.; Bejan, D.; Teutli-Le n, M.; Bunce, N. J. *Ind. Eng. Chem. Res.* **2006**, *45*, 4898.
- (219) Guo, L.; Chen, G. *Diamond Relat. Mater.* **2007**, *16*, 1530.
- (220) Tian, Y.; Chen, X.; Shang, C.; Chen, G. *J. Electrochem. Soc.* **2006**, *153*, J80.
- (221) Guo, L.; Chen, G. *J. Electrochem. Soc.* **2007**, *154*, D657.
- (222) Bringmann, J.; Ebert, K.; Galla, U.; Schmieder, H. *J. Appl. Electrochem.* **1995**, *25*, 846.
- (223) Steele, D. F. U.S. Patent 4,874,485, 1989.
- (224) Steele, D. F. *Platinum Met. Rev.* **1990**, *34*, 10.
- (225) Farmer, J. C.; Wang, F. T.; Hawley-Fedder, R. A.; Lewis, P. R.; Summers, L. J.; Foiles, L. J. *Electrochem. Soc.* **1992**, *139*, 654.
- (226) Laitinen, H. A.; Conley, J. M. *Anal. Chem.* **1976**, *48*, 1224.
- (227) Panizza, M.; Duo, I.; Michaud, P. A.; Cerisola, G.; Comninellis, C. *Electrochem. Solid State* **2000**, *3*, 550.
- (228) Ryan, J. L.; Bray, A. L.; Wheelwright, E. J.; Bryan, G. H. In *Transuranium Elements: A Half Century*; Morss, L. R., Fuger, J., Eds.; American Chemical Society: Washington, DC, 1992.
- (229) Zundelevich, Y. *J. Alloys Compd.* **1992**, *182*, 115.
- (230) Po, H. N.; Swinehart, J. H.; Allen, T. L. *Inorg. Chem.* **1968**, *7*, 244.
- (231) Steele, D. F. *Chem. Brit.* **1991**, *27*, 915.
- (232) Mentasti, E.; Baiocchi, C.; Coe, J. S. *Coord. Chem. Rev.* **1984**, *54*, 131.
- (233) Lehmani, A.; Turq, P.; Simonin, J.-P. *J. Electrochem. Soc.* **1996**, *143*, 1860.
- (234) Turner, A. D. *Membr. Technol.* **2002**, *142*, 6.
- (235) Chung, Y. H.; Park, S. M. *J. Appl. Electrochem.* **2000**, *30*, 685.

- (236) Balazs, G. B.; Lewis, P. R. U.S. Patent 5,919,350, 1999.
- (237) Farmer, J. C.; Wang, F. T.; Lewis, P. R.; Summers, L. J. *J. Electrochem. Soc.* **1992**, *139*, 3025.
- (238) Leffrang, U.; Ebert, K.; Flory, K.; Galla, U.; Schmeider, H. *Sep. Sci. Technol.* **1995**, *30*, 1883.
- (239) Sanroman, M. A.; Pazos, M.; Ricart, M. T.; Cameselle, C. *Chemosphere* **2004**, *57*, 233.
- (240) Surma, J. E.; Bryan, G. H.; Geeting, J. G. H.; Butner, R. S. U.S. Patent 5,707,508, 1998.
- (241) Surma, J. E.; Nelson, N.; Steward, G. A.; Bryan, G. H. U.S. Patent 5,968,337, 1999.
- (242) Varela, J. A.; Oberg, S. G.; Neustedter, T. M.; Nelson, N. *Environ. Prog.* **2001**, *20*, 261.
- (243) Nelson, N. *Platinum Met. Rev.* **2002**, *46*, 18.
- (244) Balaji, S.; Kokovkin, V. V.; Chung, S. J.; Moon, I. S. *Water Res.* **2007**, *41*, 1423.
- (245) Balaji, S.; Chung, S. J.; Thiruvengatachari, R.; Moon, I. S. *Chem. Eng. J.* **2007**, *126*, 51.
- (246) Balaji, S.; Chung, S. J.; Matheswaran, M.; Vasilivich, K. V.; Moon, I. S. *J. Hazard. Mater.* **2008**, *150*, 596.
- (247) Chung, S. J.; Balaji, S.; Matheswaran, M.; Ramesh, T.; Moon, I. S. *Water Sci. Technol.* **2007**, *55*, 261.
- (248) Lee, J.-W.; Chung, S.-J.; Balaji, S.; Kokovkin, V. V.; Moon, I.-S. *Chemosphere* **2007**, *68*, 1067.
- (249) Matheswaran, M.; Balaji, S.; Chung, S. J.; Moon, I. S. *Electrochim. Acta* **2007**, *53*, 1897.
- (250) Matheswaran, M.; Balaji, S.; Chung, S. J.; Moon, I. S. *Chemosphere* **2007**, *69*, 325.
- (251) Matheswaran, M.; Balaji, S.; Chung, S. J.; Moon, I. S. *Chem. Eng. J.* **2008**, *144*, 28.
- (252) Vaze, A. S.; Sawant, S. B.; Pangarkar, V. G. *J. Appl. Electrochem.* **1999**, *29*, 7.
- (253) Dhooge, P. M.; Park, S. M. *J. Electrochem. Soc.* **1983**, *130*, 1029.
- (254) Dhooge, P. M.; Stilwell, D. E.; Park, S. M. *J. Electrochem. Soc.* **1982**, *129*, 1719.
- (255) Farmer, J. C.; Wang, F. T.; Hickman, R. G.; Lewis, P. R. U.S. Patent 5,516,972, 1996.
- (256) Brillas, E.; Ouran, M. A.; Sirés, I. *Chem. Rev.* . submitted for publication.
- (257) Malpass, G. R. P.; Miwa, D. W.; Machado, S. A. S.; Olivi, P.; Motheo, A. J. *J. Hazard. Mater.* **2006**, *137*, 565.
- (258) Azzam, M. O.; Al-Tarazi, M.; Tahboub, Y. *J. Hazard. Mater.* **2000**, *75*, 99.
- (259) Rajkumar, D.; Palanivelu, K. *Ind. Eng. Chem. Res.* **2003**, *42*, 1833.
- (260) Bonfatti, F.; De Battisti, A.; Ferro, S.; Lodi, G.; Osti, S. *Electrochim. Acta* **2000**, *46*, 305.
- (261) Bonfatti, F.; Ferro, S.; Lavezzo, F.; Malacarne, M.; Lodi, G.; De Battisti, A. *J. Electrochem. Soc.* **2000**, *147*, 592.
- (262) Cameselle, C.; Pazos, M.; Sanroman, M. A. *Chemosphere* **2005**, *60*, 1080.
- (263) Panizza, M.; Barbucci, A.; Ricotti, R.; Cerisola, G. *Sep. Purif. Technol.* **2007**, *54*, 382.
- (264) Martinez-Huitle, C. A.; Ferro, S.; De Battisti, A. *Electrochem. Solid State* **2005**, *8*, D35.
- (265) Vlyssides, A.; Arapoglou, D.; Mai, S.; Barampouti, E. M. *Chemosphere* **2005**, *58*, 439.
- (266) Vlyssides, A.; Arapoglou, D.; Mai, S.; Barampouti, E. M. *Int. J. Environ. Pollut.* **2005**, *23*, 289.
- (267) Vlyssides, A.; Arapoglou, D.; Israilides, C.; Karlis, P. *J. Pestic. Sci.* **2004**, *29*, 105.
- (268) Vlyssides, A.; Arapoglou, D.; Mai, S.; Barampouti, E. M. *Fresenius Environ. Bull.* **2004**, *13*, 760.
- (269) Vlyssides, A.; Barampouti, E. M.; Mai, S.; Arapoglou, D.; Kotronarou, A. *Environ. Sci. Technol.* **2004**, *38*, 6125.
- (270) Vlyssides, A. G.; Arapoglou, D. G.; Israilides, C. J.; Barampouti, E. M. P.; Mai, S. T. *J. Appl. Electrochem.* **2004**, *34*, 1265.
- (271) Arapoglou, D.; Vlyssides, A.; Israilides, C.; Zorpas, A.; Karlis, P. *J. Hazard. Mater.* **2003**, *98*, 191.
- (272) Zhou, M. H.; Wu, Z. C.; Wang, D. H. *J. Environ. Sci. Health, Part A* **2002**, *37*, 1263.
- (273) Iniesta, J.; Gonzalez-Garcia, J.; Exposito, E.; Montiel, V.; Aldaz, A. *Water Res.* **2001**, *35*, 3291.
- (274) Korbahti, B. K.; Tanyolac, A. *Ind. Eng. Chem. Res.* **2003**, *42*, 5060.
- (275) Korbahti, B. K.; Tanyolac, A. *Chem. Eng. Commun.* **2003**, *190*, 749.
- (276) Korbahti, B. K.; Tanyolac, A. *Water Res.* **2003**, *37*, 1505.
- (277) Korbahti, B. K.; Salih, B.; Tanyolac, A. *J. Chem. Technol. Biotechnol.* **2002**, *77*, 70.
- (278) Comninellis, C.; Nerini, A. *J. Appl. Electrochem.* **1995**, *25*, 23.
- (279) Rajkumar, D.; Kim, J. G.; Palanivelu, K. *Chem. Eng. Technol.* **2005**, *28*, 98.
- (280) Lopez-Grimau, V.; Gutierrez, M. C. *Chemosphere* **2006**, *62*, 106.
- (281) Manisankar, P.; Rani, C.; Viswanathan, S. *Chemosphere* **2004**, *57*, 961.
- (282) Moraes, P. B.; Bertazzoli, R. *Chemosphere* **2005**, *58*, 41.
- (283) Chiang, L. C.; Chang, J. E.; Wen, T. C. *Water Res.* **1995**, *29*, 671.
- (284) Vlyssides, A.; Karlis, P.; Loizidou, M.; Zorpas, A.; Arapoglou, D. *Environ. Technol.* **2001**, *22*, 1467.
- (285) Vlyssides, A. G.; Karlis, P. K.; Mahnken, G. *J. Appl. Electrochem.* **2003**, *33*, 155.
- (286) Korbahti, B. K.; Aktas, N.; Tanyolac, A. *J. Hazard. Mater.* **2007**, *148*, 83.
- (287) Rajkumar, D.; Palanivelu, K. *J. Hazard. Mater.* **2004**, *113*, 123.
- (288) Panizza, M.; Cerisola, G. *Water Res.* **2006**, *40*, 1179.
- (289) Israilides, C. J.; Vlyssides, A. G.; Mourafeti, V. N.; Karvouni, G. *Bioresour. Technol.* **1997**, *61*, 163.
- (290) Belaid, C.; Kallel, M.; Khadhraou, M.; Lalleve, G.; Elleuch, B.; Fauvarque, J.-F. *J. Appl. Electrochem.* **2006**, *36*, 1175.
- (291) Giannis, A.; Kalaitzakis, M.; Diamadopoulos, E. *J. Chem. Technol. Biotechnol.* **2007**, *82*, 663.
- (292) Szpyrkowicz, L.; Naumczyk, J.; Zilio-Grandi, F. *Toxicol. Environ. Chem.* **1994**, *44*, 189.
- (293) Szpyrkowicz, L.; Naumczyk, J.; Zilio-Grandi, F. *Water Res.* **1995**, *29*, 517.
- (294) Rao, N. N.; Somasekhar, K. M.; Kaul, S. N.; Szpyrkowicz, L. *J. Chem. Technol. Biotechnol.* **2001**, *76*, 1124.
- (295) Szpyrkowicz, L.; Kelsall, G. H.; Kaul, S. N.; DeFaveri, M. *Chem. Eng. Sci.* **2001**, *56*, 1579.
- (296) Szpyrkowicz, L.; Kaul, S. N.; Neti, R. N. *J. Appl. Electrochem.* **2005**, *35*, 381.
- (297) Szpyrkowicz, L.; Kaul, S. N.; Neti, R. N.; Satyanarayan, S. *Water Res.* **2005**, *39*, 1601.
- (298) Costa, C. R.; Botta, C. M. R.; Espindola, E. L. G.; Olivi, P. *J. Hazard. Mater.* **2008**, *153*, 616.
- (299) Rajkumar, D.; Song, B. J.; Kim, J. G. *Dyes Pigm.* **2007**, *72*, 1.
- (300) Rajkumar, D.; Kim, J. G. *J. Hazard. Mater.* **2006**, *136*, 203.
- (301) Malpass, G. R. P.; Miwa, D. W.; Machado, S. A. S.; Motheo, A. J. *J. Hazard. Mater.* **2008**, *156*, 170.
- (302) Vlyssides, A. G.; Loizidou, M.; Karlis, P. K.; Zorpas, A. A.; Papaioannou, D. *J. Hazard. Mater.* **1999**, *70*, 41.
- (303) Vlyssides, A. G.; Israilides, C. J. *J. Environ. Sci. Health, Part A* **1998**, *33*, 847.
- (304) Vlyssides, A. G.; Papaioannou, D.; Loizidou, M.; Karlis, P. K.; Zorpas, A. A. *Waste Manage.* **2000**, *20*, 569.
- (305) Szpyrkowicz, L.; Radaelli, M. *Sep. Sci. Technol.* **2007**, *42*, 1493.
- (306) Szpyrkowicz, L.; Radaelli, M. *J. Appl. Electrochem.* **2006**, *36*, 1151.
- (307) Szpyrkowicz, L.; Juzzolino, C.; Daniele, S.; De Faveri, M. D. *Catal. Today* **2001**, *66*, 519.
- (308) Szpyrkowicz, L.; Juzzolino, C.; Kaul, S. N.; Daniele, S.; DeFaveri, M. *Ind. Eng. Chem. Res.* **2000**, *39*, 3241.
- (309) Naumczyk, J.; Szpyrkowicz, L.; Zilio-Grandi, F. *Water Sci. Technol.* **1996**, *34*, 17.
- (310) Szpyrkowicz, L.; Radaelli, M.; Daniele, S. *Catal. Today* **2005**, *100*, 425.
- (311) Chatzisyneon, E.; Xekoukoulotakis, N. P.; Coz, A.; Kalogerakis, N.; Mantzavinos, D. *J. Hazard. Mater.* **2006**, *137*, 998.
- (312) Mohan, N.; Balasubramanian, N. *J. Hazard. Mater.* **2006**, *136*, 239.
- (313) Mohan, N.; Balasubramanian, N.; Basha, C. A. *J. Hazard. Mater.* **2007**, *147*, 644.
- (314) Panizza, M.; Cerisola, G. *Electrochim. Acta* **2003**, *48*, 1515.
- (315) Katoh, M.; Nishiki, Y.; Nakamatsu, S. *J. Appl. Electrochem.* **1994**, *24*, 489.
- (316) Babak, A. A.; Amadelli, R.; De Battisti, A.; Fateev, V. N. *Electrochim. Acta* **1994**, *39*, 1597.
- (317) Da Silva, L. M.; De Faria, L. A.; Boodts, J. F. C. *Electrochim. Acta* **2003**, *48*, 699.
- (318) Park, S.-G.; Kim, G.-S.; Park, J.-E.; Einaga, Y.; Fujishima, A. *J. New Mater. Electrochem. Syst.* **2005**, *8*, 65.
- (319) Foller, P. C.; Tobias, C. W. *J. Electrochem. Soc.* **1982**, *129*, 506.
- (320) Foller, P. C.; Goodwin, M. L. *Chem. Eng. Prog.* **1985**, *81*, 49.
- (321) Foller, P. C.; Goodwin, M. L. *Ozone: Sci. Eng.* **1984**, *6*, 29.
- (322) El-Shal, W.; Khordagui, H.; El-Sebaie, O.; El-Sharkawi, F.; Sedahmed, G. H. *Desalination* **1994**, *99*, 149.
- (323) Wang, J.; Jing, X. *Electrochemistry* **2006**, *74*, 539.
- (324) Tatapudi, P.; Fenton, J. M. *J. Electrochem. Soc.* **1993**, *140*, 3527.
- (325) Tatapudi, P.; Fenton, J. M. *J. Electrochem. Soc.* **1994**, *141*, 1174.
- (326) Kim, J.; Korshin, G. V. *Ozone: Sci. Eng.* **2008**, *30*, 113.
- (327) Wang, Y.-H.; Cheng, S.; Chan, K.-Y.; Li, X. Y. *J. Electrochem. Soc.* **2005**, *152*, 197.
- (328) Cheng, S.-A.; Chan, K.-Y. *Electrochem. Solid State* **2004**, *7*, 4.
- (329) Santana, M. a. H. P.; De Faria, L. A.; Boodts, J. F. C. *Electrochim. Acta* **2004**, *49*, 1925.
- (330) Da Silva, L. M.; Franco, D. V.; De Faria, L. A.; Boodts, J. F. C. *Electrochim. Acta* **2004**, *49*, 3977.
- (331) Awad, M. I.; Saleh, M. M.; Ohsaka, T. *J. Electrochem. Soc.* **2006**, *153*, D207.

- (332) Kaneda, K.; Ikematsu, M.; Koizumi, Y.; Minoshima, H.; Rakuma, T.; Takaoka, D.; Yasuda, M. *Electrochem. Solid State* **2005**, *8*, 13.
- (333) Foller, P. C.; Kelsall, G. H. *J. Appl. Electrochem.* **1993**, *23*, 996.
- (334) Katsuki, N.; Takahashi, E.; Toyoda, M.; Kurosu, T.; Iida, M.; Wakita, S.; Nishiki, Y.; Shimamune, T. *J. Electrochem. Soc.* **1998**, *145*, 2358.
- (335) Arihara, K.; Terashima, C.; Fujishima, A. *J. Electrochem. Soc.* **2007**, *154*, E71.
- (336) Michaud, P. A.; Panizza, M.; Ouattara, L.; Diaco, T.; Foti, G.; Comninellis, C. *J. Appl. Electrochem.* **2003**, *33*, 151.
- (337) Kraft, A.; Stadelmann, M.; Wunsche, M.; Blaschke, M. *Electrochem. Commun.* **2006**, *8*, 883.
- (338) Da Silva, L. M.; Franco, D. V.; Forti, J. C.; Jardim, W. F.; Boodts, J. F. C. *J. Appl. Electrochem.* **2006**, *36*, 523.
- (339) Onda, K.; Ohba, T.; Kusunoki, H.; Takezawa, S.; Sunakawa, D.; Araki, T. *J. Electrochem. Soc.* **2005**, *152*, D177.
- (340) Ravera, M.; Ciccarelli, C.; Gianotti, V.; Scorza, S.; Osella, D. *Chemosphere* **2004**, *57*, 587.
- (341) Canizares, P.; Larrondo, F.; Lobato, J.; Rodrigo, M. A.; Saez, C. *J. Electrochem. Soc.* **2005**, *152*, D191.
- (342) Saha, M. S.; Furuta, T.; Nishiki, Y. *Electrochem. Solid State* **2003**, *6*, D5.
- (343) Canizares, P.; Garcya-Gomez, J.; Lobato, J.; Rodrigo, M. A. *Ind. Eng. Chem. Res.* **2004**, *43*, 1915.

CR9001319